

AD-A276 017

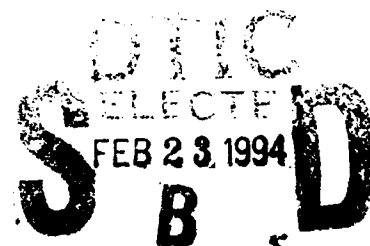
(2)

NPSEC-93-020



NAVAL POSTGRADUATE SCHOOL

Monterey, California



Analysis Using Bi-Spectral Related Technique

by

Ralph Hippenstiel

November 17, 1993



94-05749

DP

94 2 22 136

Approved for public release; distribution unlimited.

Prepared for: Naval Command Control & Ocean Surveillance Center
Code 732
271 Catalina Blvd.
San Diego, CA 92152-5000

QUALITY

Naval Postgraduate School
Monterey, California 93943-5000

Rear Admiral T. A. Mercer
Superintendent

H. Shull
Provost

This report was funded by the Naval Command Control and Ocean Surveillance Center.

Reproduction of all or part of this report is authorized.

This report was prepared by:

Ralph Hippensiel

RALPH HIPPENSTIEL
Associate Professor,
Department of Electrical and
Computer Engineering

Reviewed by:

Michael A. Morgan
MICHAEL A. MORGAN
Chairman,
Department of Electrical and
Computer Engineering

Released by:

PJ. Marto
PAUL J. MARTO
Dean of Research

REPORT DOCUMENTATION PAGE

*Form Approved
OMB No 0704-0188*

Public reporting burden for this collection of information is estimated to average 1 hour per response, including the time for reviewing instructions, searching existing data sources, gathering and maintaining the data needed, and completing and reviewing the collection of information. Send comments regarding this burden estimate or any other aspect of this collection of information, including suggestions for reducing this burden, to Washington Headquarters Services, Directorate for Information Operations and Reports, 1215 Jefferson Davis Highway, Suite 1204, Arlington, VA 22202-4302 and to the Office of Management and Budget, Paperwork Reduction Project (0704-0188), Washington, DC 20503.

1. AGENCY USE ONLY (Leave blank)			2. REPORT DATE	3. REPORT TYPE AND DATES COVERED	
			November 17, 1993	Final Report	Oct 1, 92-Sep 30, 93
4. TITLE AND SUBTITLE			5. FUNDING NUMBERS		
Analysis Using Bi-Spectral Related Techniques					
6. AUTHOR(S)					
Ralph Hippenstiel					
7. PERFORMING ORGANIZATION NAME(S) AND ADDRESS(ES)			8. PERFORMING ORGANIZATION REPORT NUMBER		
Naval Postgraduate School Monterey, CA 93943-5000			NPSEC-93-020		
9. SPONSORING / MONITORING AGENCY NAME(S) AND ADDRESS(ES)			10. SPONSORING / MONITORING AGENCY REPORT NUMBER		
Naval Command Control & Ocean Surveillance Center Code 732 271 Catalina Blvd. San Diego, CA 92152-5000					
11. SUPPLEMENTARY NOTES The views expressed in this report are those of the authors and do not reflect the official policy or position of the Department of Defense or the United States Government.					
12a. DISTRIBUTION / AVAILABILITY STATEMENT Approved for public release; distribution unlimited.			12b. DISTRIBUTION CODE		
13. ABSTRACT (Maximum 200 words) This report investigates the use of Bi-spectral related techniques to extract detection/classification clues from time-frequency representations. Earlier results have indicated that 1.5-D spectral techniques (a degenerate version of the Bi-spectrum) has potential Signal to Noise Ratio (SNR) gain over conventional techniques. This is partially due to the rejection of Gaussian like perturbations by the cumulant based techniques. The third order moment for Gaussian zero mean random processes is essentially zero. It is assumed that i) the independence of the Instantaneous Power Spectrum (IPS) from analytic signal representations and ii) the Gaussian character of the noise causes minimal distortion of the output variables, hence permit signal characterization at low to moderate SNRs. The performance is demonstrated on i) synthetic signals and ii) on segment(s) of the NOSC data set.					
14. SUBJECT TERMS spectral estimation, instantaneous spectrum, Bi-spectrum, cumulant based spectrum, detection			15. NUMBER OF PAGES 60		
			16. PRICE CODE		
17. SECURITY CLASSIFICATION OF REPORT UNCLASSIFIED	18. SECURITY CLASSIFICATION OF THIS PAGE UNCLASSIFIED	19. SECURITY CLASSIFICATION OF ABSTRACT UNCLASSIFIED	20. LIMITATION OF ABSTRACT SAR		

Analysis Using Bi-Spectral Related Techniques.

Ralph Hippenstiel

Electrical and Computer Engineering Department
Naval Postgraduate School
Monterey, CA 93943-5000

November 17, 1993

Final Report
on Research sponsored by
Naval Ocean System Center
San Diego, CA

Accession For	
NTIS GRA&I	<input checked="" type="checkbox"/>
DTIC TAB	<input type="checkbox"/>
Unnumbered	<input type="checkbox"/>
Journal Article	<input type="checkbox"/>
By _____	
Distribution _____	
Availability _____	
Dist	Aval and/or Special
A-1	

Analysis Using Bi-Spectral Related Techniques.

Table of Content.

- i. Objectives.
- 1. Introduction.
- 2. Instantaneous power spectrum (IPS), cumulant based instantaneous power spectrum (CUM), and spectrogram based representation (LOFAR).
 - 2.1 IPS
 - 2.2 CUM
 - 2.3 LOFAR
- 3. Theoretical results for averaged surfaces.
 - 3.1 Averaged IPS
 - 3.2 Averaged CUM
 - 3.3 Averaged LOFAR
 - 3.4 Deflection ratio comparison
- 4. Simulation results using sinusoids embedded in white Gaussian noise.
- 5. Processing results using NOSC data base.
- 6. Conclusion and recommendation.
- 7. Program listings.
- 8. References.
- 9. Appendix A.

i. Objectives:

This report investigates the use of Bi-spectral related techniques to extract detection/classification clues from time-frequency representations.

Earlier results have indicated that 1.5-D spectral techniques (a degenerate version of the Bi-spectrum) has potential Signal to Noise Ratio (SNR) gain over conventional techniques. This is partially due to the rejection of Gaussian like perturbations by the cumulant based techniques. The third order moment for Gaussian zero mean random processes is essentially zero. It is assumed that i) the independence of IPS from analytic signal representations and ii) the Gaussian character of the noise causes minimal distortion of the output variables, hence permit signal characterization at low to moderate SNR's.

The performance is demonstrated on i) synthetic signals and ii) on segment(s) of the NOSC data set.

1. Introduction:

This report examines the instantaneous power spectrum (IPS) and the cumulant based version of IPS (CUM) to address the question whether or not these techniques offer possible improvements relative to conventional spectral processing (i.e. spectrogram, Lofargram, periodogram).

Section 2 provides the mathematical definition for IPS, CUM, and LOFAR while section 3 allows a theoretical comparison of these techniques. The comparison is performed using a deflection criterion (i.e. maximum signal magnitude versus standard deviation of the detector output under noise only conditions).

Section 4 contains simulation results, while section 5 provides actual SONAR data results.

Section 6, and 7 contain the conclusion and program listings, respectively. Section 8 provides the list of references.

2. IPS, CUM and LOFAR

2.1 IPS:

IPS is a member of the Cohen's class [1], and is also known as the real part of the Rihaczec distribution. Our particular implementation differs in that filtering is employed as the data is processed (equation 1). Earlier results have shown that in contrast to the Wigner-Ville Distribution (WVD) no spectral cross modulation terms are generated. However, it has wider spectral peaks and superimposed spectral auto modulation terms [2]. These auto terms do not interfere with the interpretation of T-F surfaces, but can help in the detection of a weak stable spectral line component. The digital implementation of IPS is given by

$$IPS(n, k) = \frac{1}{2} \sum_{m=-N/2}^{N/2-1} (x(n)x^*(n-m) + x^*(n)x(n+m)) w(m) \exp -j2\pi km/N$$

eq. 1

where k = frequency index, n = time index, N = the length of data used, m = shift parameter and $w()$ = lag window.

Some earlier results are published in [2,3,4].

2.2 CUM:

In general the Bi-spectrum is defined as

$$S_X(\omega_1, \omega_2) = \sum_{l_1} \sum_{l_2} C_X(l_1, l_2) e^{-j(\omega_1 l_1 + \omega_2 l_2)}$$

where the cumulant is given by [5]

$$C_X(l_1, l_2) = E(X^*(n)X(n+l_1)X(n+l_2)).$$

A degenerate version of the cumulant is given by

$$C_X(0, l_2) = E(X^*(n) X(n) X(n+l_2)) = E(|X(n)|^2 X(n+l_2)).$$

When replacing the expected value with the instantaneous value the degenerate Bi-spectrum, also called the $1\frac{1}{2}$ D spectrum, becomes

$$S_X(\omega) = \sum_l |x(n)|^2 x(n+l) e^{-j\omega l}.$$

The cumulant version of IPS is given by

$$CUM(n, k) = \frac{1}{2} \sum_{m=-N/2}^{N/2-1} (|x(n)|^2 x^*(n-m) + |x(n)|^2 x(n+m)) w(m) \exp -j2\pi km/N$$

eq. 2

Cross terms at locations where the true spectrum has no support are not created. Also contrary to the conventional Bi-spectrum none of the spectrally related components are suppressed.

In part of the work in [6], the approach of Petropulu [7] which uses an instantaneous higher order moment slice was utilized. This approach works well, but does not permit separation of spectral components having the same spectral dynamics. That is, all stationary spectral components (i.e. stable line components) map to the same detection cell, making this technique useless in scenarios with several similarly behaving spectral components.

2.3 LOFAR:

The LOFAR algorithm uses a Hamming windowed Fast Fourier Transform (FFT) and displays the magnitude of the transform.

To keep T-F dimensions relative small, no zero padding is used.

$$P_x(n, k) = \left| \sum_{m=n}^{n+N-1} x(m) e^{-j2\pi km/N} \right|$$

eq. 3

The IPS, CUM, and LOFAR surfaces are averaged (in magnitude) over some segments of the time axis leaving only a display of spectral magnitude versus frequency. For each segment one spectral line is created resulting again in a time frequency display. The averaging technique is also known as power or incoherent averaging.

3. Theoretical results for averaged surfaces.

The analysis in this section is done by disregarding any window effects and assuming that under the noise only hypothesis (H_0) Gaussian white noise and under the signal only hypothesis (H_1) a deterministic signal of the form $x(n)=A \cos(2\pi k_0 n/N)$ is present. The value of k_0 , n , and N are assumed to be integers which ensures that the spectrum peaks at a bin center of an N -point Fourier transform. In all detection schemes (averaged IPS, averaged CUM, and averaged LOFAR) magnitudes are averaged since they are numerically more conveniently computed than the magnitude squared values.

The comparison is done for normalized versions of

$$I(k) = \sum_n |\text{IPS}(n, k)| ,$$

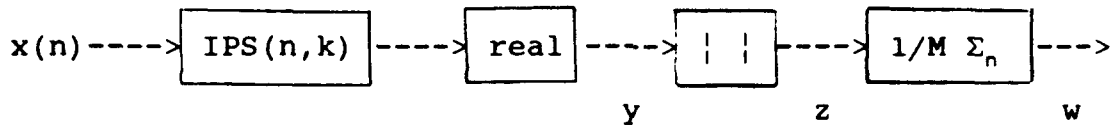
$$C(k) = \sum_n |\text{CUM}(n, k)| , \text{ and}$$

$P(k) = \sum_n |\text{windowed Fourier transform } \{x(n_1, k)\}|$; where n_1 is the time counted from reference point n .

In what follows the time (n) and frequency (k) dependency is

usually suppressed.

3.1 Averaged IPS.



where $x(n) \sim N(0, \sigma^2)$ i.i.d. and M is the appropriate number of degrees of freedom.

Under H_0 :

Under noise only condition (H_0) the random variable Y denoted by Y_0 has the following moments [6]:

$$E(Y_0) = \sigma^2, \quad E(Y_0)^2 = [(N+5)/2] \sigma^4, \quad \text{var}(Y_0) = [(N+3)/2] \sigma^4.$$

For the transformation $Z = \text{SQRT}(Y^2)$,

the resulting probability density function is given by

$$f_z(z) = (f_Y(z) + f_Y(-z)) U(z).$$

Making the assumption that for large enough number of data points the random variable Y is approximately Gaussian distributed we can derive the moments for Z as

$$E(Z_0) = \text{SQRT}\{(N+3)/16\pi\} \sigma^2 e^{-(2/(N+3))}$$

$$E(Z_0^2) = E(Y_0)^2 = ((N+5)/2) \sigma^4$$

$$\text{var}(Z_0) = [(N+5)/2 - ((N+3) e^{-(4/(N+3))})/16\pi] \sigma^4$$

$$\text{var}(W_0) \approx 1/M \text{ var}(Z_0) \quad (\text{for large } N)$$

$$\approx (1/M) 0.48 N \sigma^4.$$

A typical surface has about $N/3$ degrees of freedom [6], providing a standard deviation (under the H_0 hypothesis) of

$$\sigma(W_0) \approx 1.2 \sigma^2 .$$

Under H_1 (at spectral location $\pm k_0$):

$$Z_1 = |Y_1| = (NA^2) \cos^2(2\pi k_0 n/N)$$

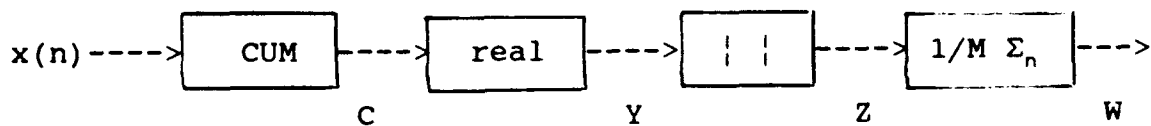
$$W_1 = (NA^2)/M \sum_n \cos^2(2\pi k_0 n/N)$$

$$\approx (NA^2)/2.$$

The deflection D_{PSI} for IPS becomes

$$D_{PSI} = W_1/\sigma(W_0) = (NA^2/2)/(1.2 \sigma^2) = (N/2.4)(A^2/\sigma^2).$$

3.2 Averaged CUM.



Under H_0 :

$$E(C_0) = 0 + j0$$

$$E(C_0)^2 = \text{var}(C_0)$$

$$= (6N+54)/4(\sigma^2)^3 = \text{var}(Y_0) ; [6]$$

(since real part of cum is zero).

$$Z_0 = |Y_0|$$

$$f_z(z) = 2/(2\pi\sigma_y^2)^{1/2} \exp(-z^2/(2\sigma_y^2)) U(z)$$

$$E(Z_0) = \text{SQRT}(2/\pi) \sigma_y$$

$$E(Z_0)^2 = 3/2 \sigma_y^2$$

$$\text{var}(Z_0) = (3/2 - 2/\pi) \sigma_y^2$$

$$E(W_0) = E(Z_0) = \text{SQRT}(2/\pi) \sigma_y$$

$$E(W_0)^2 = 1/M \{E(Z_0)^2 + (M-1)E^2(Z_0)\}$$

$$\text{var}(W_0) = 1/M \left\{ (3/2 - 2/\pi)(6N+54)/4 \right\} \sigma^6$$

$$\sigma(W_0) = \text{SQRT}\{1/M (3/2 - 2/\pi)(6N+54)\}/2 \sigma^3.$$

A typical surface has about $N/3$ degrees of freedom [6] , so the standard deviation becomes

$$\sigma(W_0) \approx \text{SQRT}(3/N (3/2 - 2/\pi)(6N+54))/2 \sigma^3.$$

Under H_1 (at spectral location $\pm k_0$):

$$x(n) = A \cos(2\pi k_0 n/N)$$

$$Y_1 = NA^3/2 \cos^3(2\pi k n/N) \quad \text{if } k = \pm k_0$$

$$Z_1 = NA^3/2 |\cos^3(2\pi k n/N)| \quad \text{if } k = \pm k_0$$

From numerical evaluations we know that the summation is lower bounded by

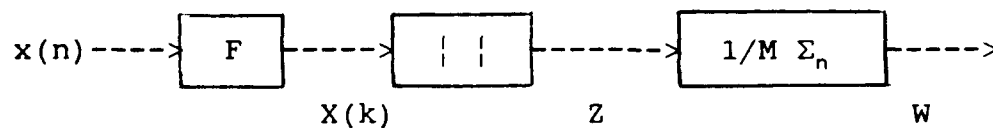
$$\frac{1}{M} \sum_{n=0}^{M-1} |\cos^3(2\pi 1n/M)| > 0.424 .$$

$$\text{Hence } Z_1 > 0.424 NA^3/2.$$

The deflection D_{CUM} becomes

$$\begin{aligned} D_{\text{CUM}} &= (0.424 NA^3/2) \text{SQRT}(M) / \{\text{SQRT}[(3/2 - 2/\pi)(6N+54)/4] \sigma^3\} \\ &\approx 0.1075 N (A/\sigma)^3 . \end{aligned}$$

3.3 LOFAR:



Under H_0 :

$$X(k) = X_r(k) + j X_i(k)$$

$= \sum_{m=n}^{n+N-1} x(m) \exp-j(2\pi km/N)$; where n is the reference time

$$E(X_r(k)) = E(X_r) = E(X_i(k)) = E(X_i) = 0$$

$$E(X_r)^2 = \text{var}(X_r) = \text{var}(X_i) = \sigma^2 N/2$$

$$Z = \text{SQRT}(X_r^2 + X_i^2)$$

$$E(Z_0) = \text{SQRT}(\pi/2) \text{ SQRT}(N/2) \sigma$$

$$\text{var}(Z_0) = (2-\pi/2)\sigma^2 N/2$$

$$E(W_0) = E(Z_0) = \text{SQRT}(\pi/2) \text{ SQRT}(N/2) \sigma$$

$$E(W_0)^2 = 1/M \{ E(Z_0)^2 + (M-1)E^2(Z_0) \}$$

$$\text{var}(W_0) = 1/M \text{ var}(Z_0) = (1/M) (2-\pi/2)\sigma^2(N/2)$$

$$\sigma(W_0) = \text{SQRT}\{(1/M) (2-\pi/2) (N/2)\} \sigma$$

Under H_1 (at spectral location $\pm k_0$):

$$X_1(k) = A N/2 \quad \theta k = \pm k_0$$

$$Z_1 = A N/2 \quad \theta k = \pm k_0$$

$$E(W_1) = E(Z_1) = A N/2$$

The deflection D_{LOFAR} becomes

$$\begin{aligned} D_{\text{LOFAR}} &= (AN/2) / \{(1/M) (2-\pi/2) \sigma^2(N/2)\}^{1/2} \\ &= N^{1/2} [3 A^2 / ((4-\pi) \sigma^2)]^{1/2}. \end{aligned}$$

3.4 Deflection ratio comparison:

We can now plot the deflection ratio, that is compare and determine which detector is more advantageous under which conditions.

Comparing D_{IPS} and D_{LOFAR} :

$$D_{\text{IPS}} > D_{\text{LOFAR}}$$

simplifies to

$$N > 20.13 (\sigma^2/A^2)$$

Comparing D_{CUM} and D_{LOFAR} :

$D_{CUM} > D_{LOFAR}$

simplifies to

$$N > 302.4 (\sigma^4/A^4).$$

We notice that the processing length variable N, for IPS relative to LOFAR has a $(SNR)^{-1}$ and for CUM relative to LOFAR has a $(SNR)^{-2}$ dependency.

4. Simulation results for sinusoid in white Gaussian noise.

Ten test sets, of length 4096, consisting of sinusoidal signals embedded in white Gaussian noise are processed by IPS, CUM and LOFAR. Each test set contains seven (7) sinusoids whose SNR goes from -3 dB to -21 dB in 3 dB steps. The decrease is monotonic relative to the spectral locations so that the SNR decreases in 3 dB steps as the frequency increases. The sinusoidal frequencies are fixed in all test sets at digital frequencies:

$\{\omega\} = \{11\%, 17\%, 29\%, 37\%, 59\%, 77\%, 111\%\} * 2\pi/256$. The phases within each set and over all set are independently distributed (i.e. no harmonic relationship between different spectral components and different realizations). We note that none of the sinusoids has an integer number of cycles over 4096 data points ensuring all signals will have side lobes if processed by an FFT of size 4096 or less. To demonstrate potential gain the deflection ratio as defined in section 3 is computed for each sinusoid and averaged over the 10 realizations.

Figures 1, 2, 3, 4, 5 and 6 are plots of the outcomes of the simulation for 128, 256, 512, 1024, 2048 and 4096 data points,

respectively. The top part of each figure superimposes all of the 10 realizations while the bottom part shows the average of the 10 realizations. We note for example, that the weakest sinusoid (bin 223-224 of 512 point data length) clearly shows up in the CUM and IPS representation (figure 3.A) but is not detectable in the LOFAR representation (figure 3.B). This illustrates that the alternative representations (i.e. averaged JPS or averaged CUM) can complement the traditional (averaged LOFAR) representation. Figures 7-12 provide plots of the experimental deflection ratios versus SNR in the top half of the figures. The solid, dashed, and dotted lines represent the experimental deflection for CUM, IPS, and LOFAR, respectively. The bottom halves are plots of the difference of deflection ratios ($D_{IPS} - D_{CUM}$). Figure 13 attempts to reconcile theoretical bounds from section 3 with the experimental evidence from this section. The straight solid lines demarcate the theoretical transitions points at which CUM works better than LOFAR (upper straight line) and where IPS works better than LOFAR (lower straight line). We mention again that no window action was accounted for in the derivation of these lines. Superimposed are (zigzag lines) the results taken from figures 7 through 12. The upper zigzag line shows the demarcation line where the experimental evidence indicates IPS will do better than CUM (in terms of deflection ratios). The lower zigzag line consists of the points, as a function of SNR and processing length, where the experimental performance of all three techniques (IPS, CUM and LOFAR) tends to coincide. Above this line the CUM and IPS technique outperform the LOFAR approach with improvements increasing as the input SNR increases.

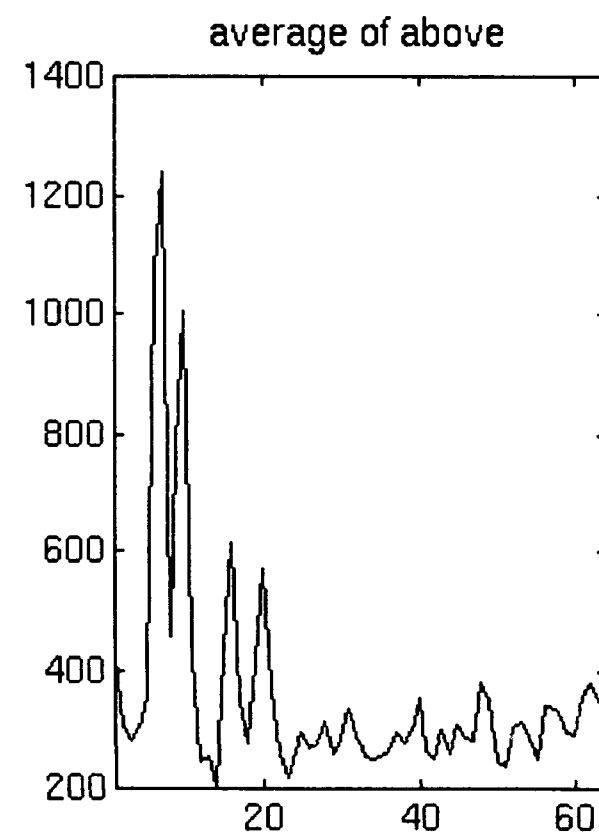
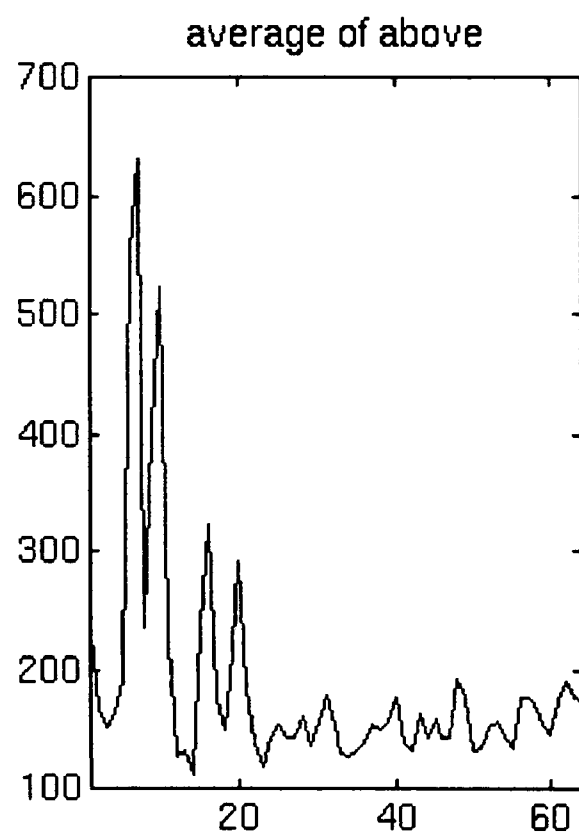
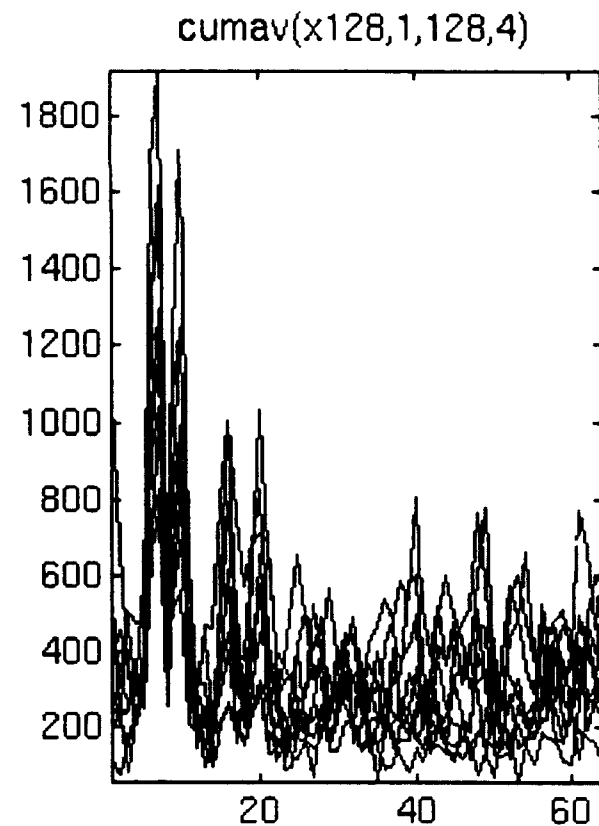
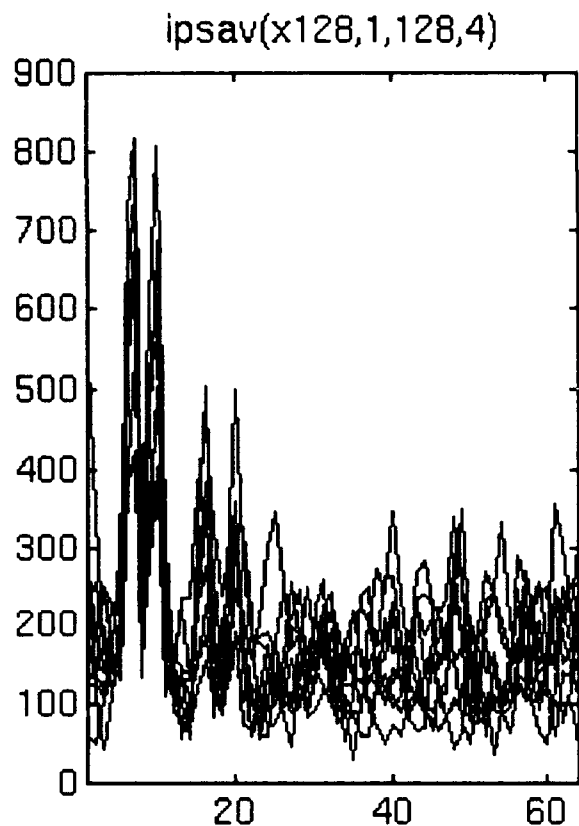
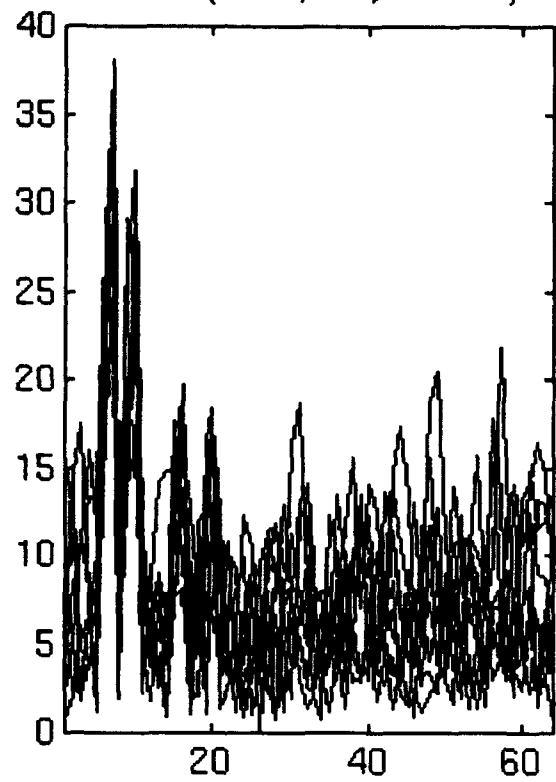


Fig. 1.A

lofarm(x128,128,128128)



average of above

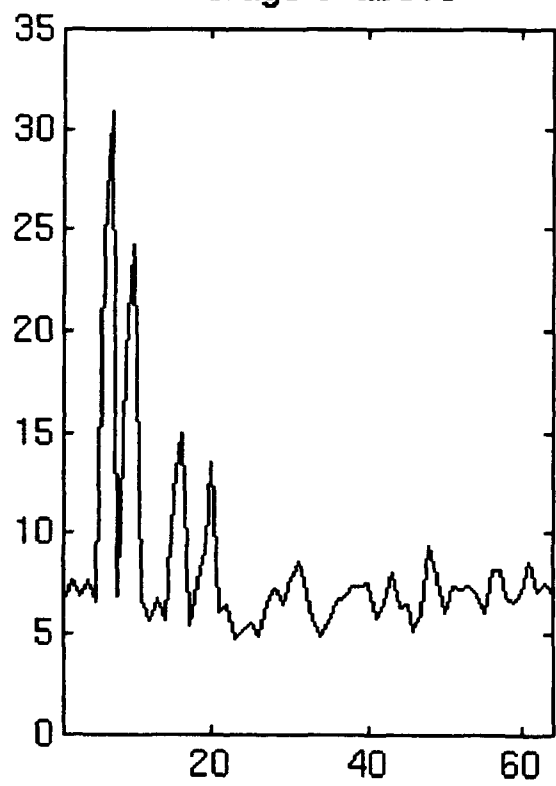


Fig. 1.B

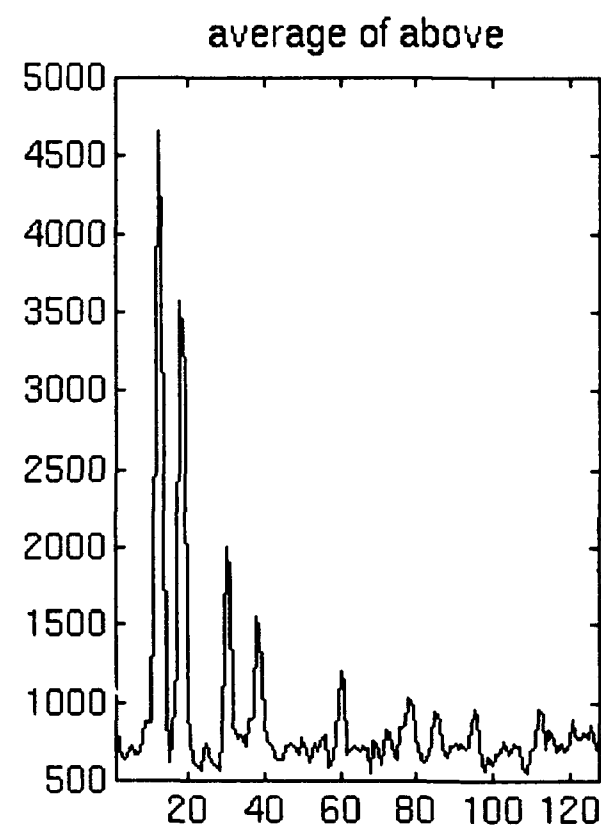
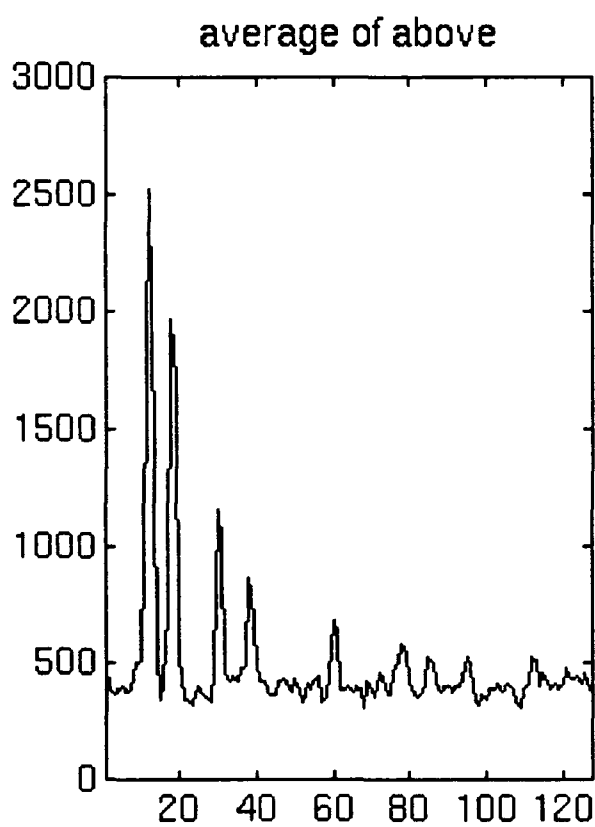
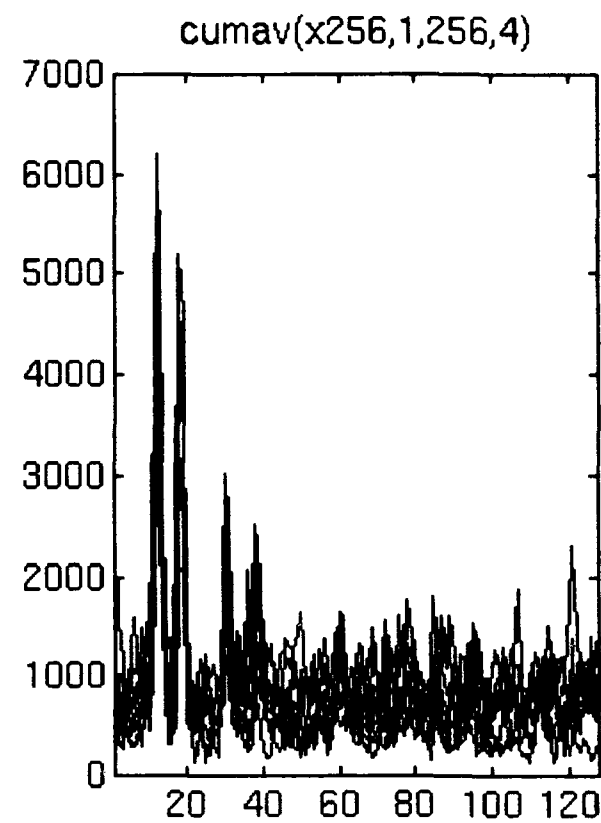
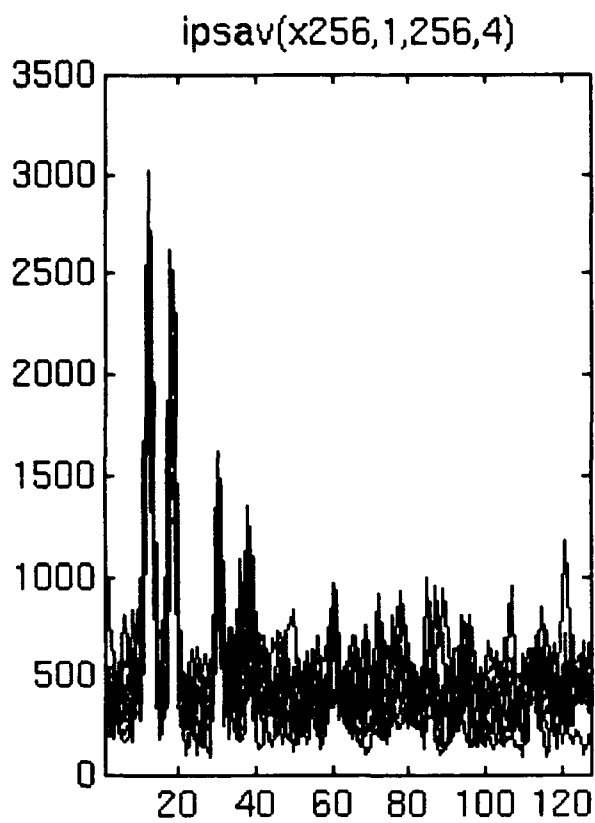


Fig. 2.A

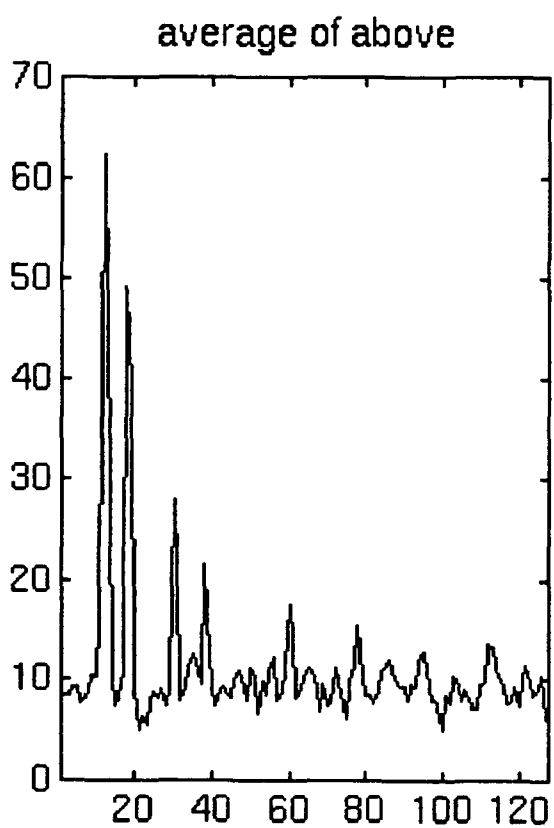
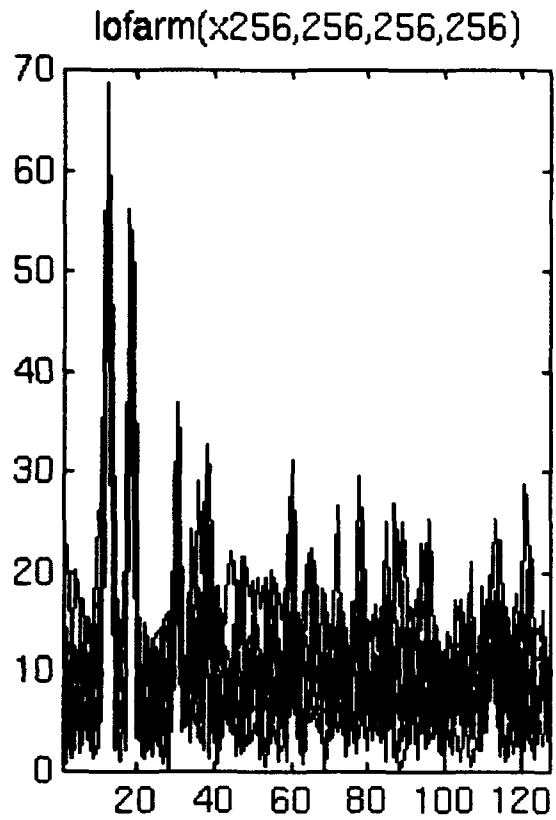


Fig. 2.B

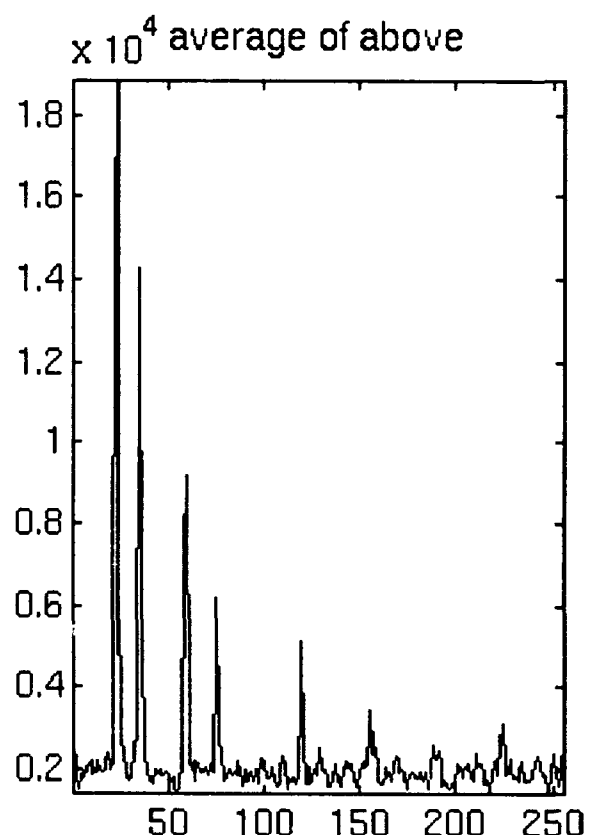
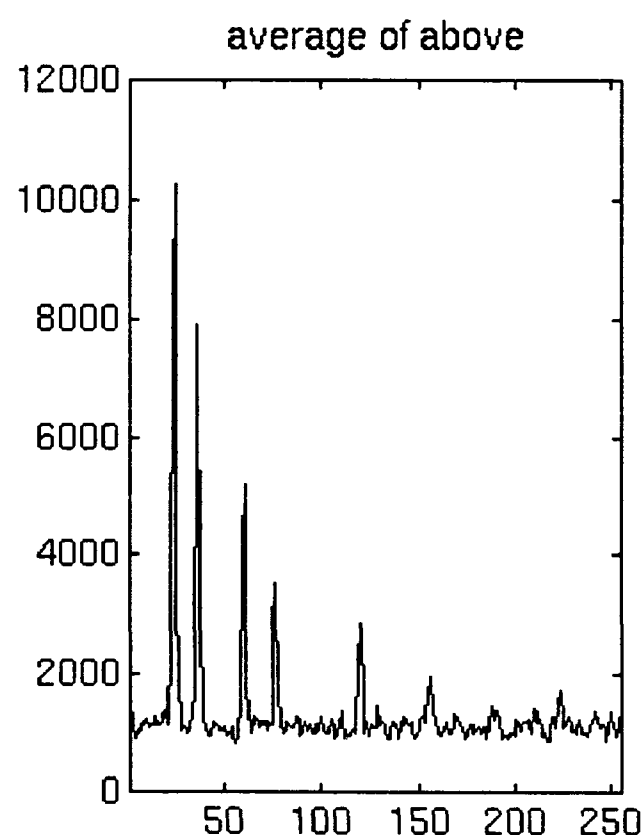
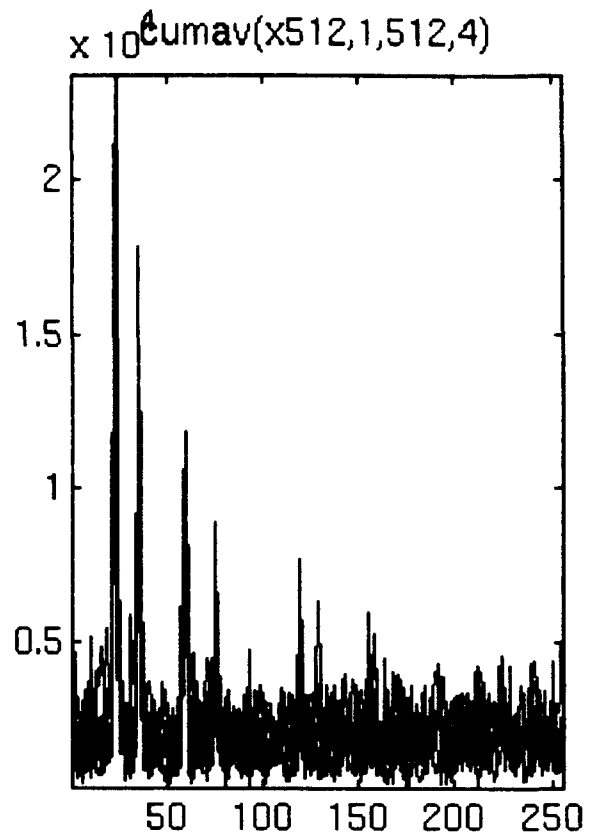
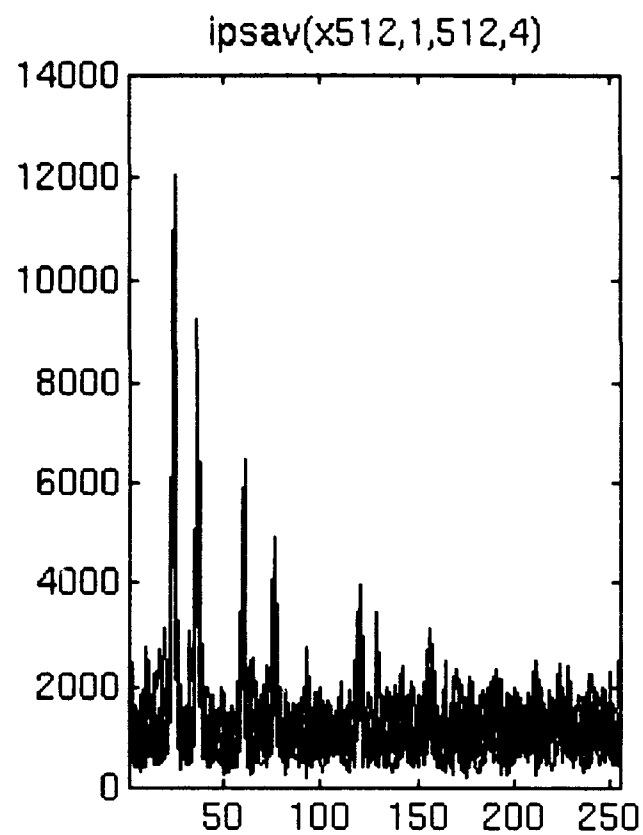
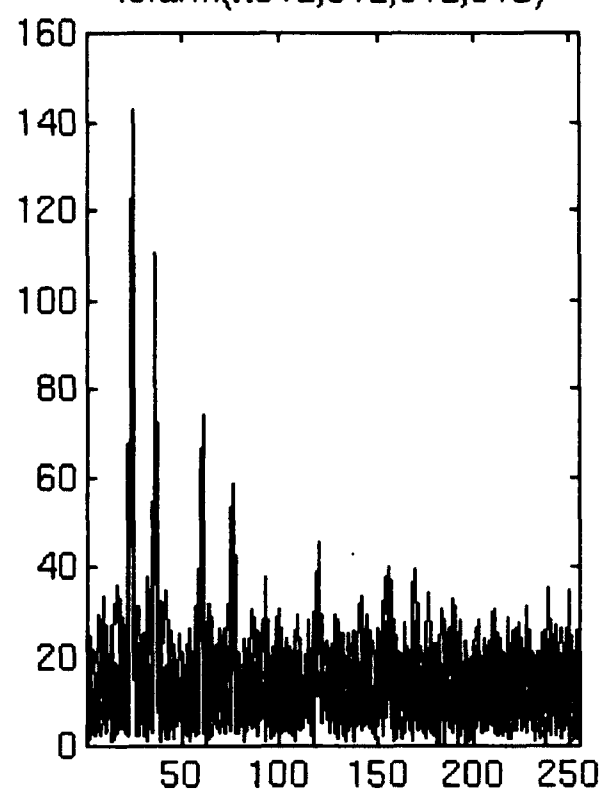


Fig. 3.A

lofarm(x512,512,512,512)



average of above

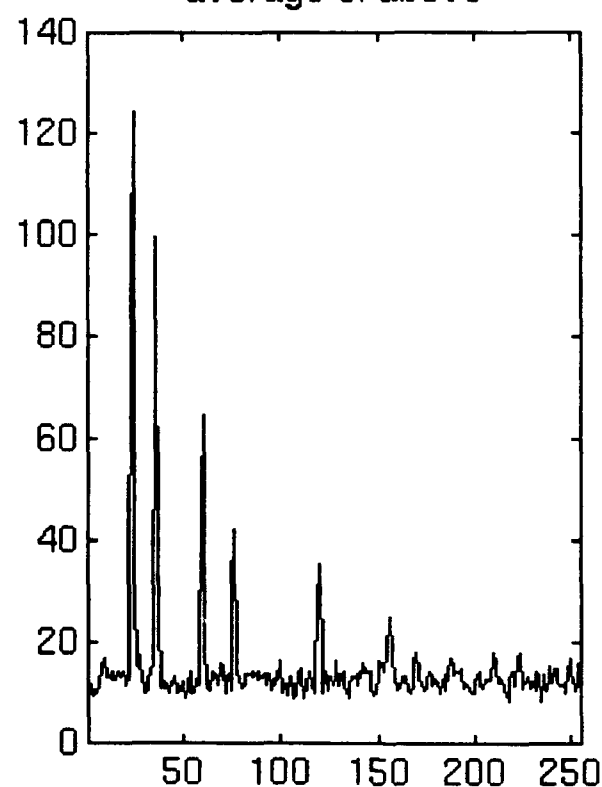


Fig. 3.B

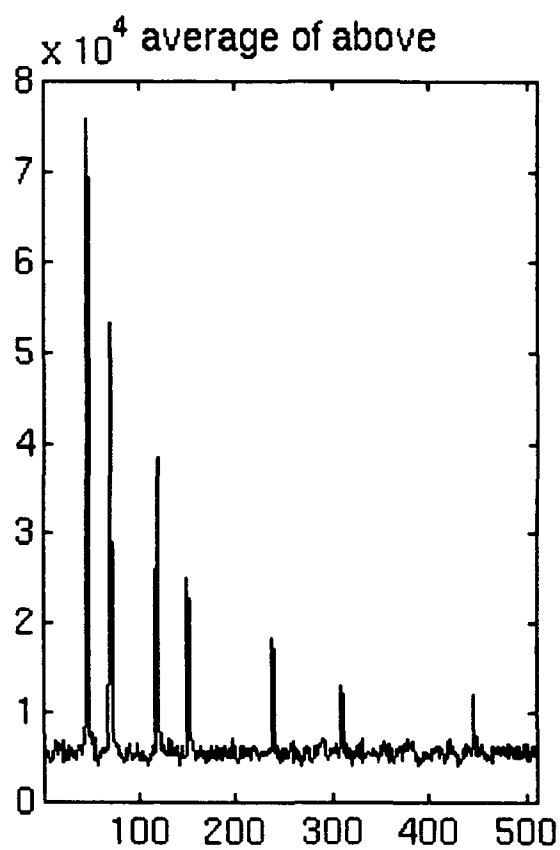
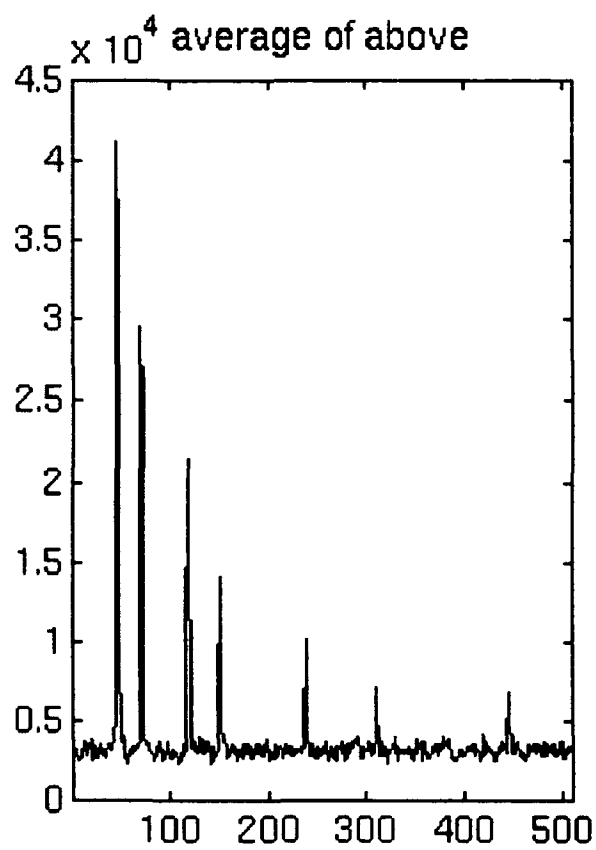
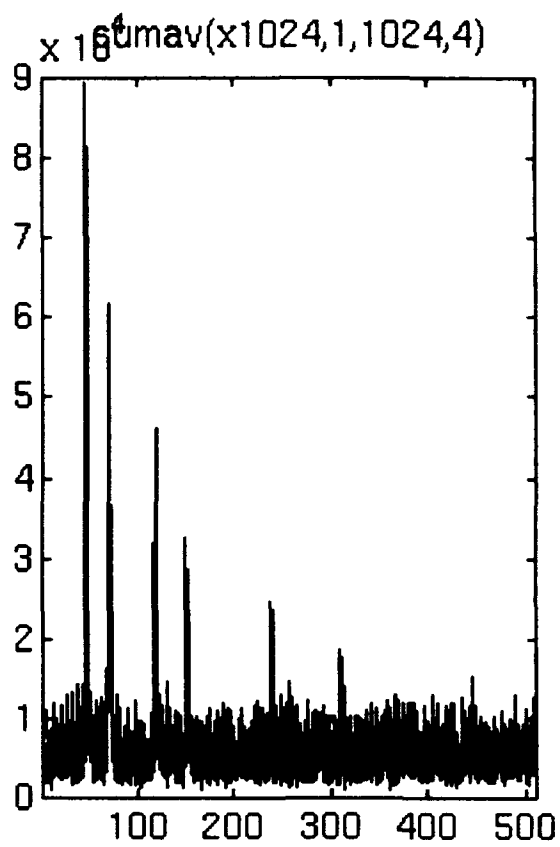
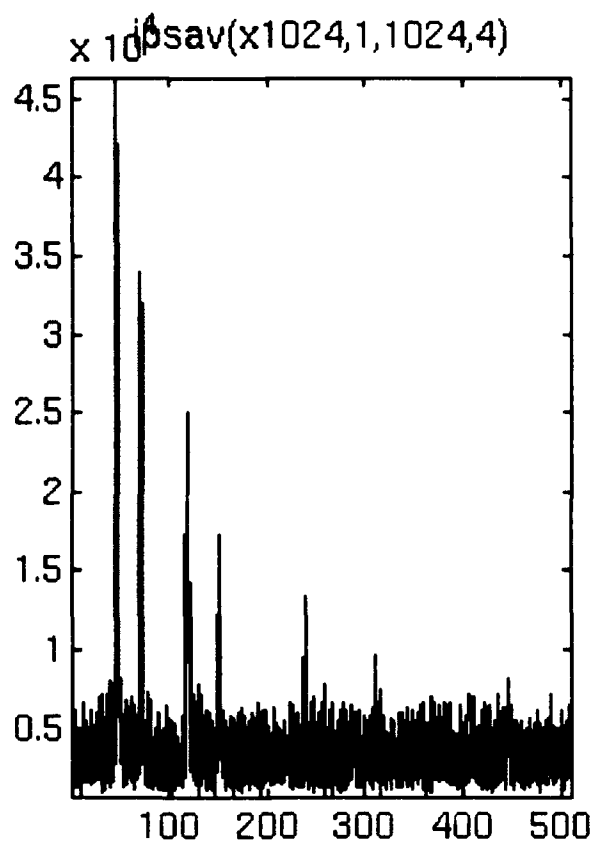


Fig. 4.A

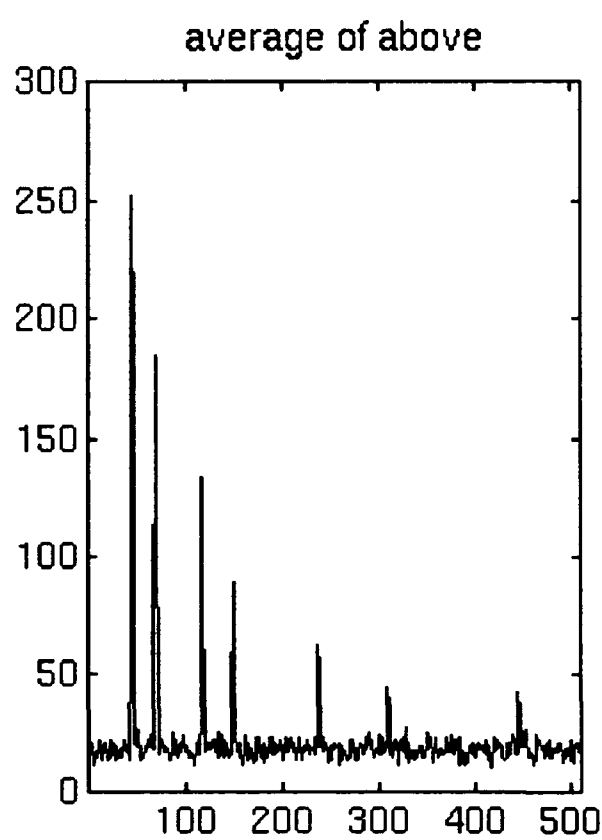
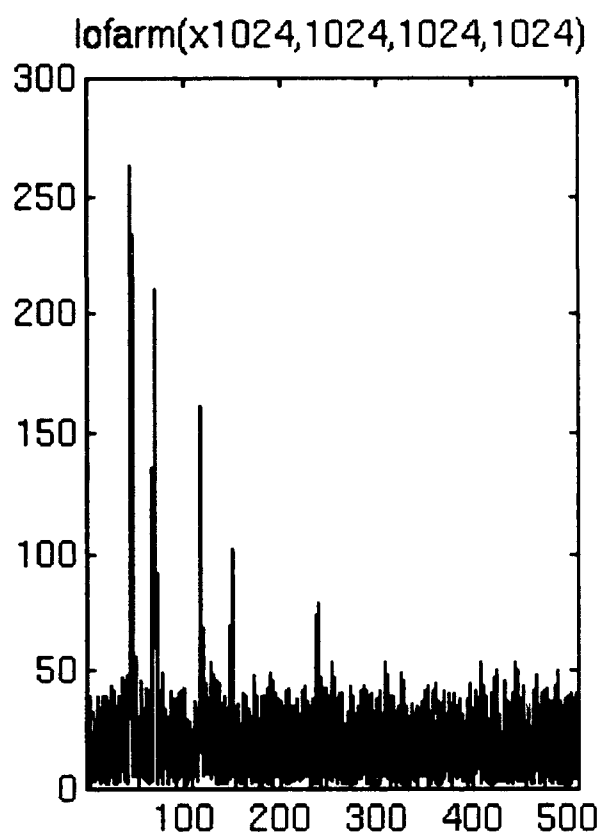


Fig. 4.B

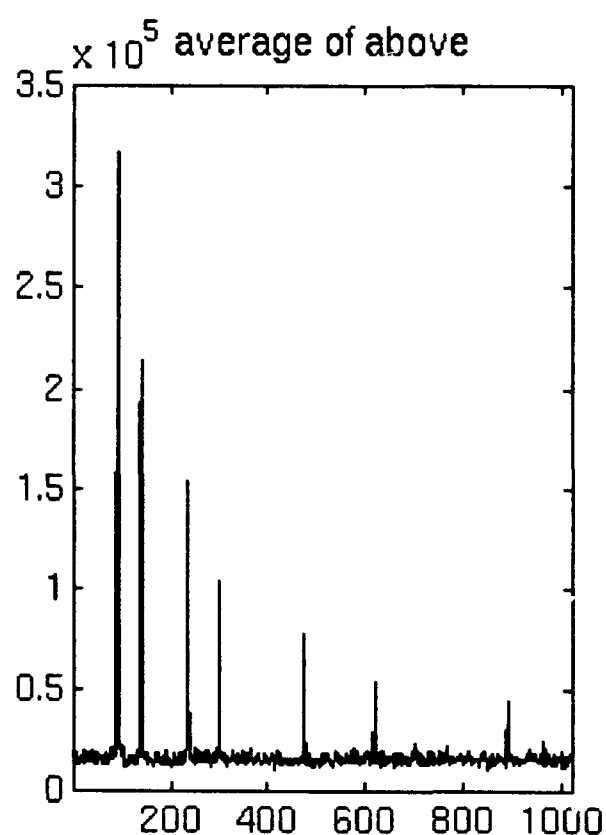
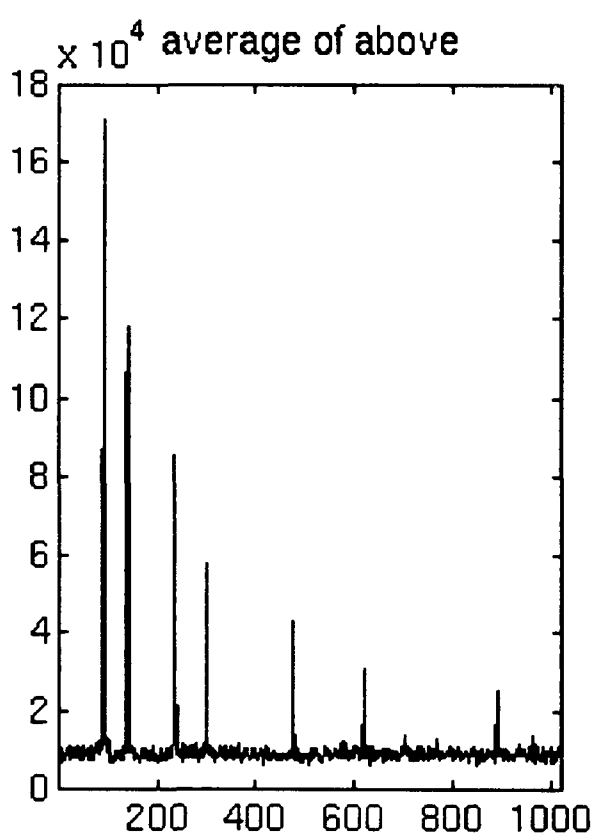
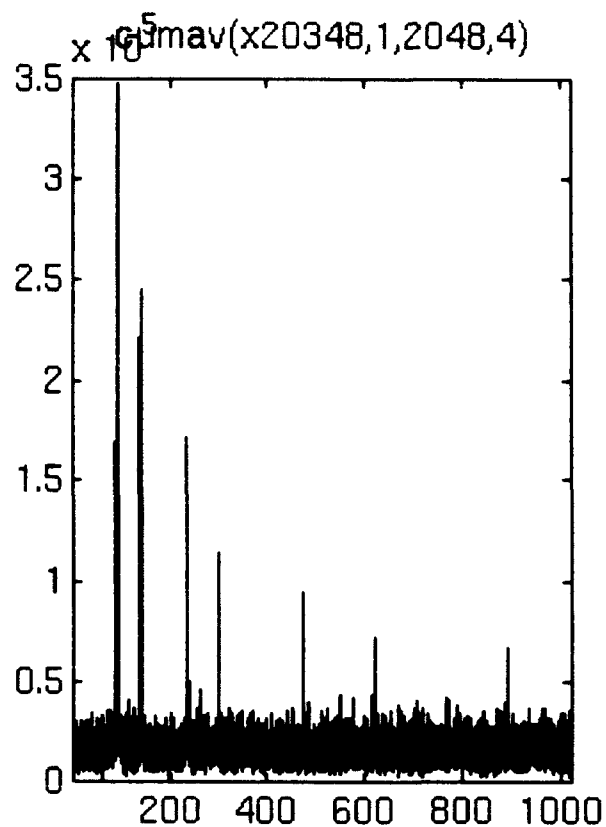
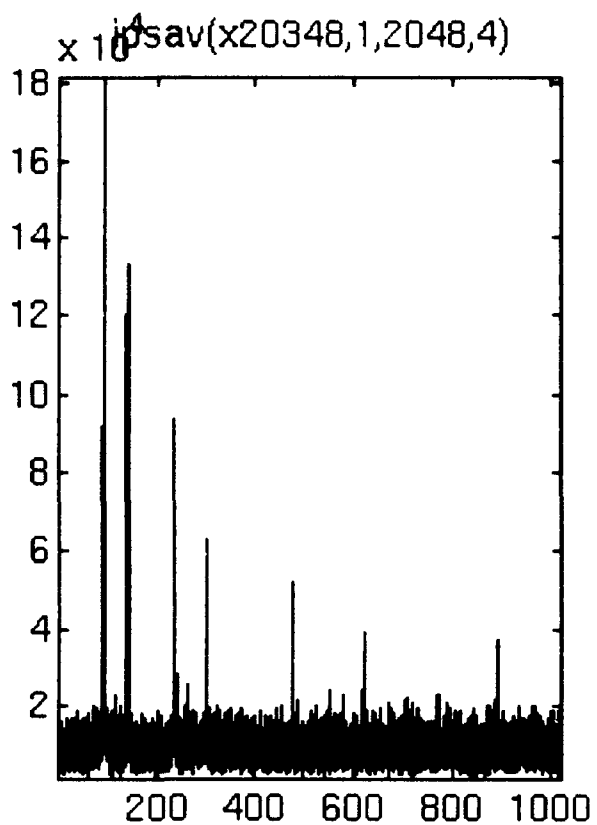


Fig. 5.A

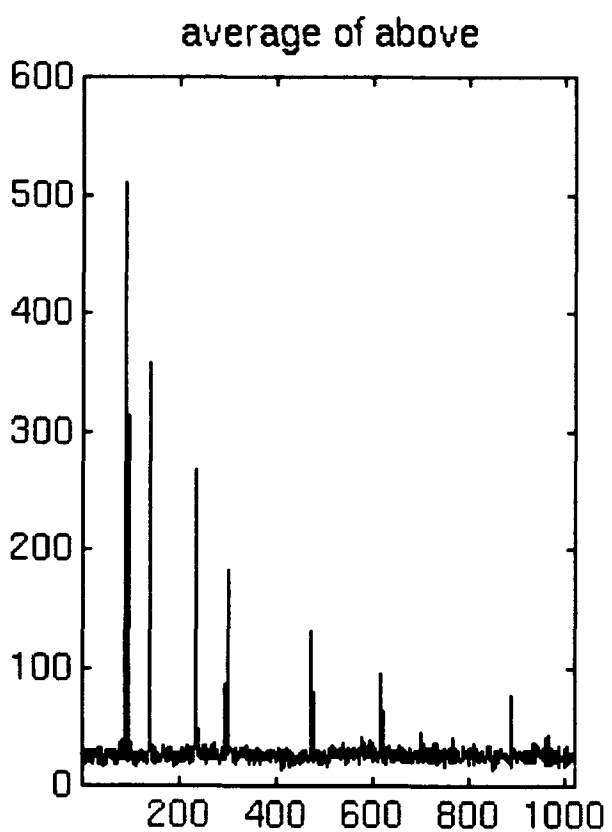
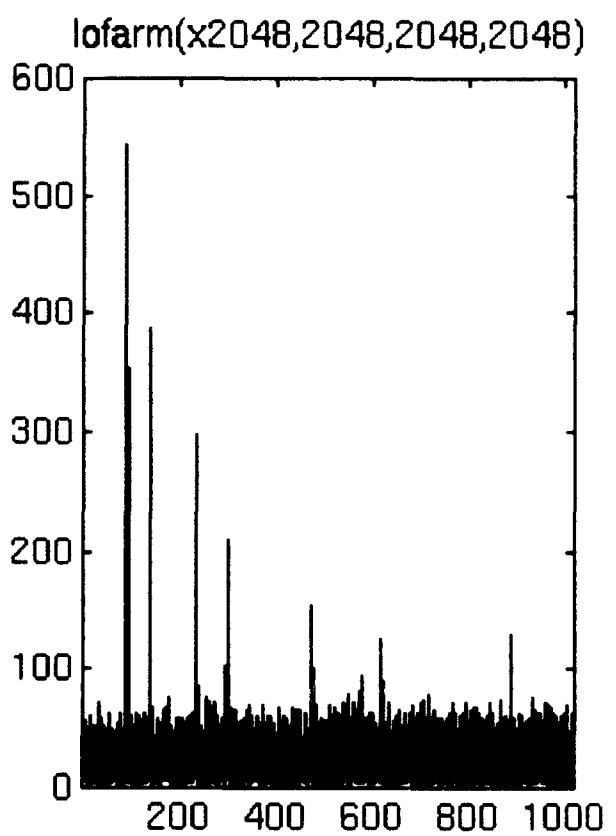


Fig. 5.B

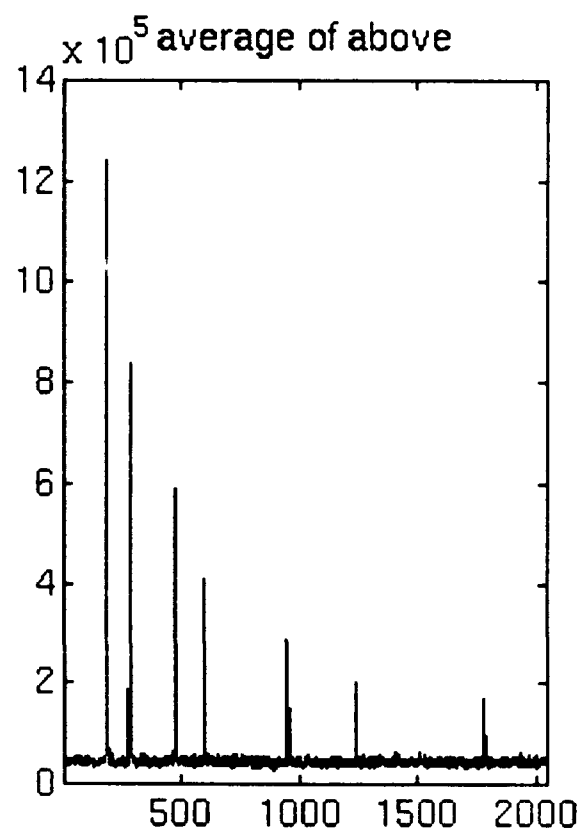
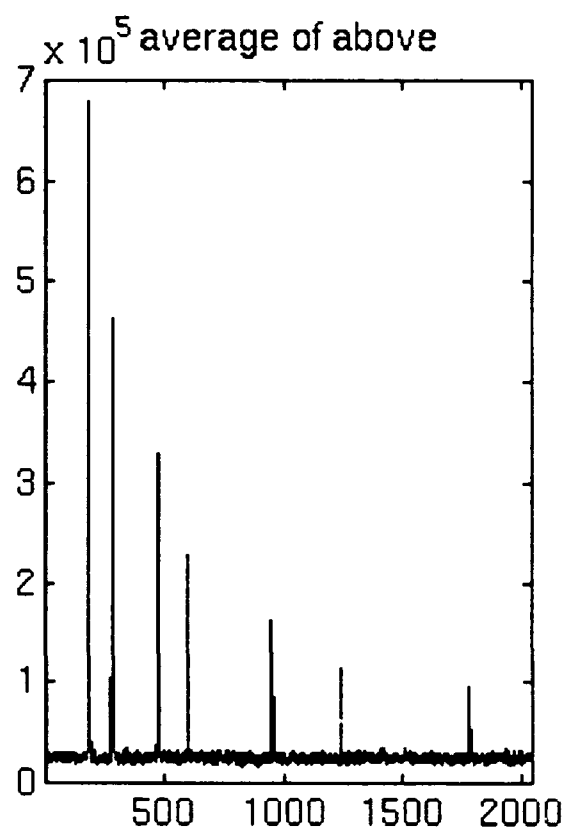
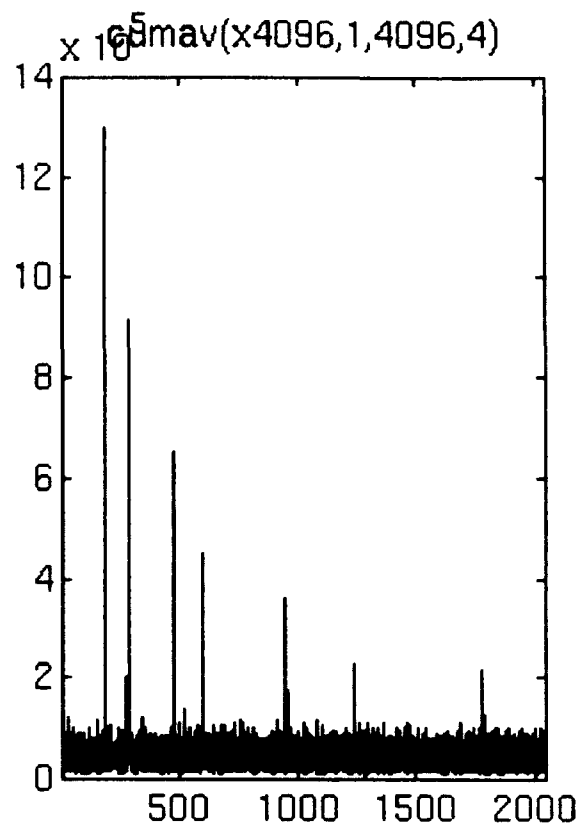
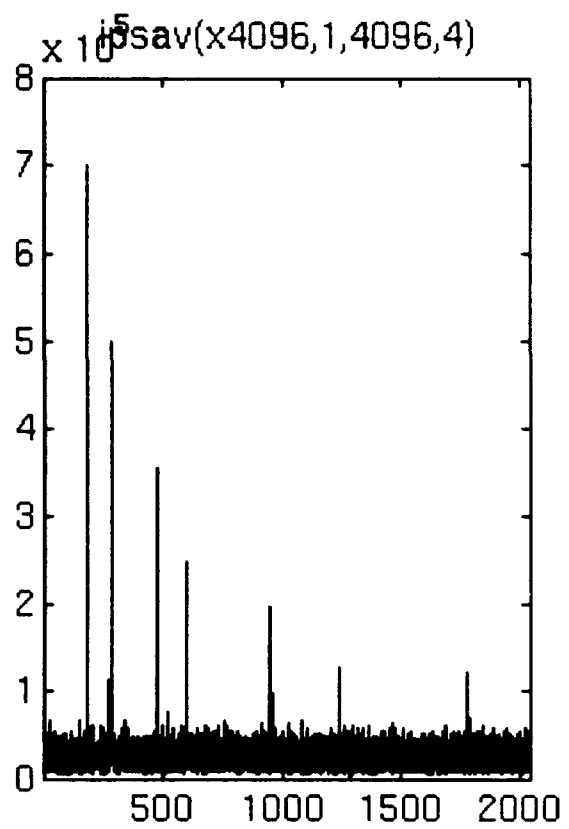
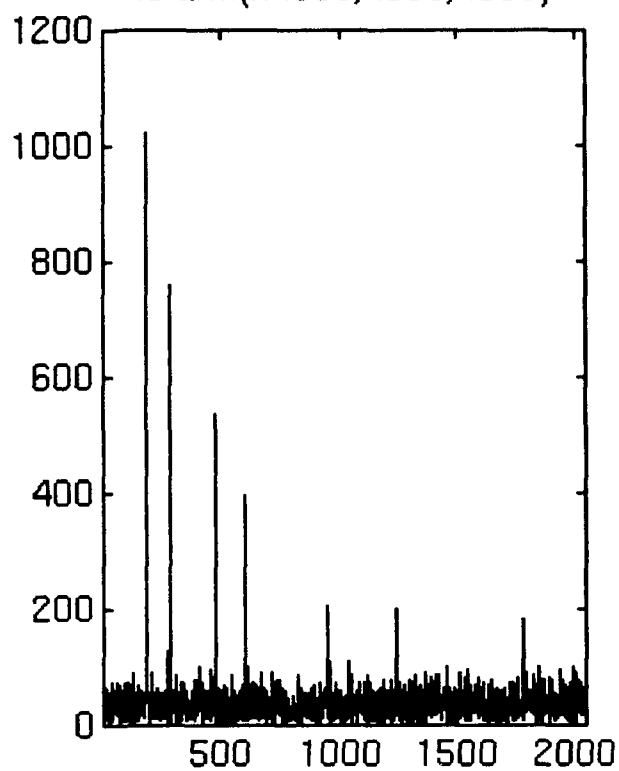


Fig. 6.A

lofarm(x4096,4096,4096)



average of above

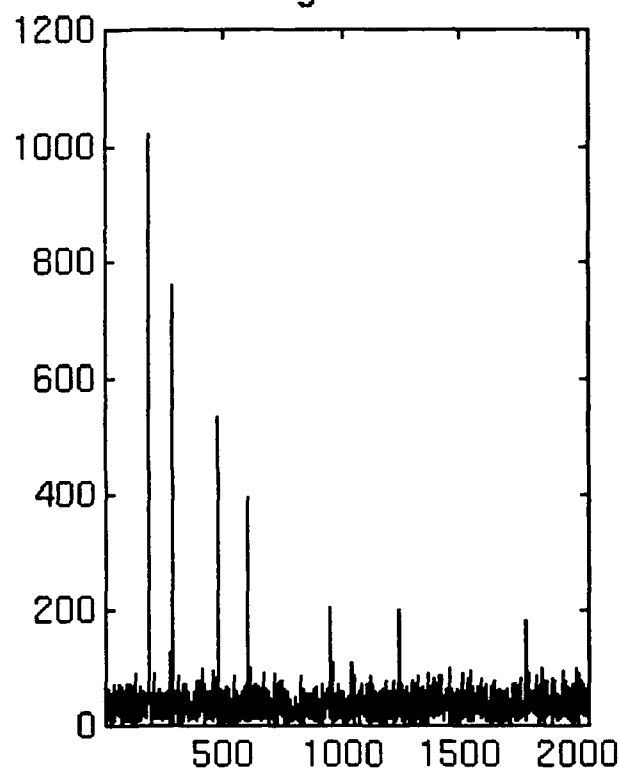


Fig. 6.B

data size 128, proc length 128

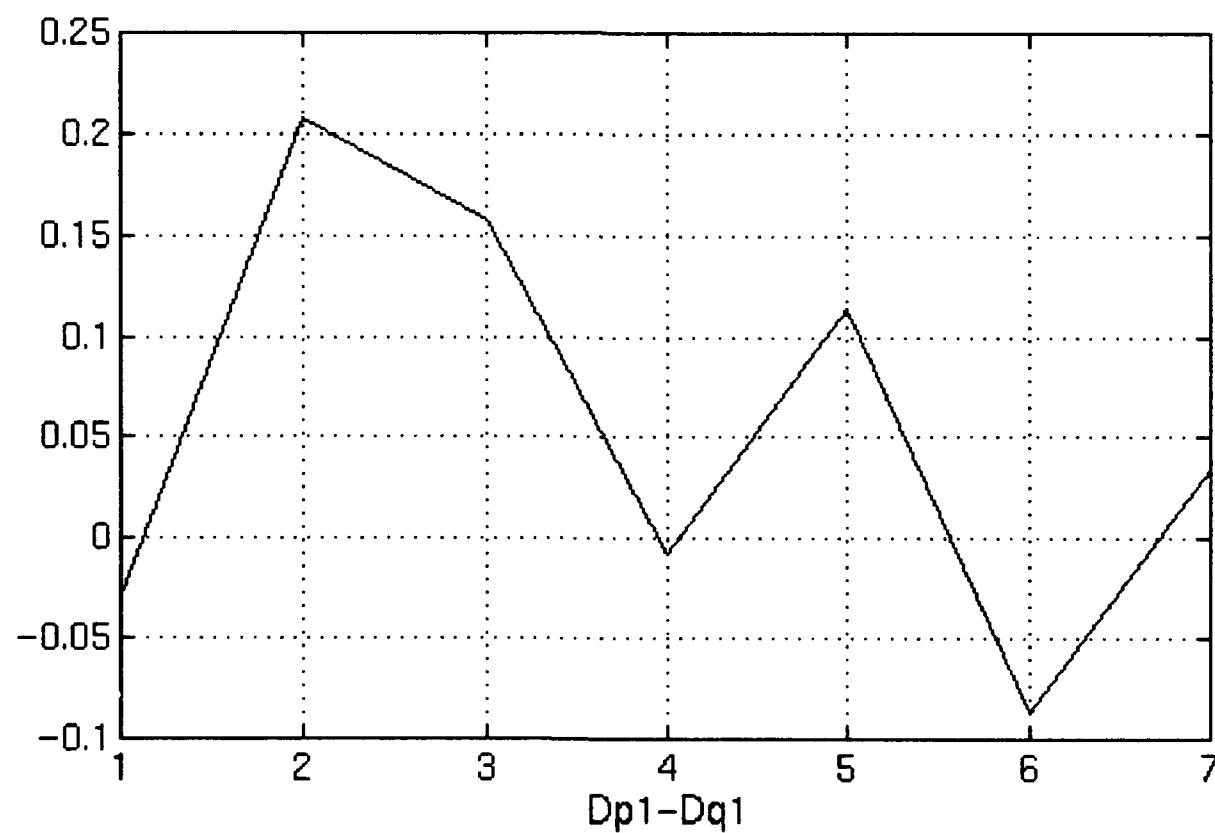
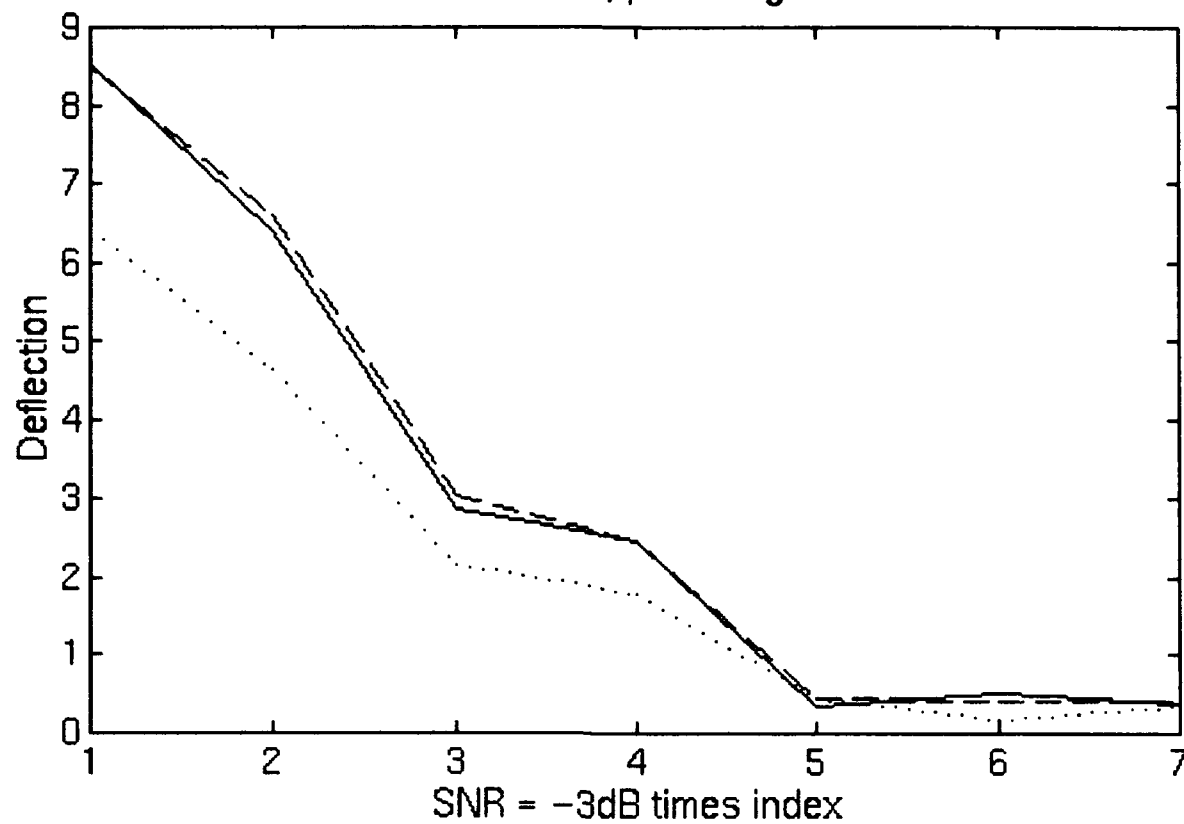


Fig. 7

data size 256, proc length 256

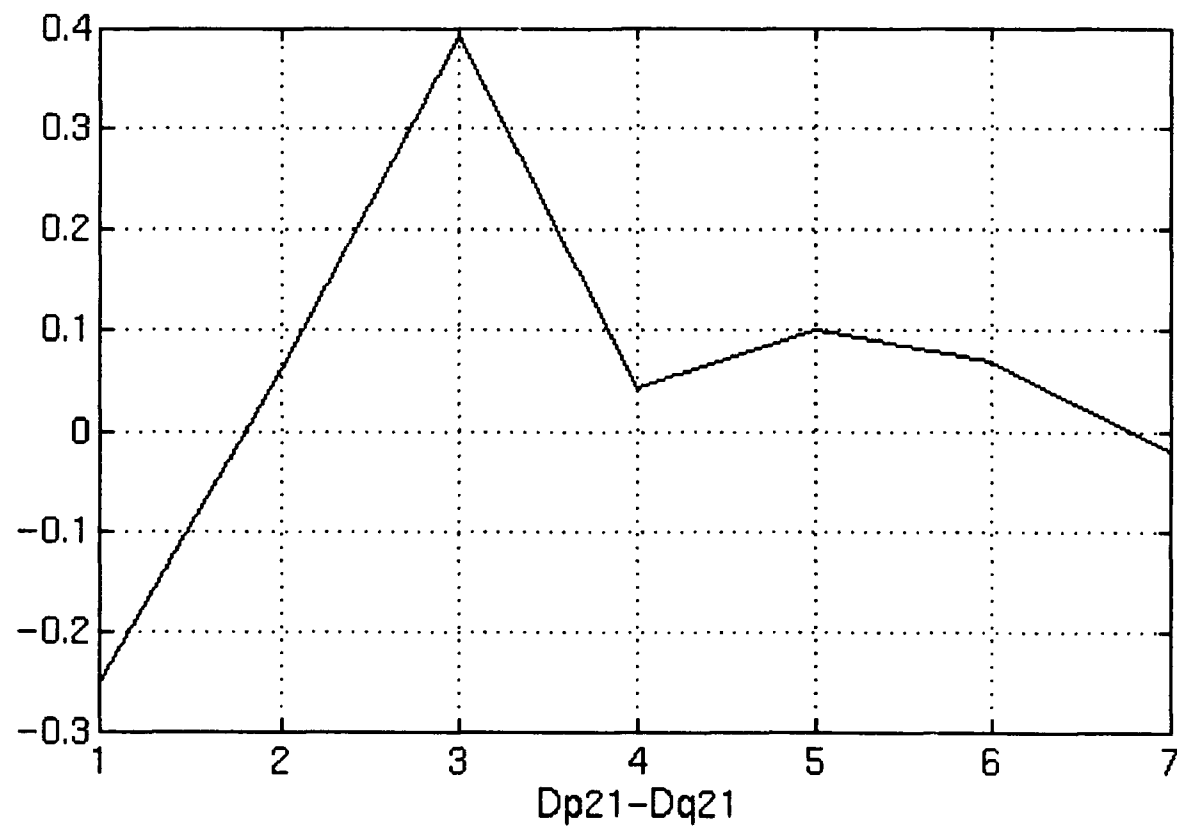
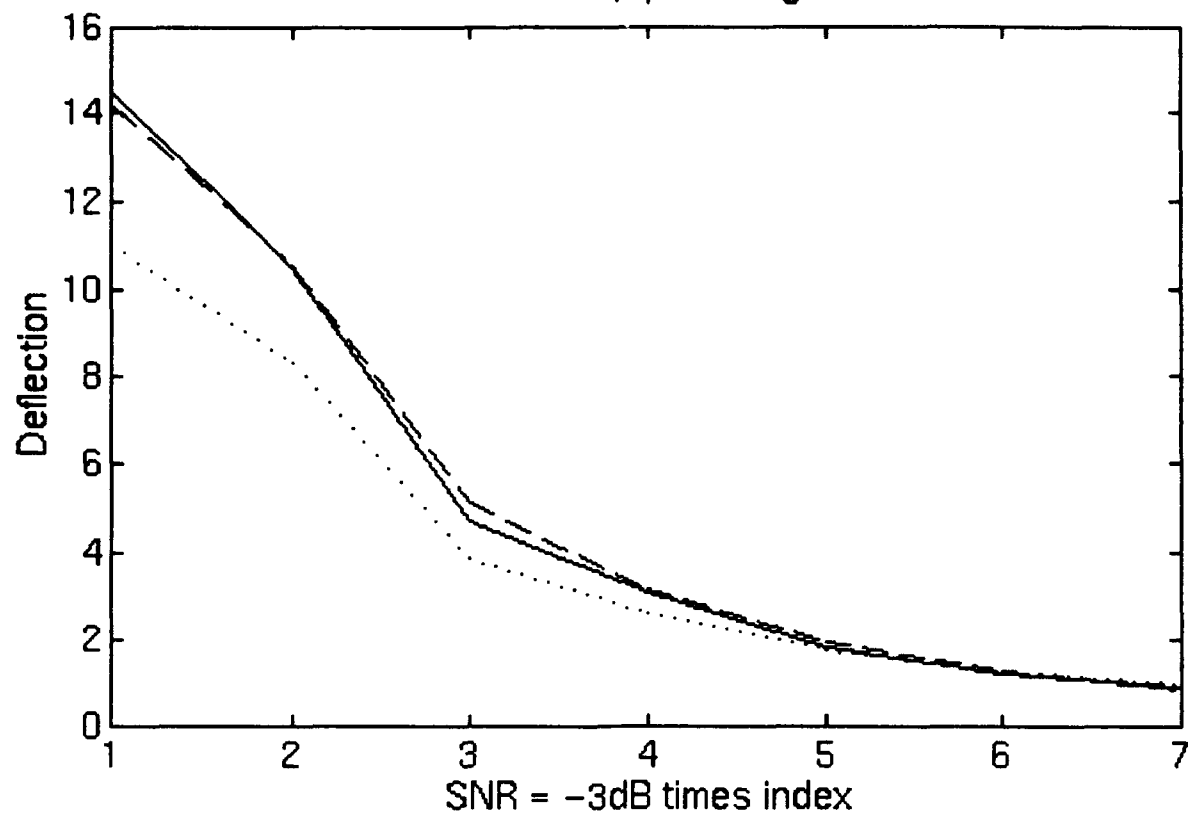


Fig. 8

data size 512, proc length 512

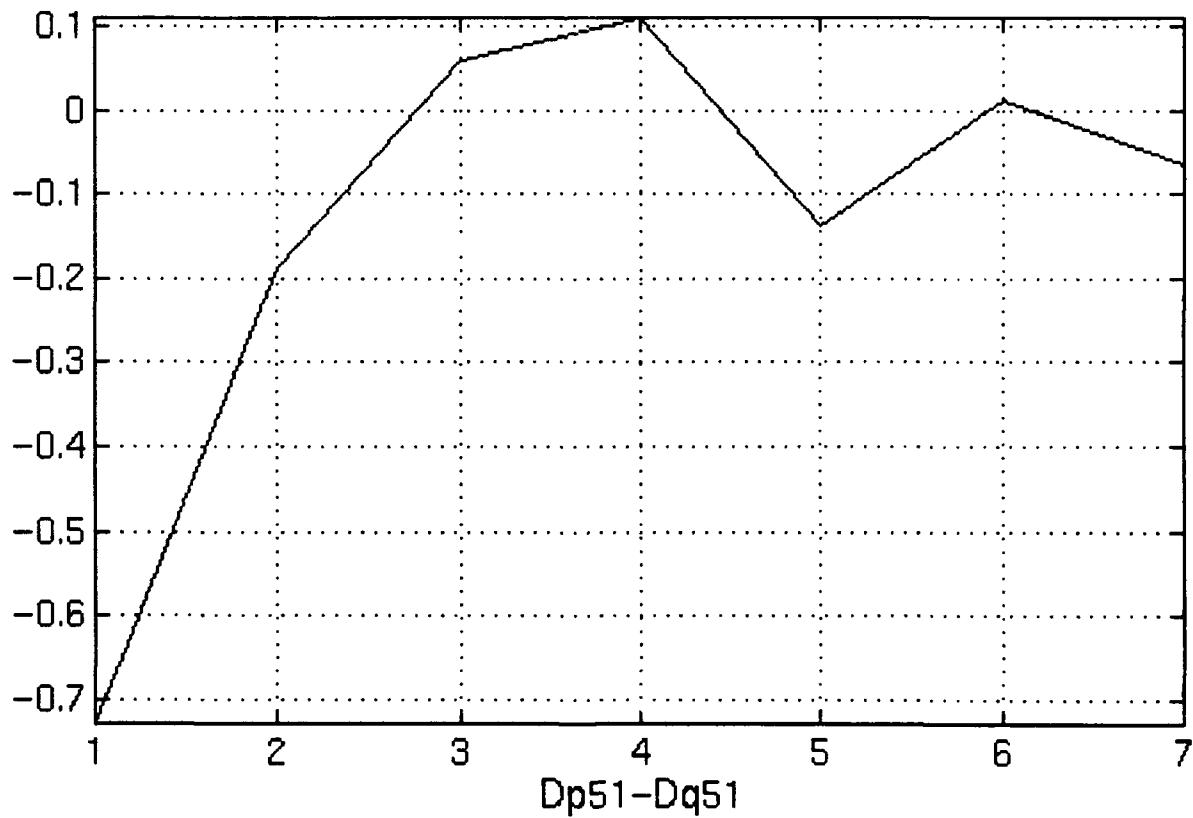
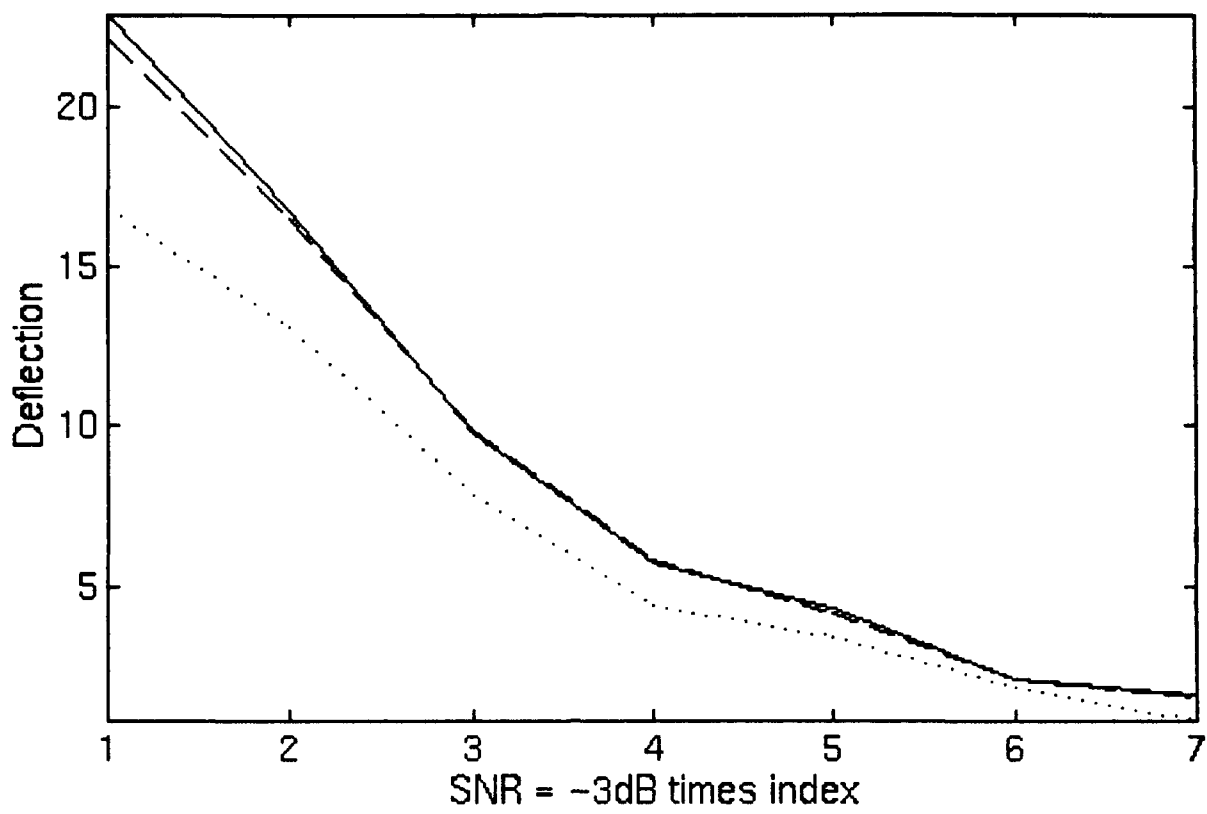


Fig. 9

data size 1024, proc length 1024

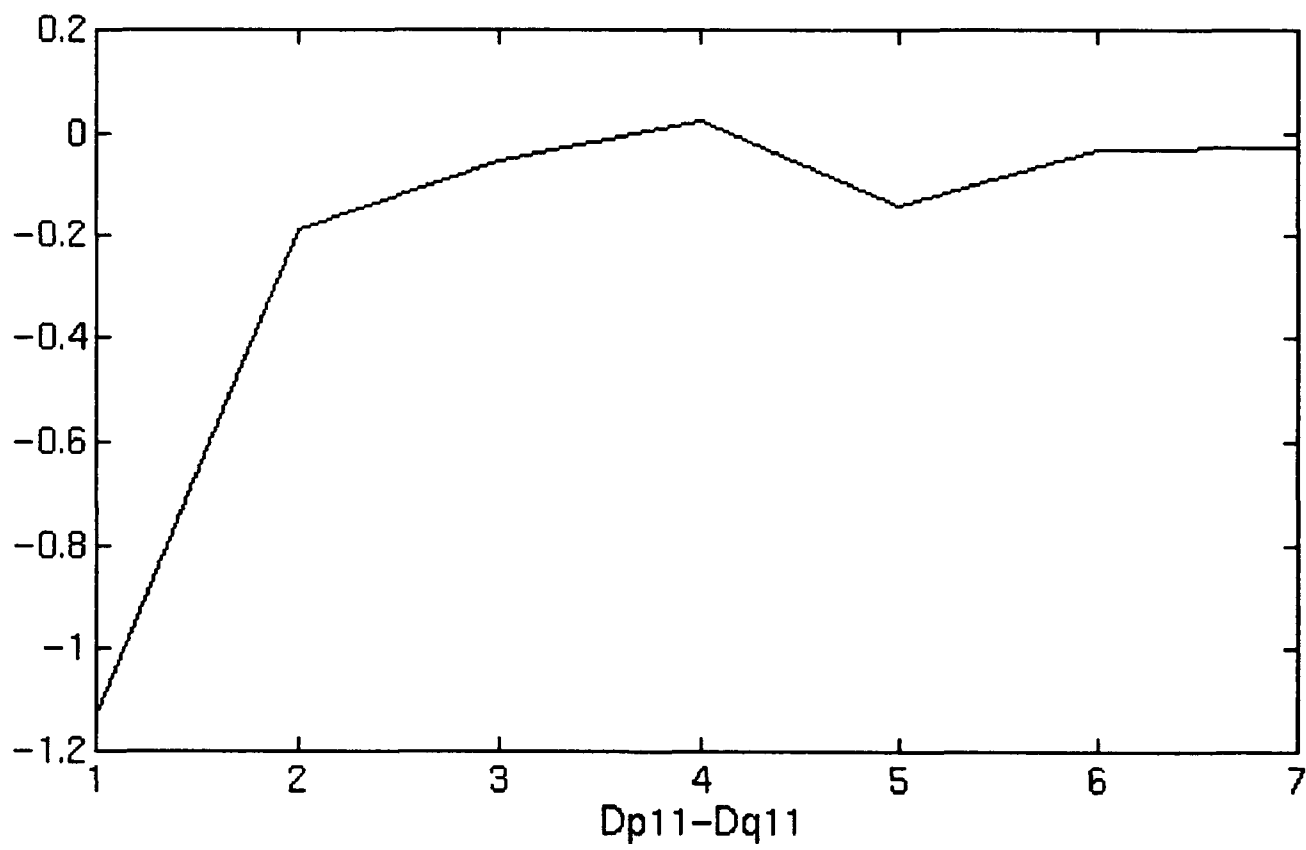
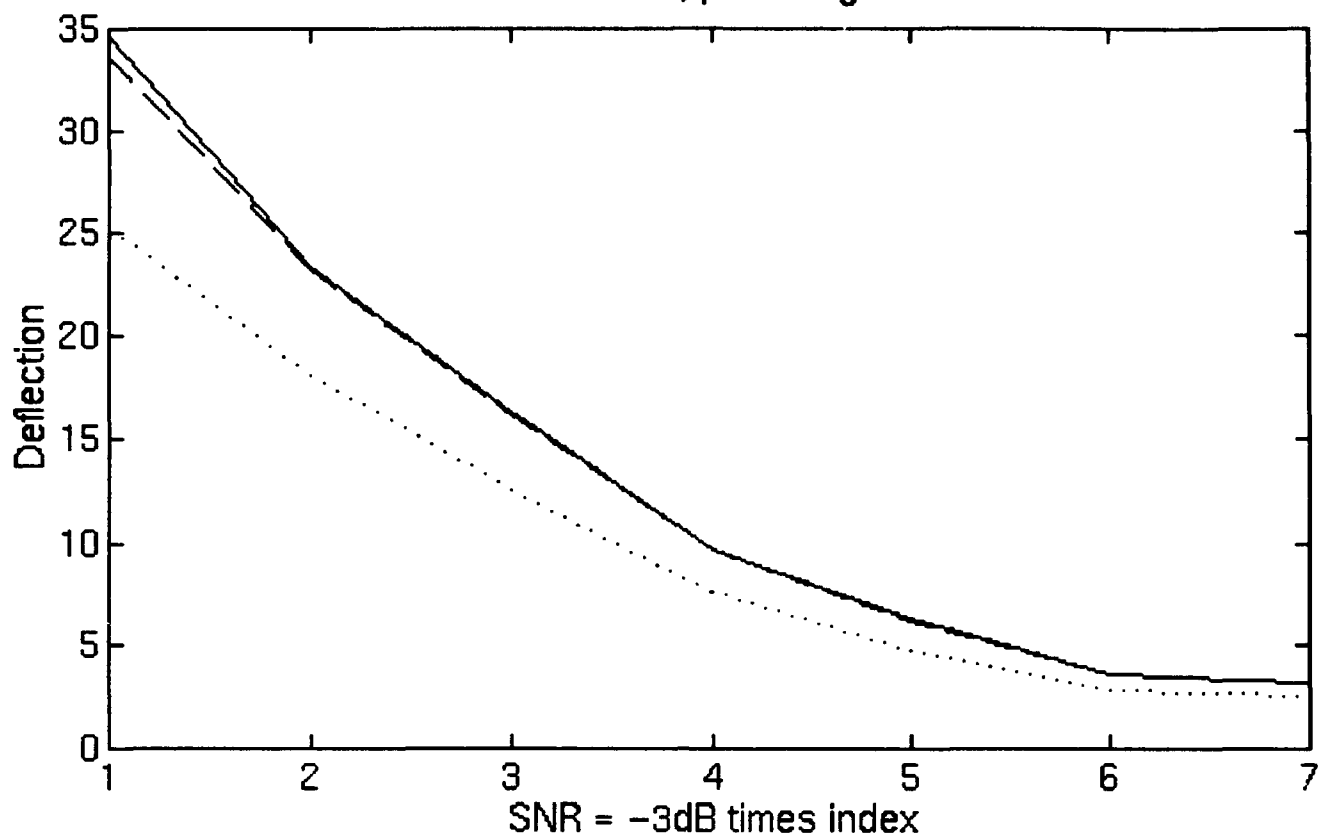


Fig. 10

data size 2048, proc length 2048

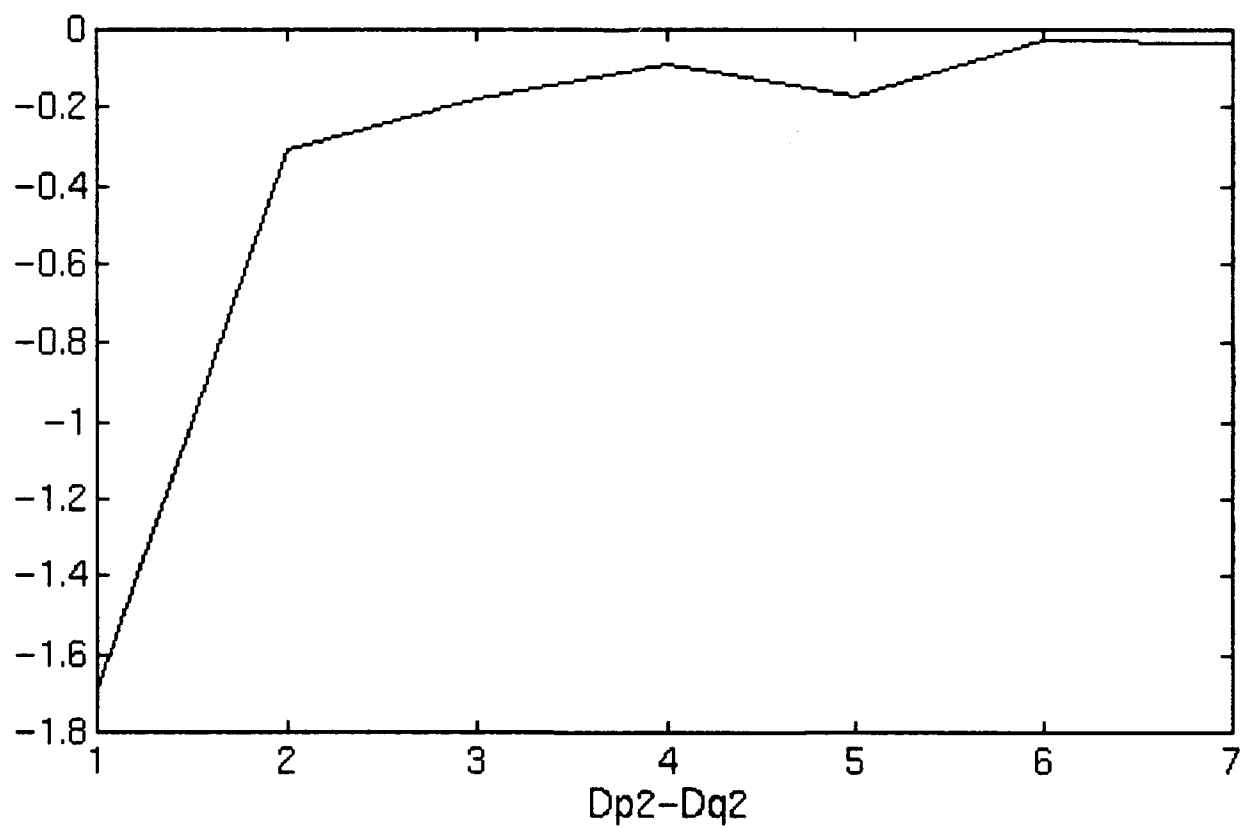
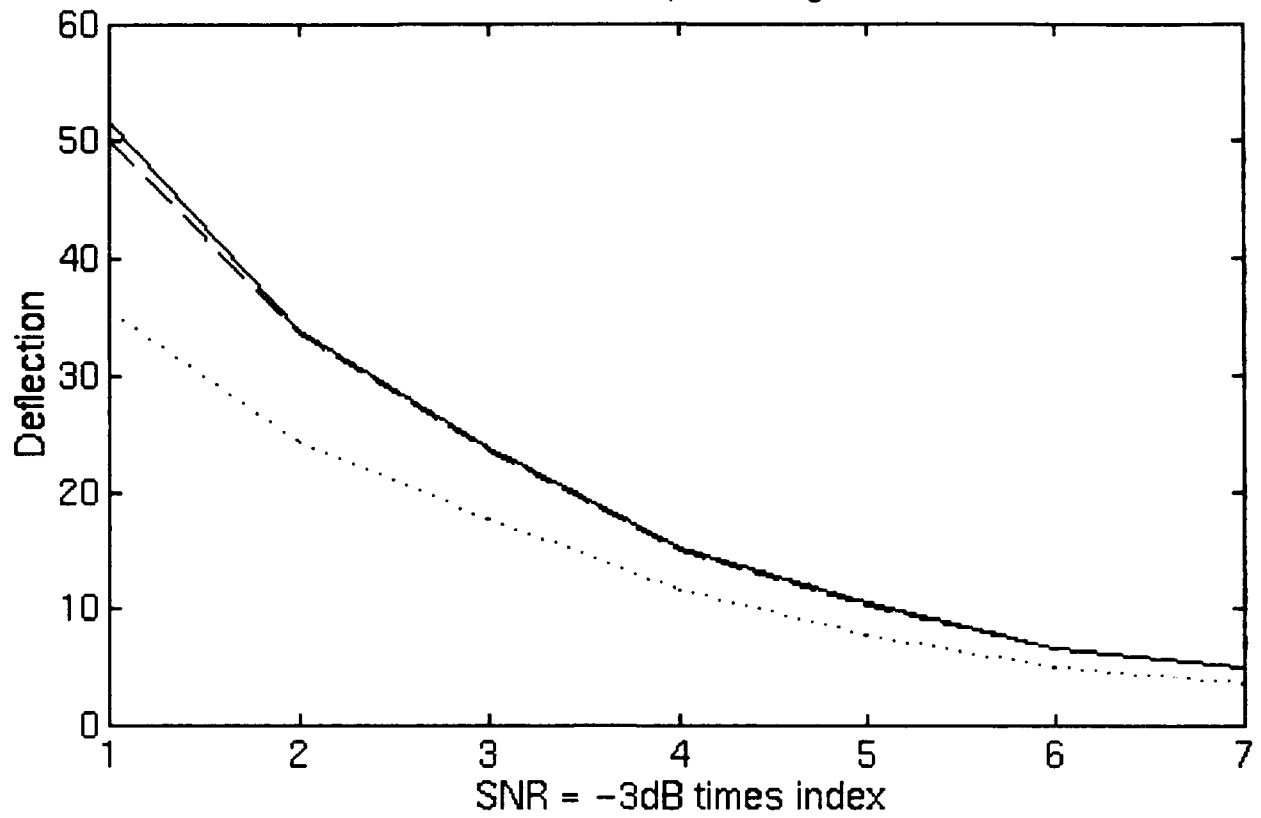
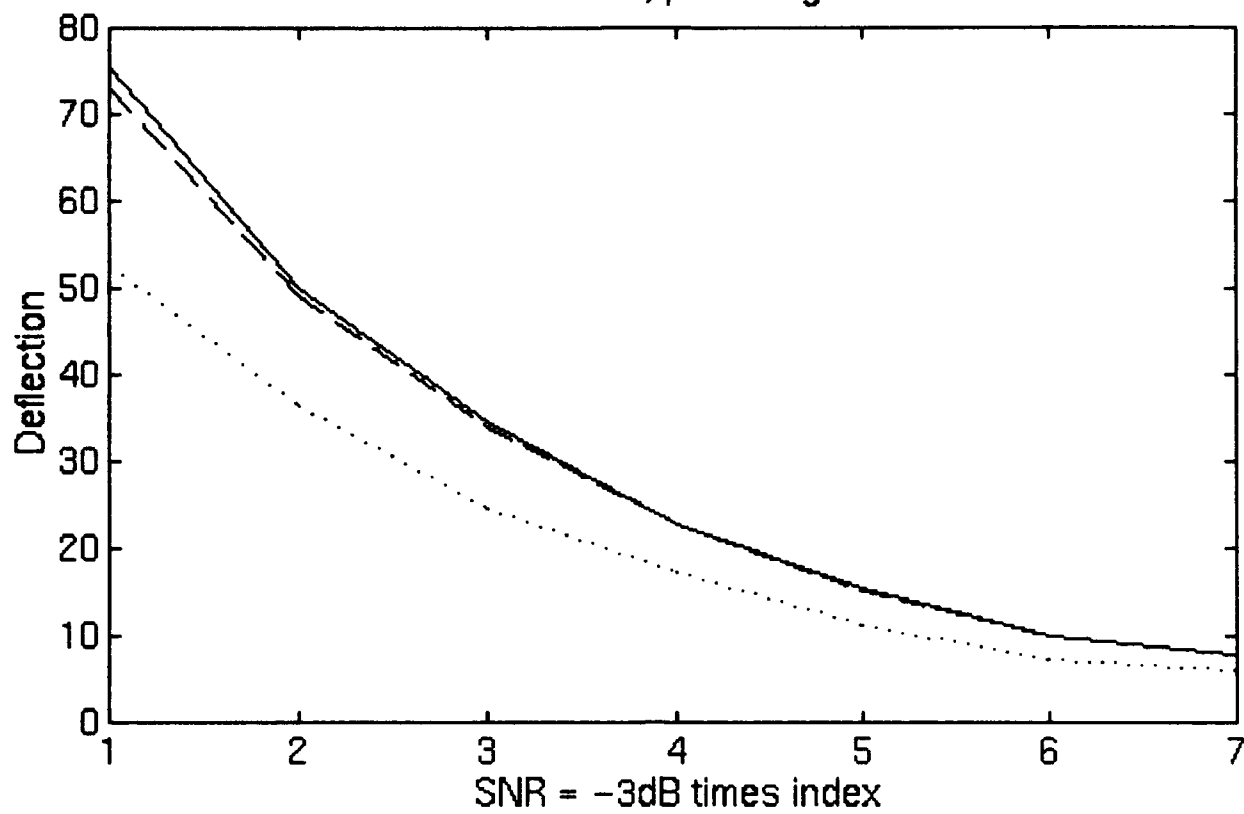


Fig. 11

data size 4096, proc length 4096



SNR = -3dB times index

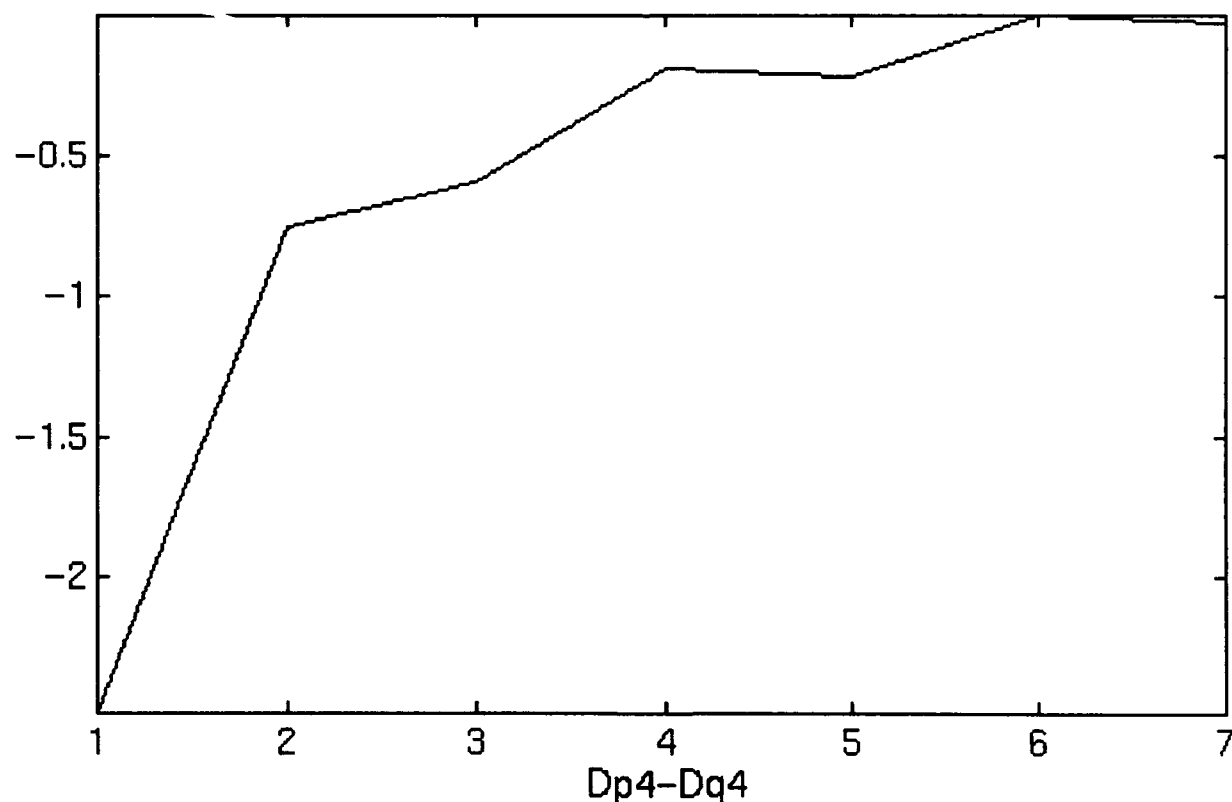


Fig. 12

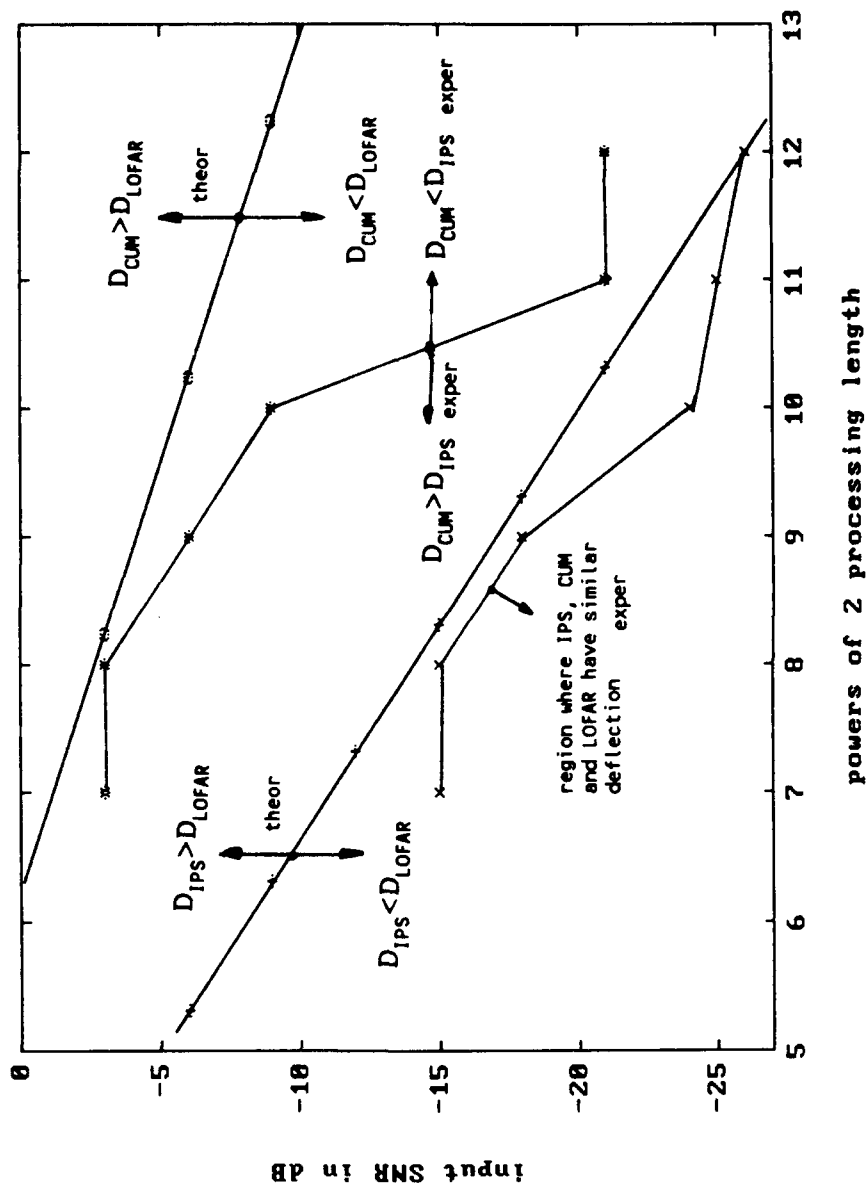


Fig. 13

5. Processing Results using NOSC Data Base.

In this section the data set supplied by NOSC is processed. Figure 14 is a LOFARGRAM of the data set r2A_14 which is 4,128,769 data points long. The time origin for all grams is chosen to be at the top of each figure. Figure 15.A and 15.B are LOFARGRAMS produced at NPS to verify the fidelity of the data transfer from NOSC to NPS. To see representative spectral plots we selected the most interesting segment, that is from time sample 1,024,001 to 1,228,800. This corresponds to the region 508 to 408 along the time (vertical) axis of figure 15.A. Initial processing using IPS and especially CUM showed heavy modulation of the time frequency displays. This is caused by the low frequency spikes observable on figure 14 and 15.A (i.e. strong DC like pulsations (about 5800 sample points apart)). In the top part of figure 16 which displays the time series, used in the experiments, these modulation spikes are clearly seen. To minimize the unwanted amplitude modulation effects on the time frequency plots, the data is soft limited by scaling all values larger than +90 by dividing them by 4 and by scaling all values less than -90 by dividing them by 2. The resulting time series is plotted in the bottom part of figure 16.

The contour plots of the remainder of this section show now little amplitude modulation allowing the approximation to gray scale via contour plots to work. On a color monitor, with a sufficient number of color levels of quantization, the modulation may not be bothersome. Figure 17 displays 49 traces (along the y-axis) which corresponds to 49 individual estimates of the spectral density. Closer examination reveals some details on the IPS plot

not so easily seen on the lower LOFARGRAM plot. In particular we refer to 3 areas:

- 1) tick mark 38-48 (vertical axis) about bin 700 (horizontal axis),
- 2) tick mark 1-33 (vertical axis) about bin 850 (horizontal axis), and
- 3) tick mark 1-20 (vertical axis) about bin 1300 (horizontal axis).

A word of caution however when using the simple minded contour (MATLAB) plots: peaks of identical height but of different width will appear differently. In appendix A the effects of choosing different contour levels is illustrated. However for all plots the best choice of level was manually selected by examining several plots differing in the number of levels selected and then retaining the one with the best features.

Figure 18.A and 18.B are displays of IPS, CUM and LOFAR with the lines created 512 time data points apart. Figure 18.A (as well as 19.A and 20.A) displays spectral location 51 through 1500 while figure 18.B (as well as 19.B and 20.B) displays spectral location 351 through 1500. This allows better interpretation of the different spectral regions.

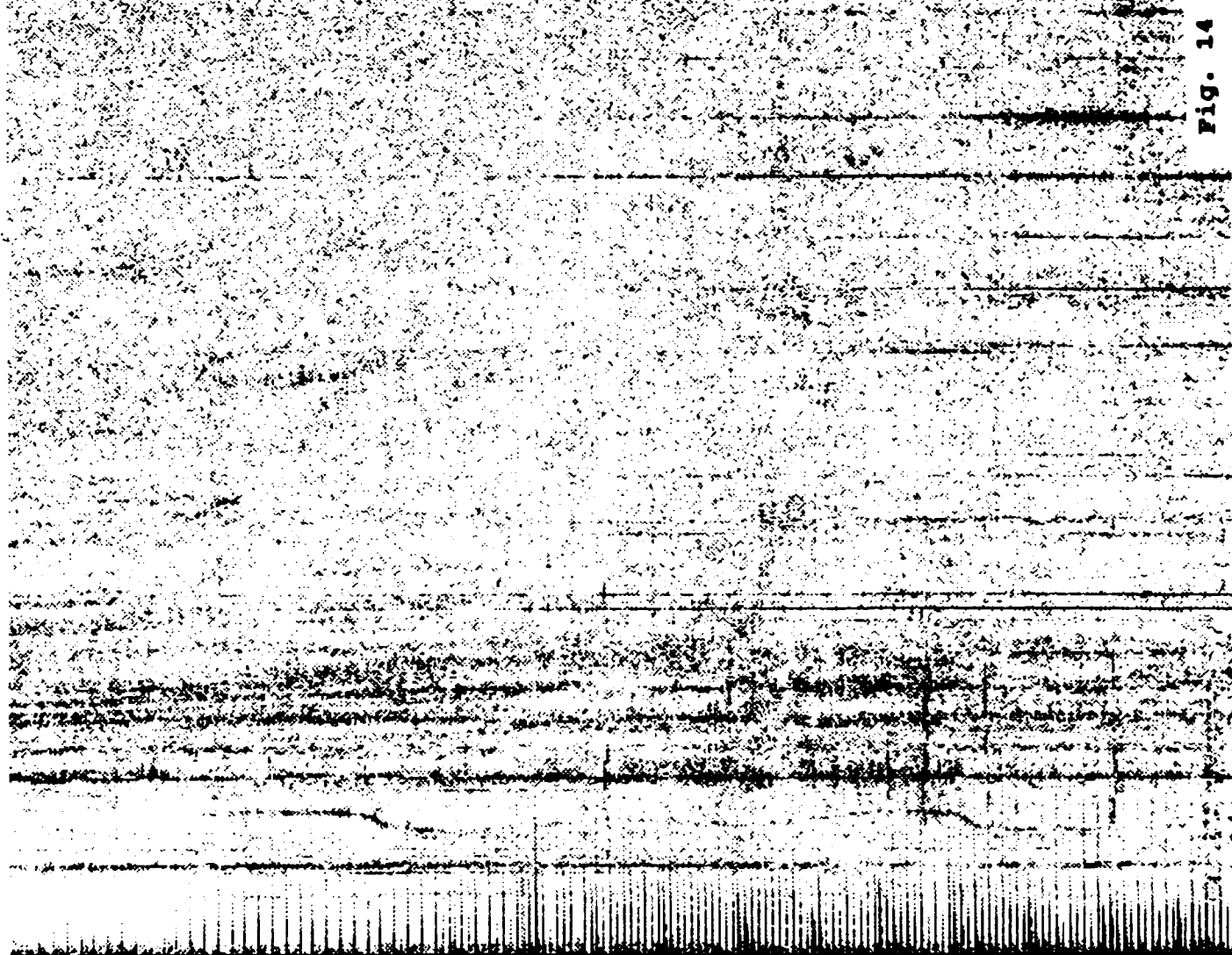
Figures 18, 19 and 20 have the same processing parameters, they differ in the number of spectral lines computed. Figure 18 uses a shift of 512 (i.e. 8:1 overlap) resulting in 390 lines, figure 19 uses a shift of 1024 (i.e. 4:1 overlap) resulting in 197 lines, while figure 20 uses a shift of 4096 (i.e. no overlap) resulting in 49 spectral lines.

Figure 21 illustrates performance as the processing length is increased to 8102 (shift 8192, no overlap) providing 25 spectral lines (bin 51 through 3300 are displayed).

6. Conclusion and recommendation.

As illustrated in section 3 and 4 processing gain can be obtained for IPS and/or CUM relative to the LOFAR processing technique. This is a function of signal and processing parameters. It may allow glimpses of targets which otherwise maybe hidden. However, the processing gain when achievable is bought at the increase in processing cost. IPS and CUM are actually tools designed more for transient type signals but as shown can be used to obtain gain on stable narrow band signals. Simplified processing was not attempted but deserve future examination. The analysis in section 3 is done totally disregarding lag and data windows which typically are used. Future analysis should address the influence of the window function on processing. Extensions to extract phase information is not attempted but should be pursued.

Fig. 14



nosc 1-st half, 0 on top

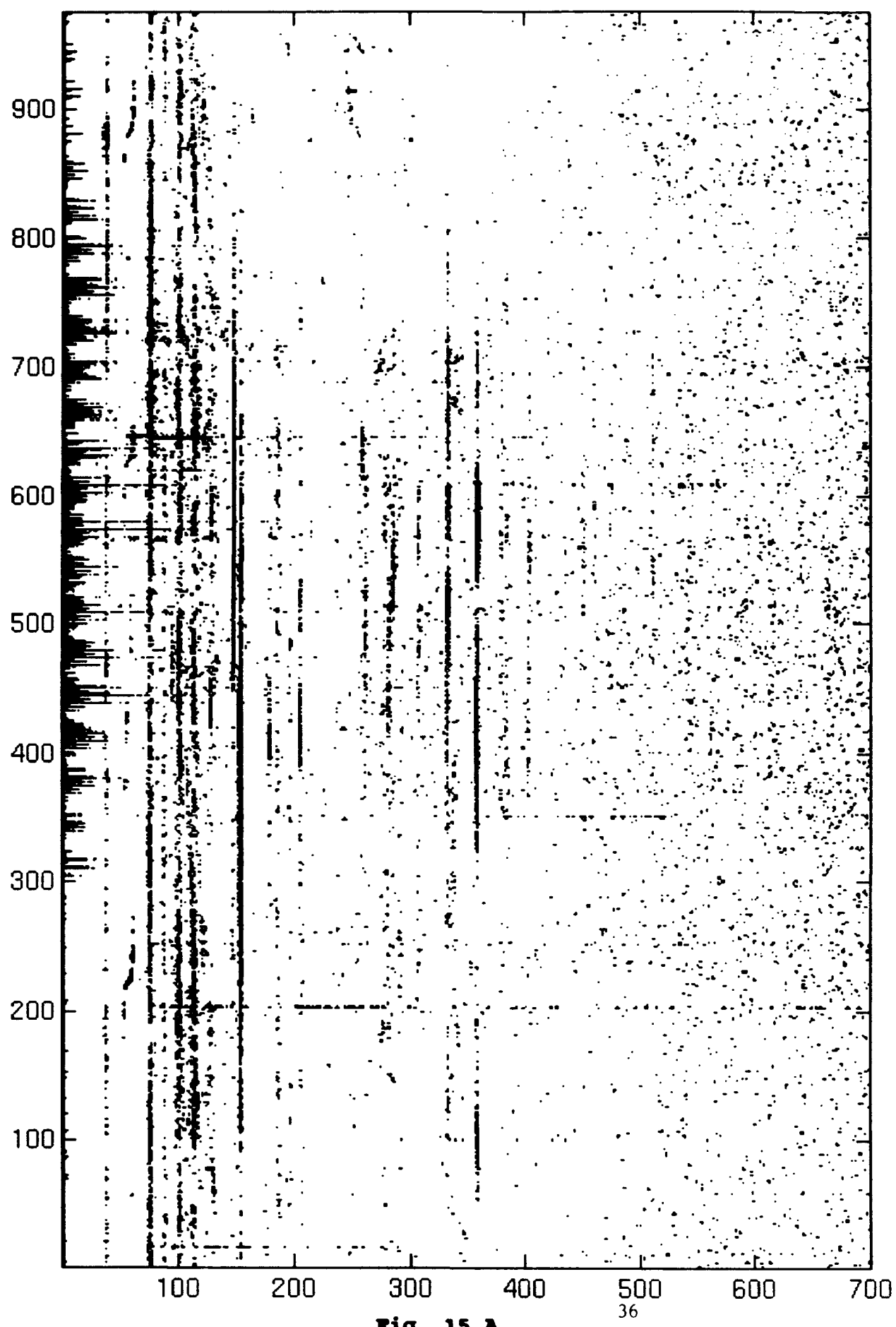


Fig. 15.A

nosc 2-nd half , 0 on top

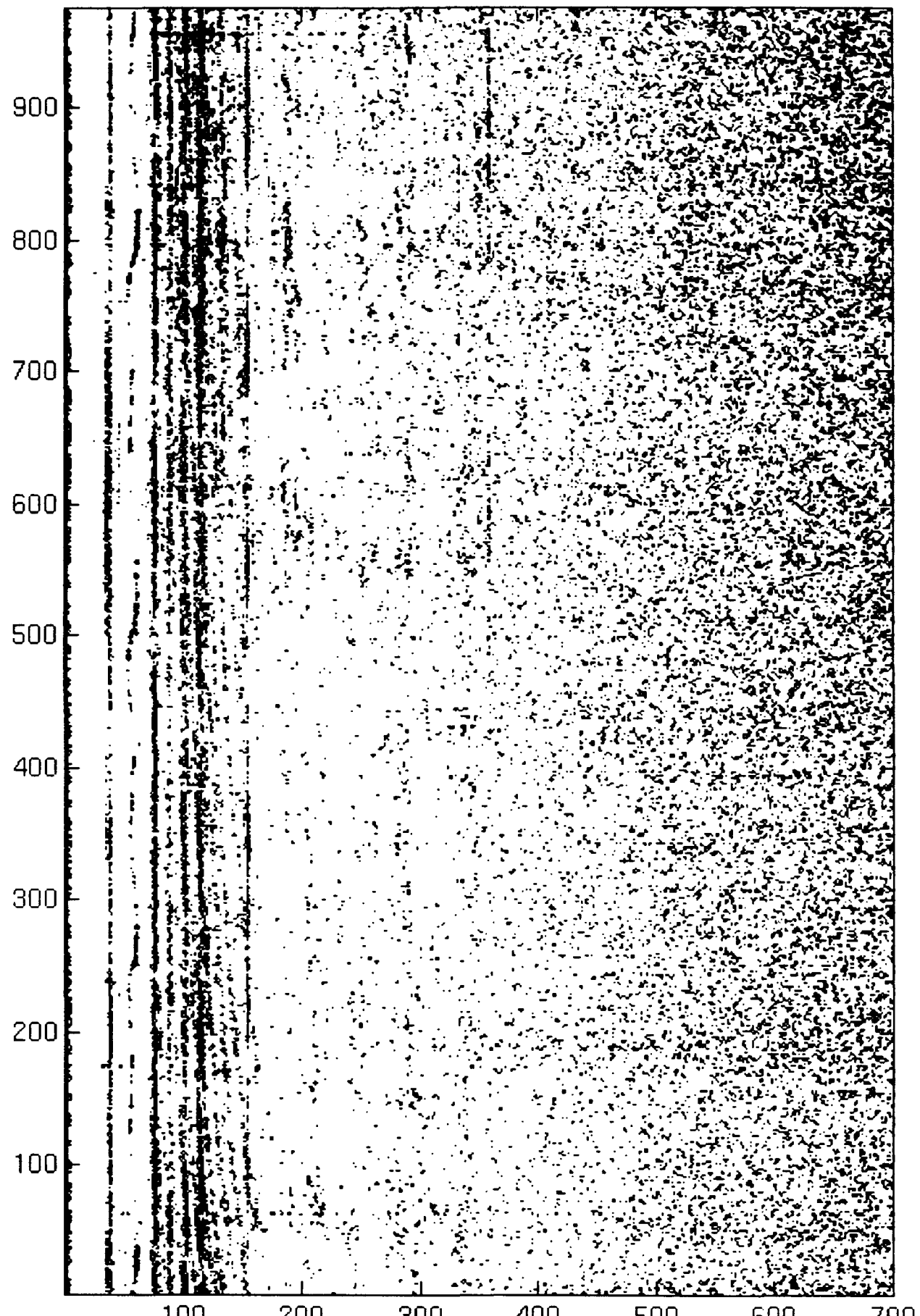


Fig. 15.B

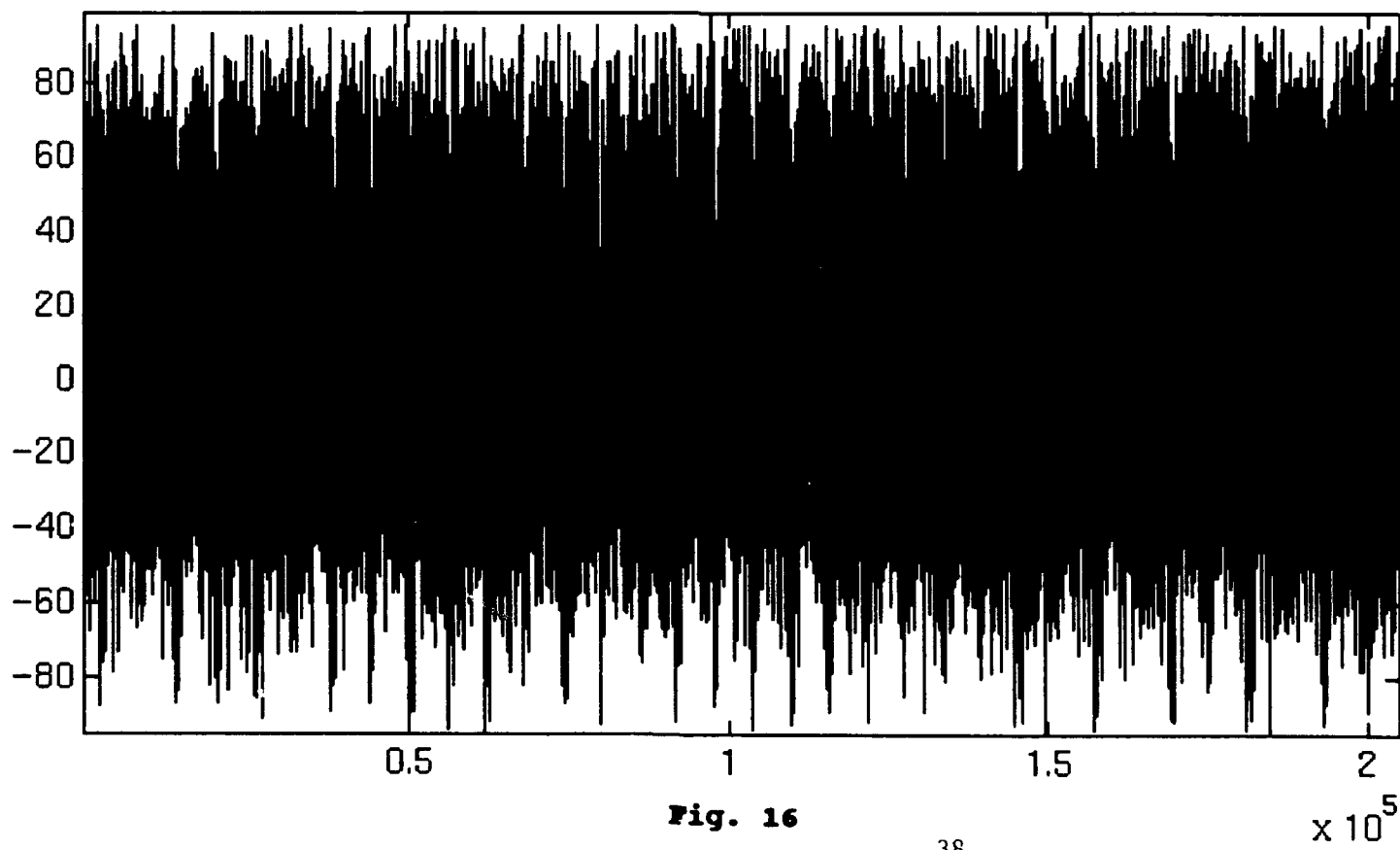
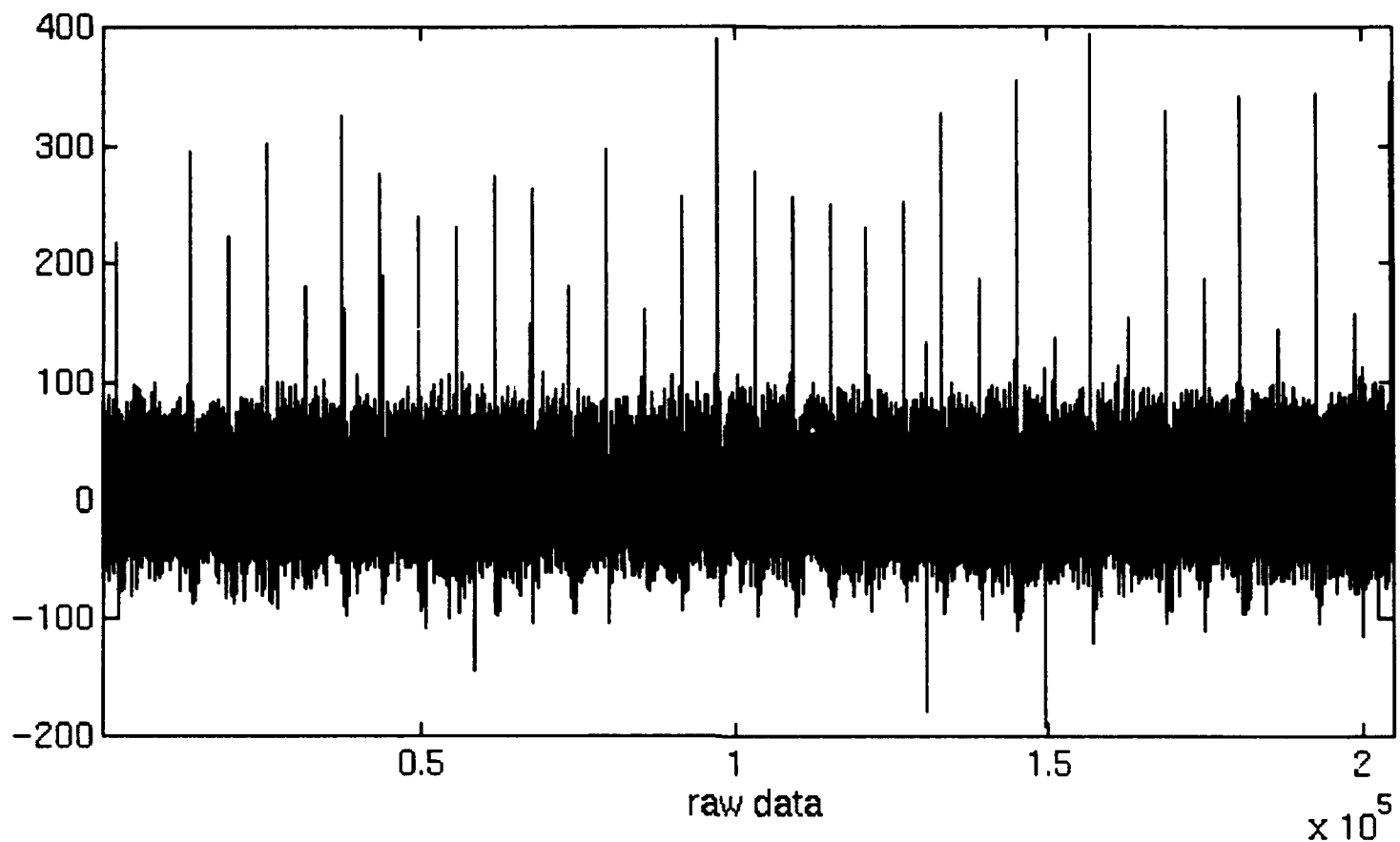
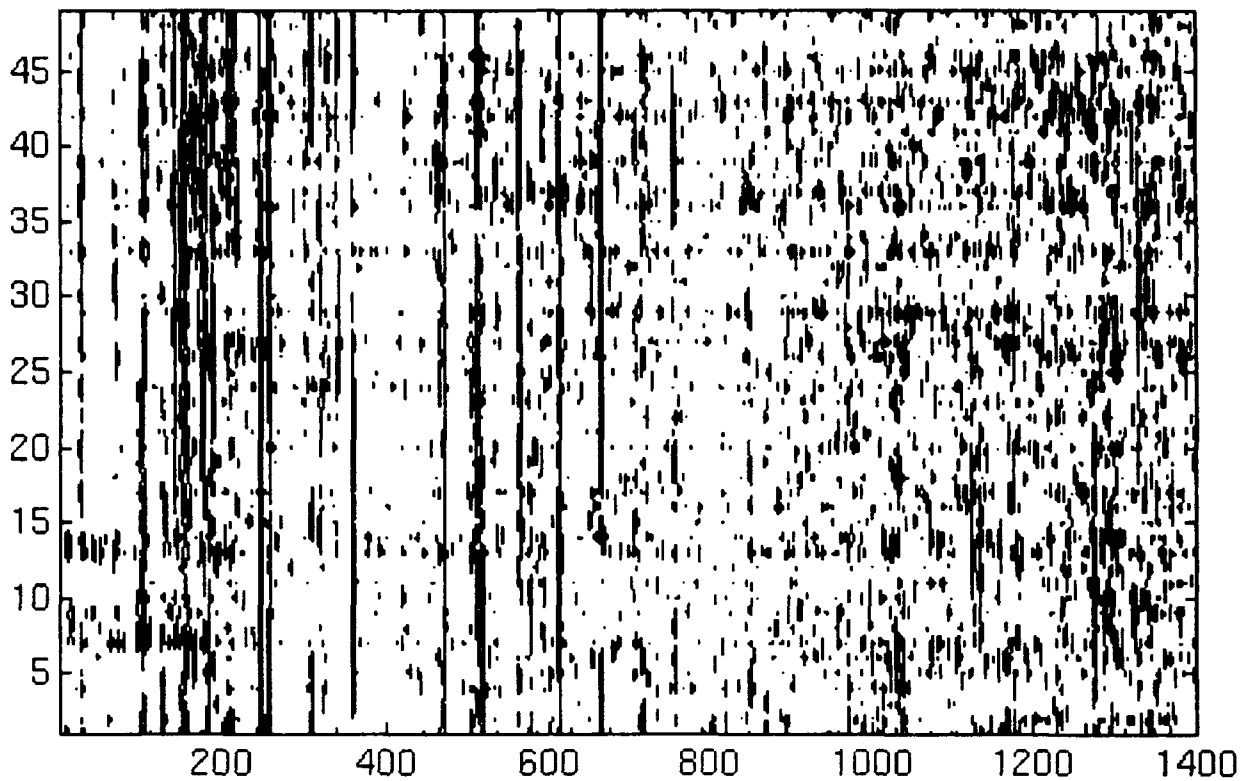


Fig. 16

ipsav(clipped to +/-90 redata x,1,4096,,32) bin 51:1450



lofarm(clipped to +/-90 redata,4096,4096,4096) bin 51:1450

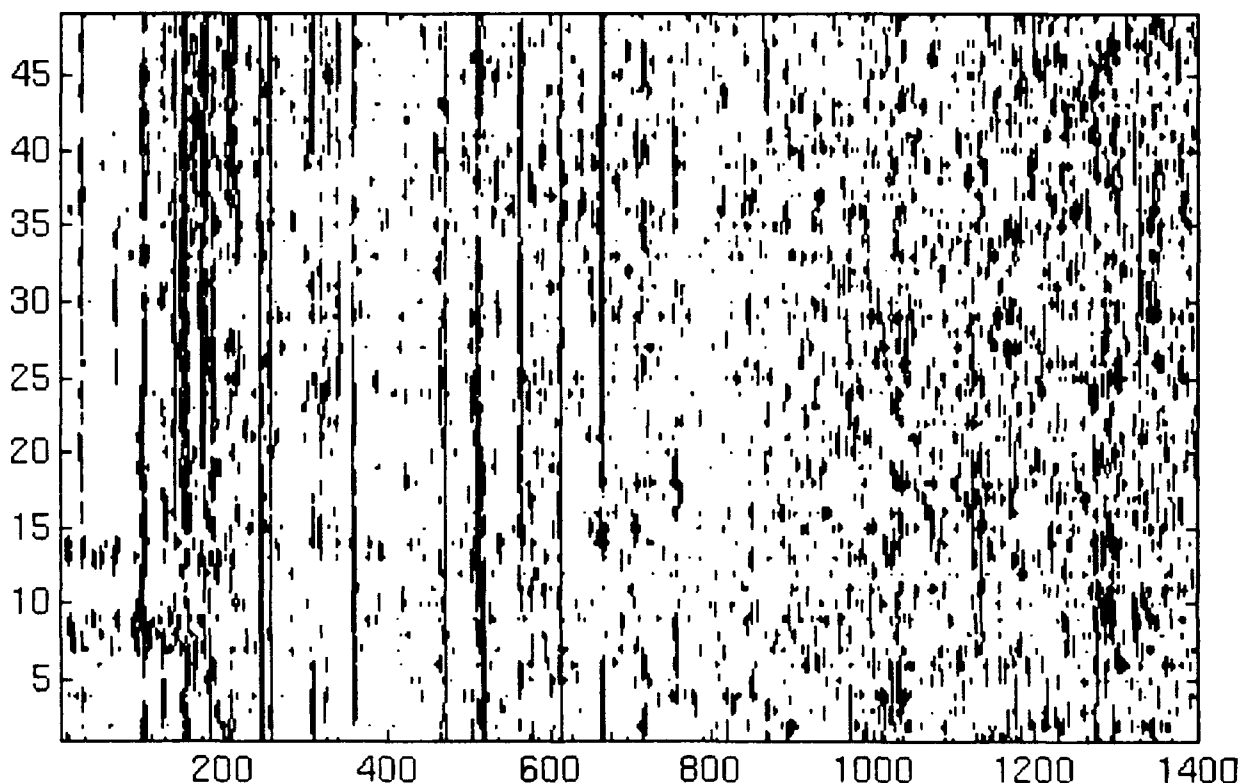
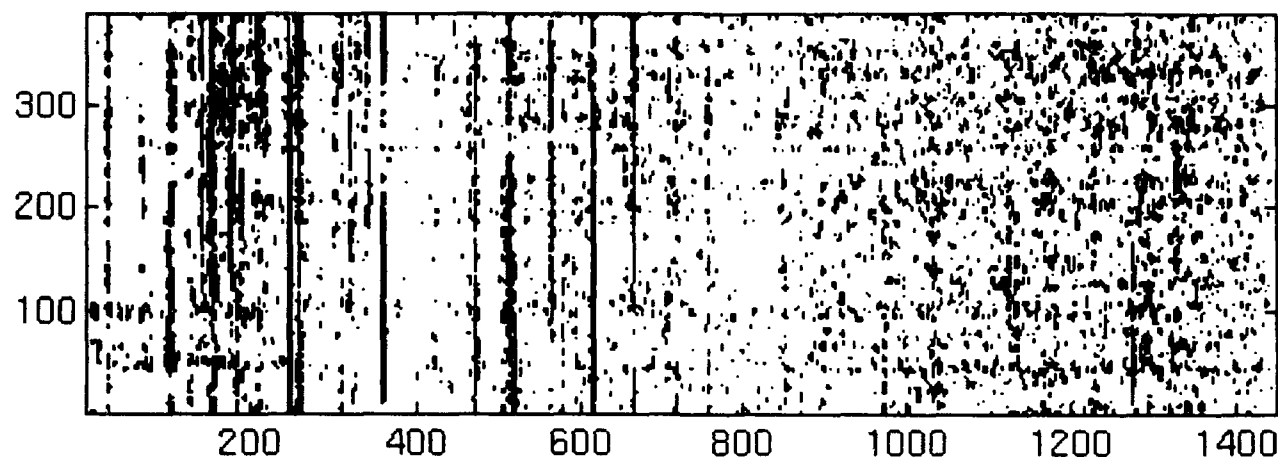
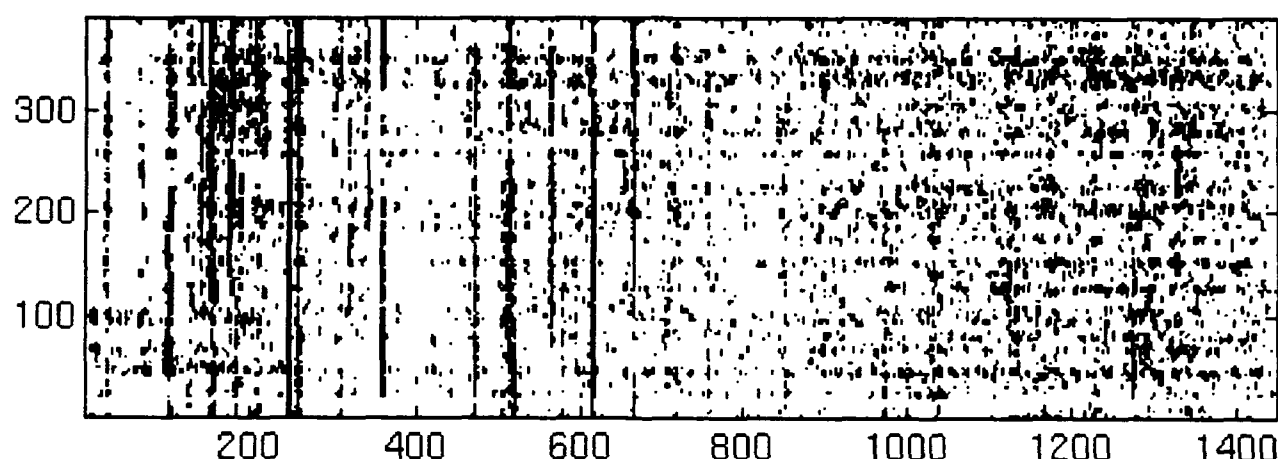


Fig. 17

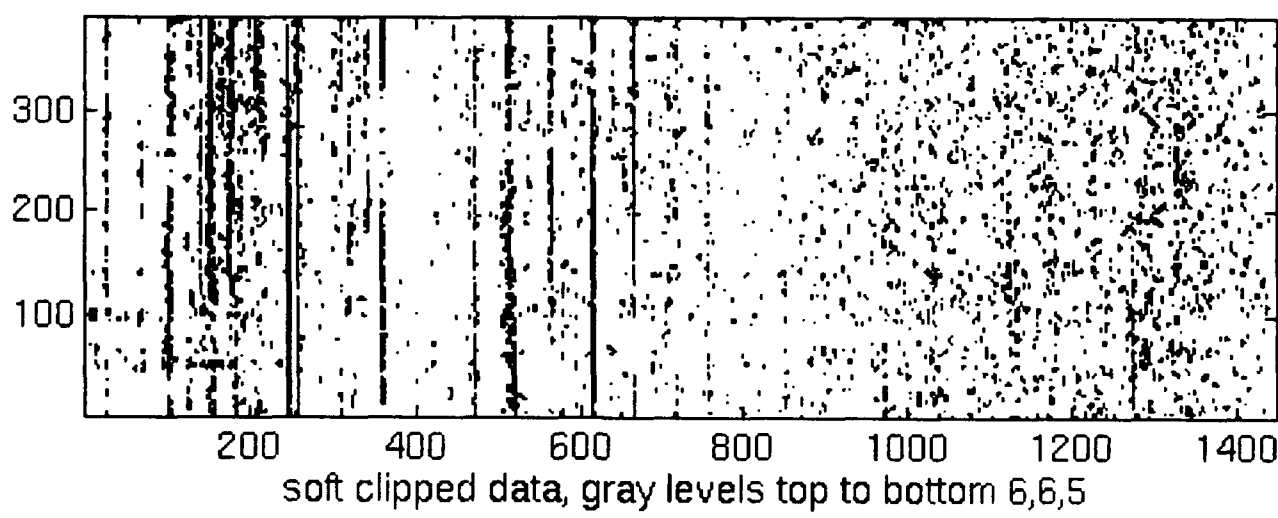
ipsav(rf,1,4096,32) bin 51:1500, shft 512



cumav(rf,1,4096,32) bin 51:1500, shft 512



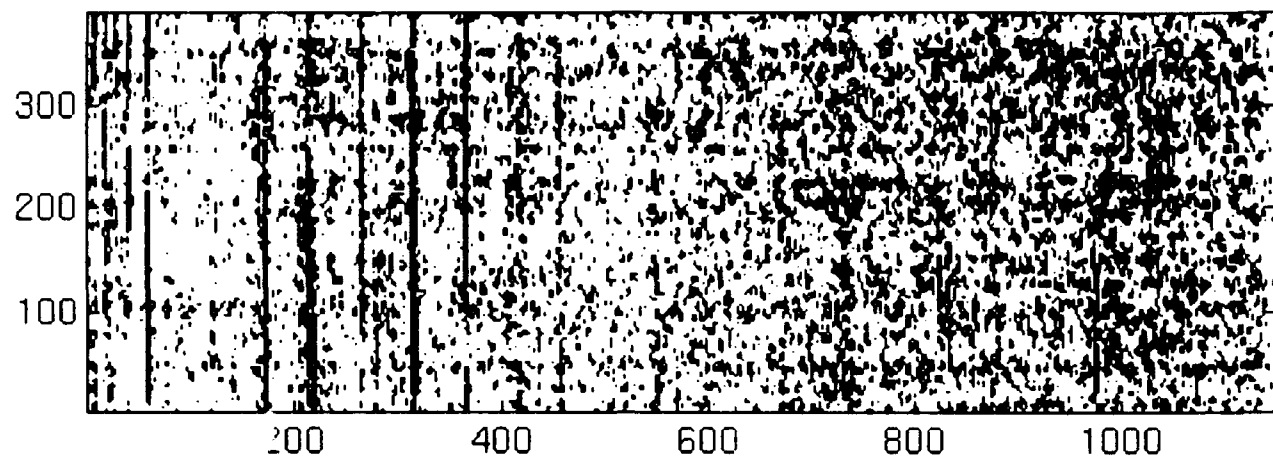
lofarm(rf,4096,4096,4096) bin 51:1500, shft 512



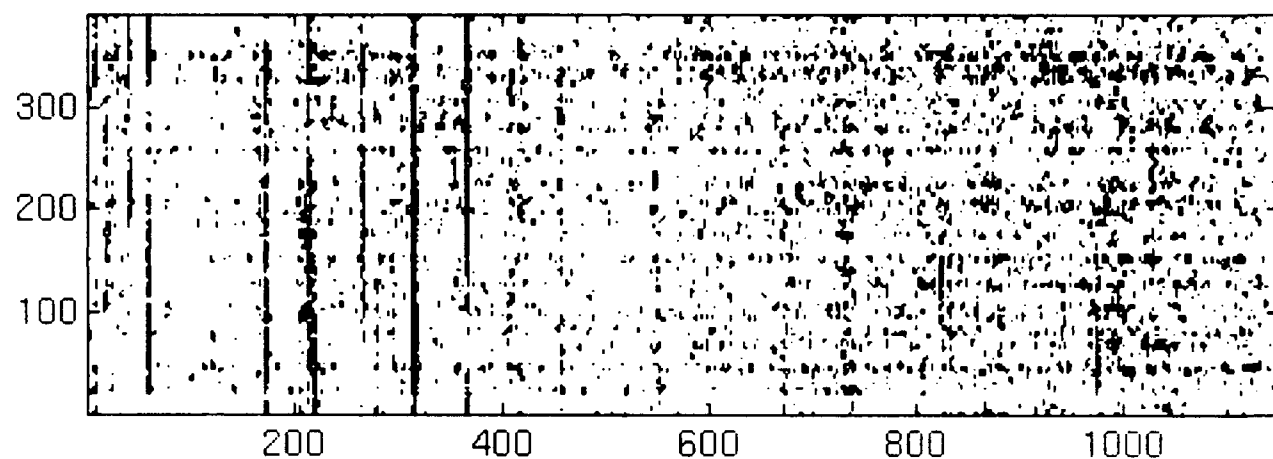
soft clipped data, gray levels top to bottom 6,6,5

Fig. 18.A

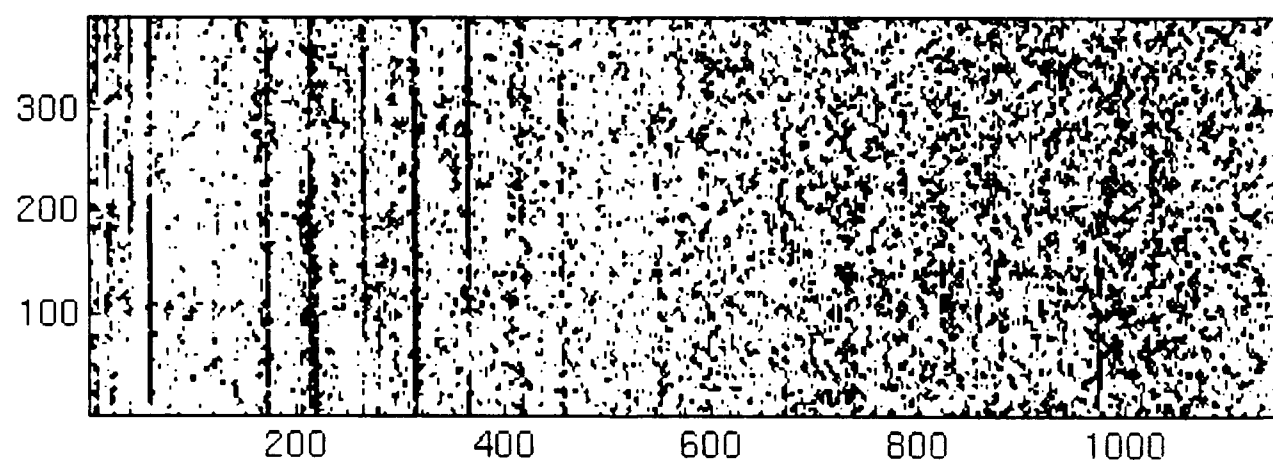
ipsav(rf,1,4096,32) bin 351:1500, shft 512



cumav(rf,1,4096,32) bin 351:1500, shft 512

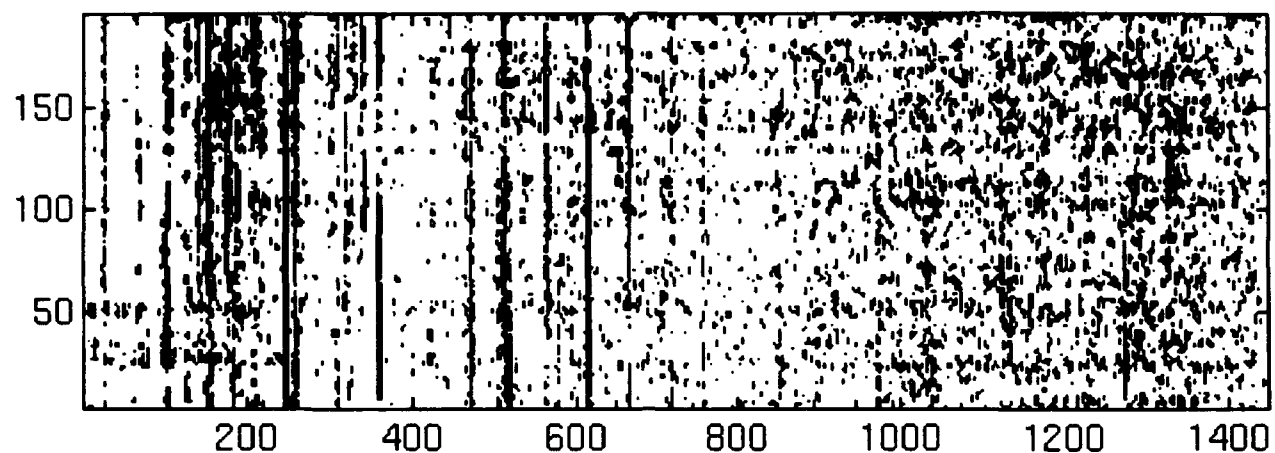


lofarm(rf,4096,4096,4096) bin 351:1500, shft 512

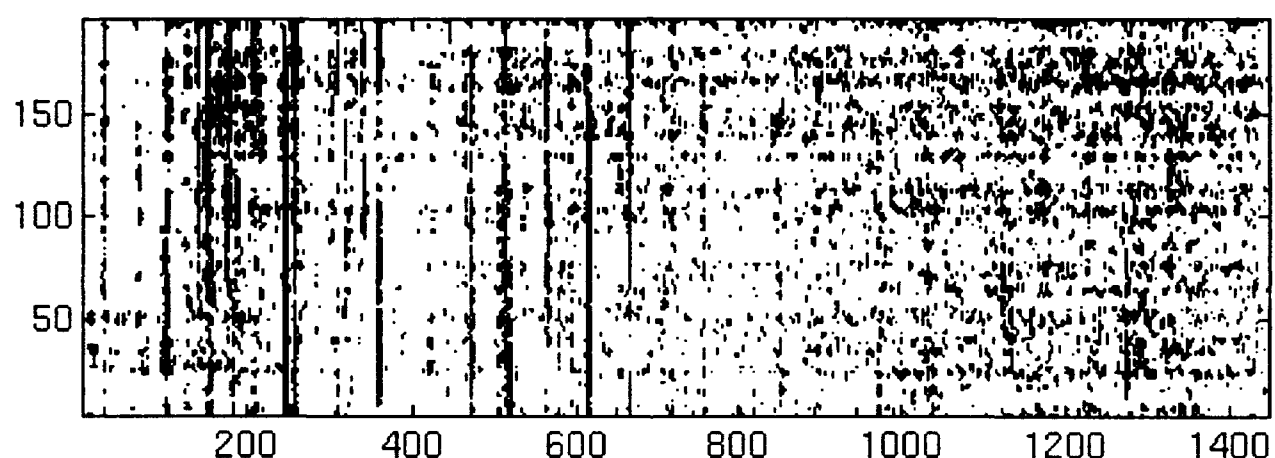


soft clipped data, gray levels top to bottom 5,4,4

ipsav(rf,1,4096,32) bin51:1500, shft 1024



cumav(rf,1,4096,32) bin51:1500, shft 1024



lofarm(rf,4096,4096,4096) bin51:1500, shft 1024

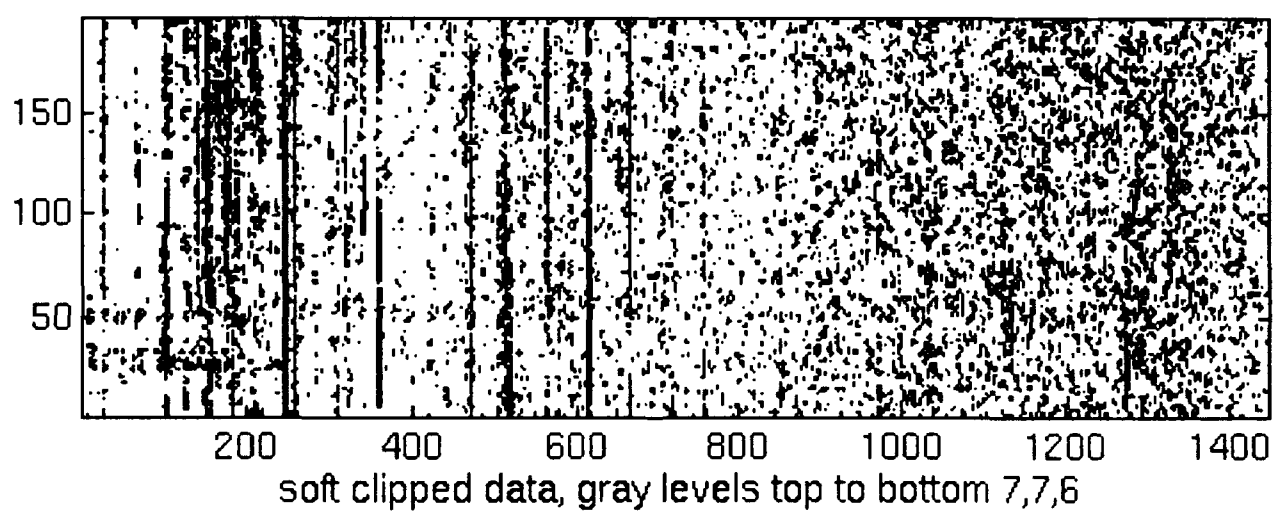
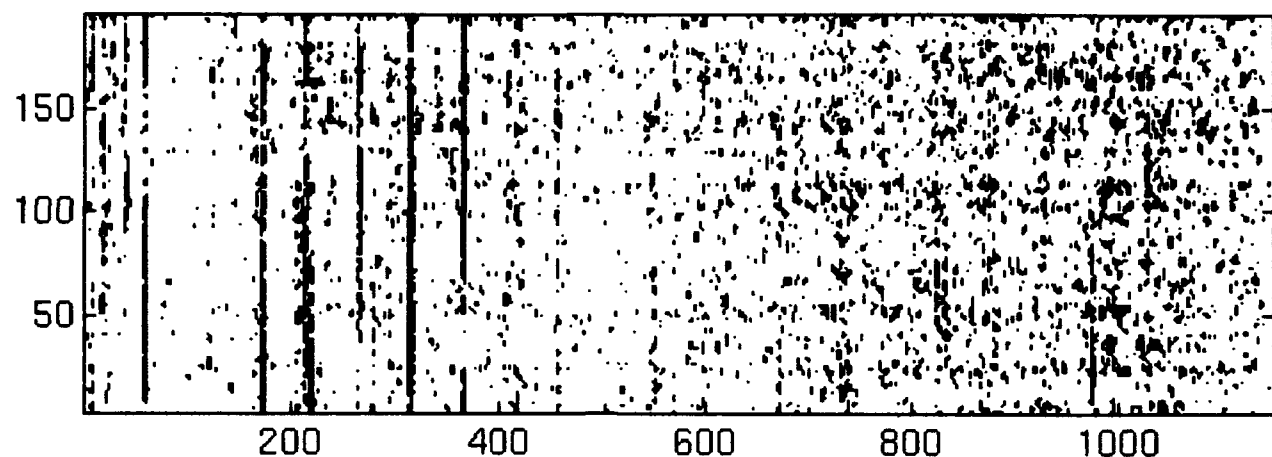
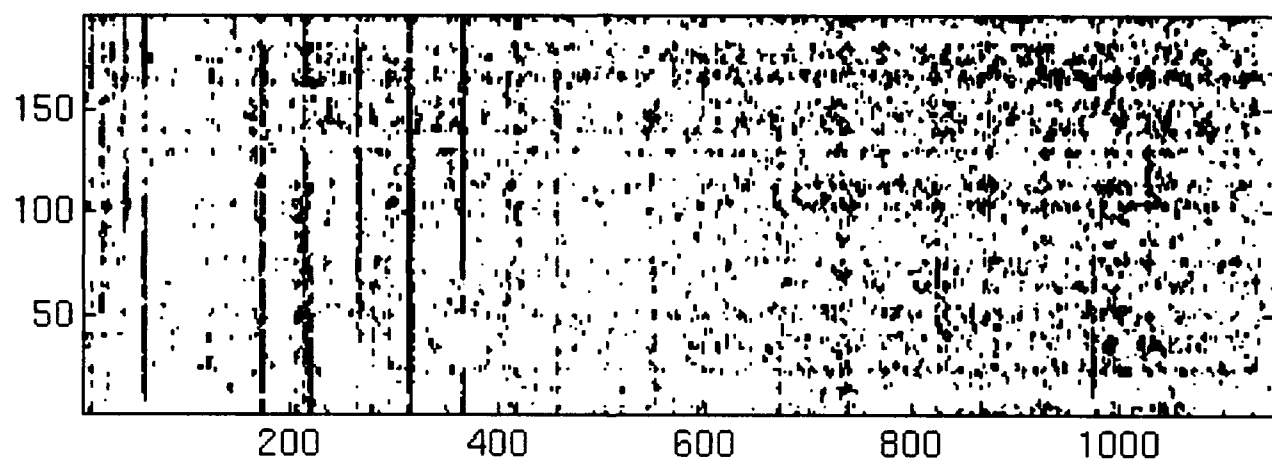


Fig. 19.A

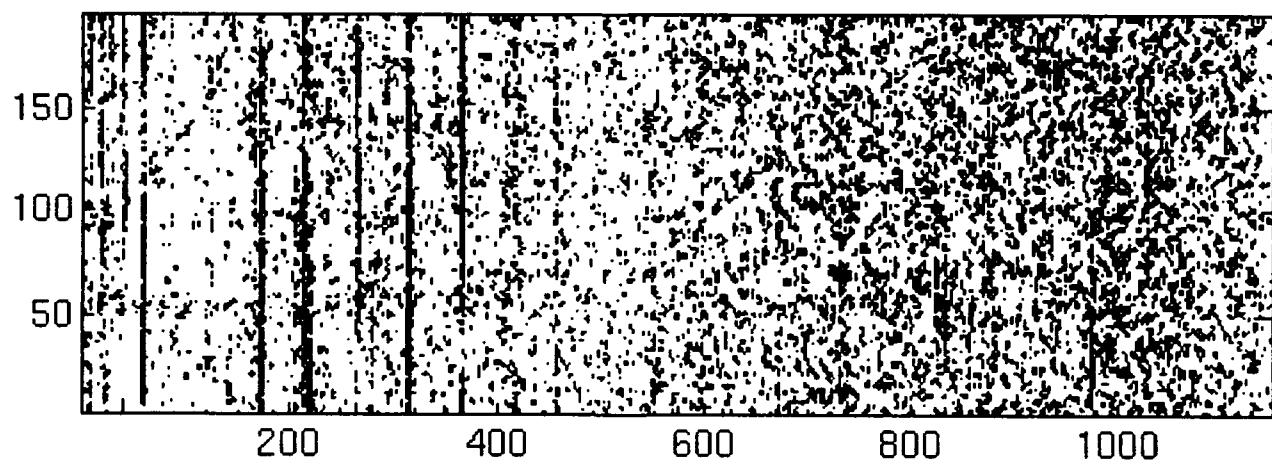
ipsav(rf,1,4096,32) bin 351:1500, shft 1024



cumav(rf,1,4096,32) bin 351:1500, shft 1024

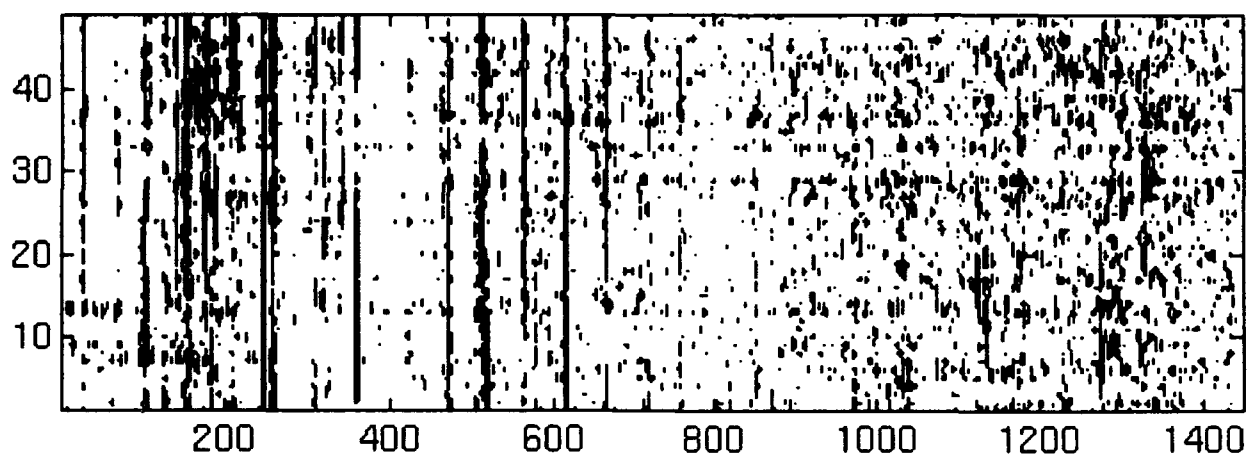


lofarm(rf,4096,4096,4096) bin 351:1500, shft 1024

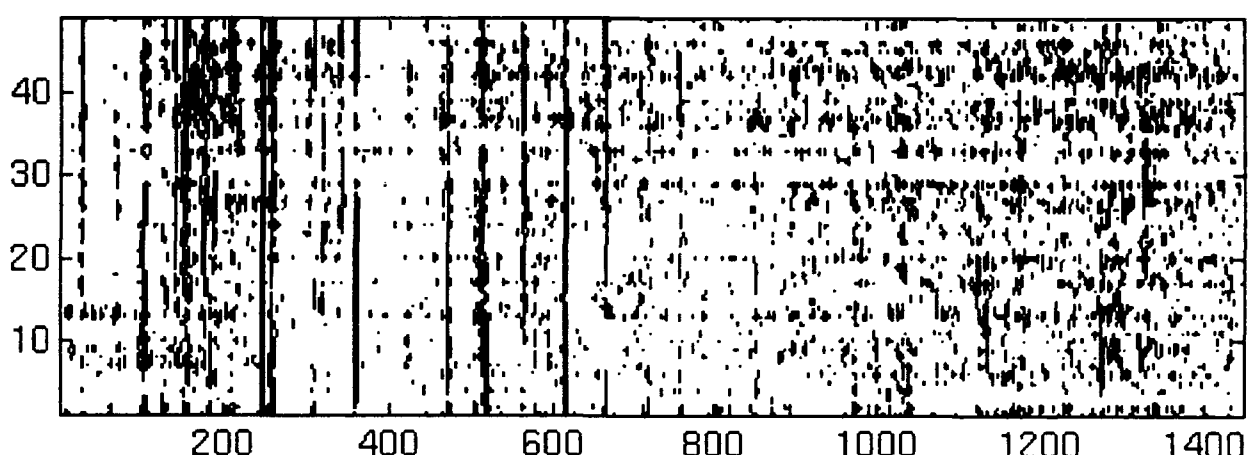


soft clipped data, gray levels top to bottom 4,4,4

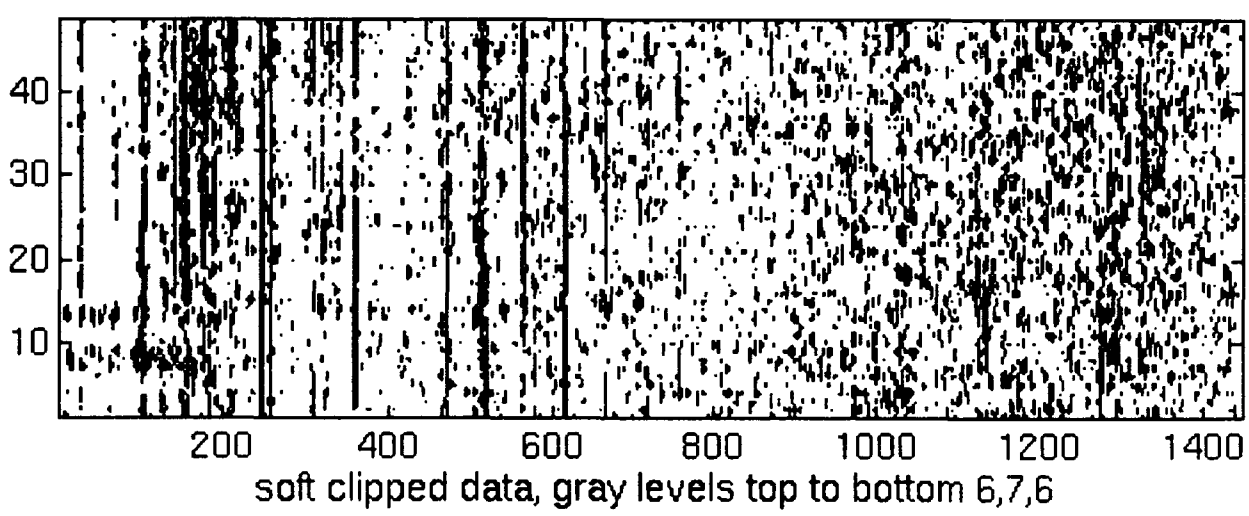
ipsav(rf,1,4096,32) bin 51:1500, shft 4096



cumav(rf,1,4096,32) bin 51:1500, shft 4096

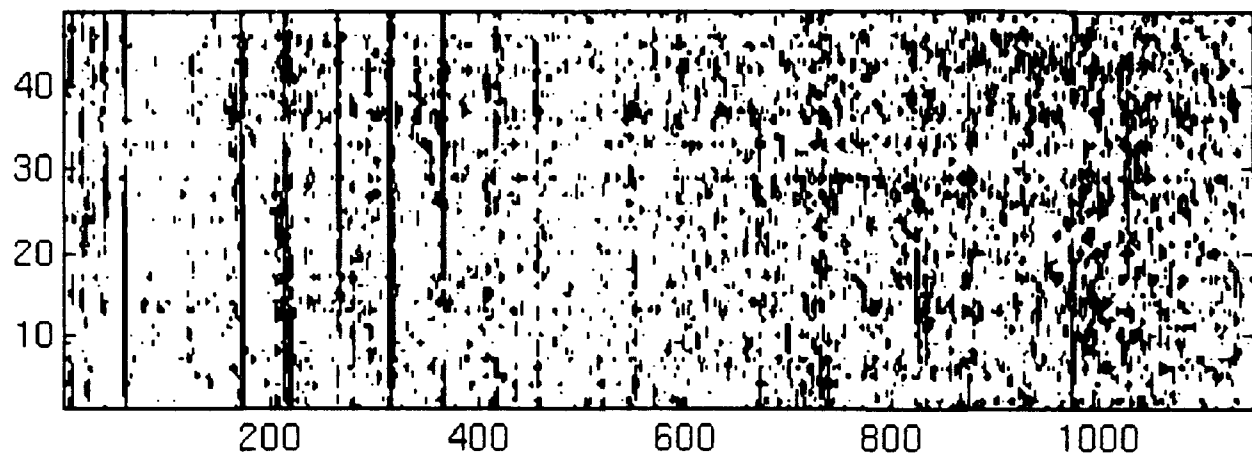


lofarm(rf,4096,4096,4096) bin 51:1500, shft 4096

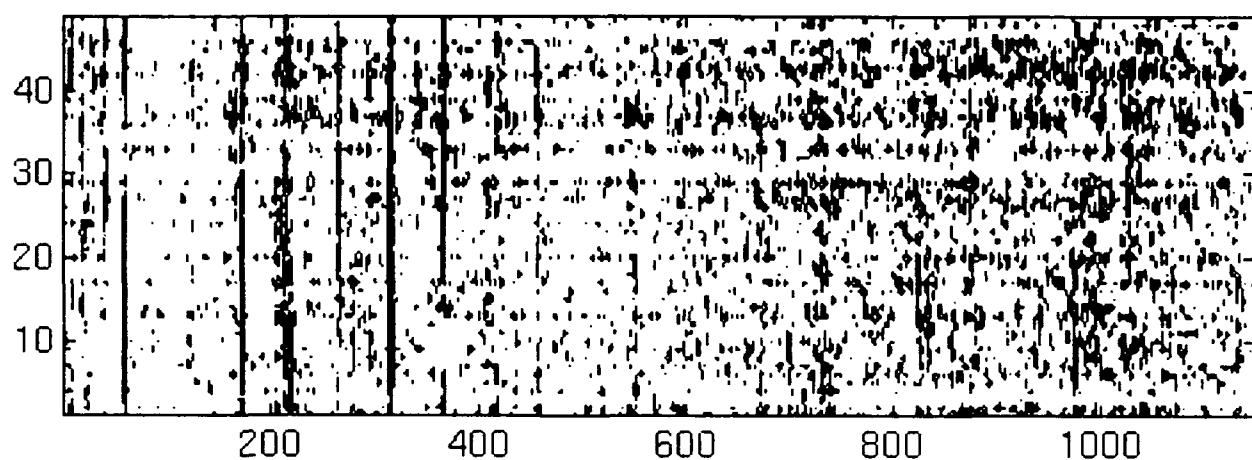


soft clipped data, gray levels top to bottom 6,7,6

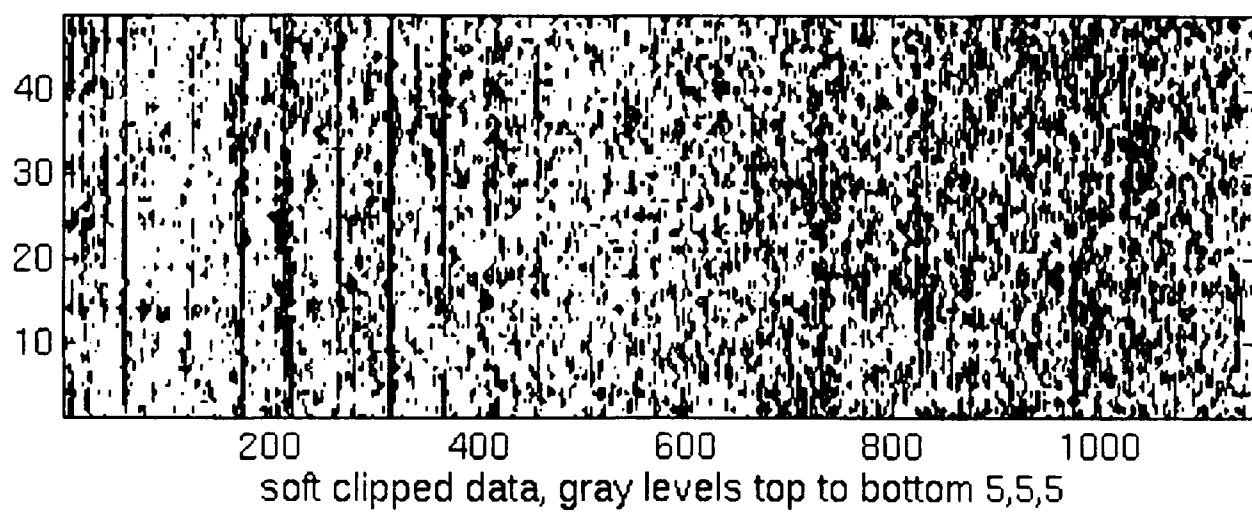
ipsav rf,1,4096,32 bin 351:1500, shft 4096



cumav rf,1,4096,32 bin 351:1500, shft 4096



lofarm rf,4096,4096,4096 bin 351:1500, shft 4096



soft clipped data, gray levels top to bottom 5,5,5

Fig. 20.B

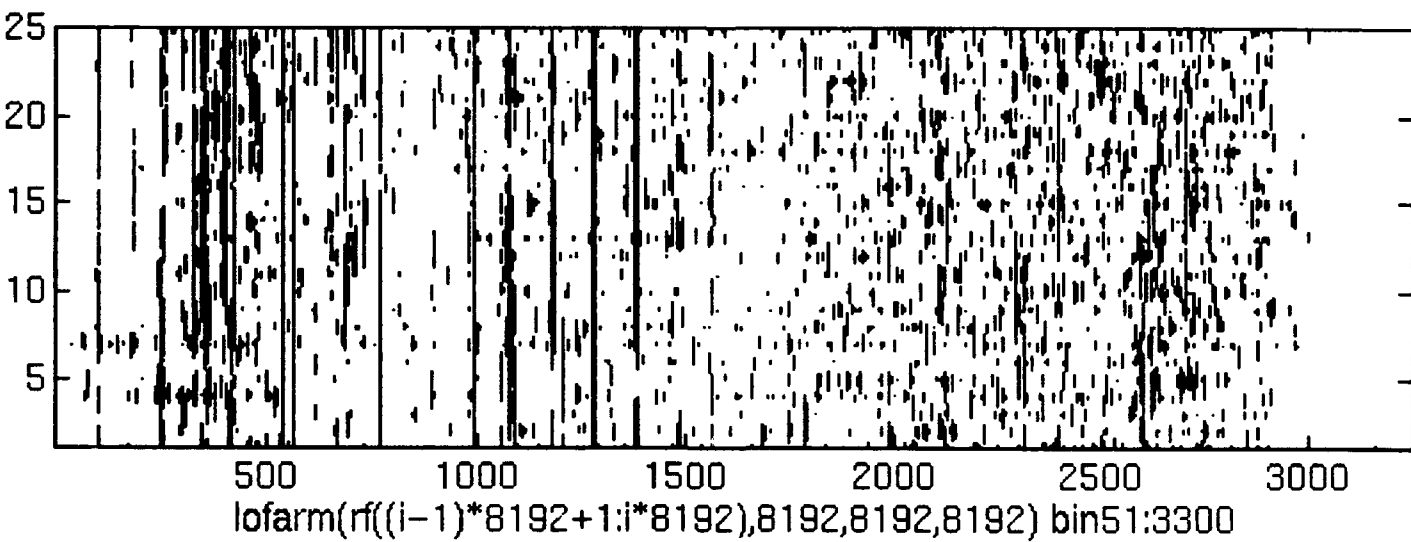
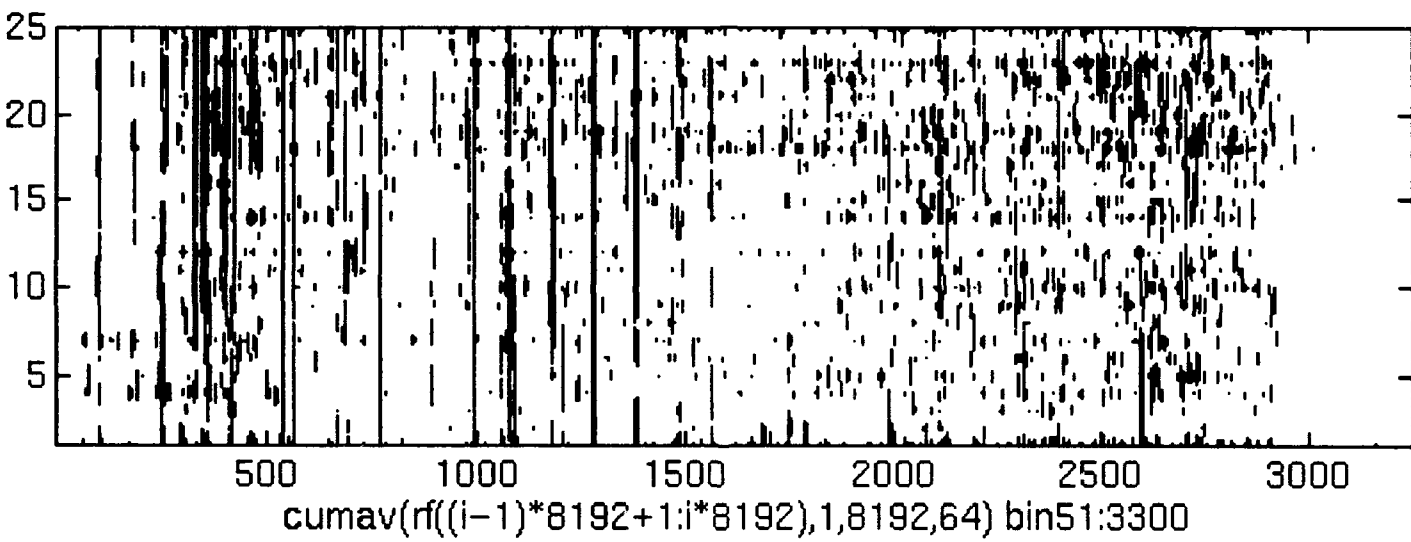
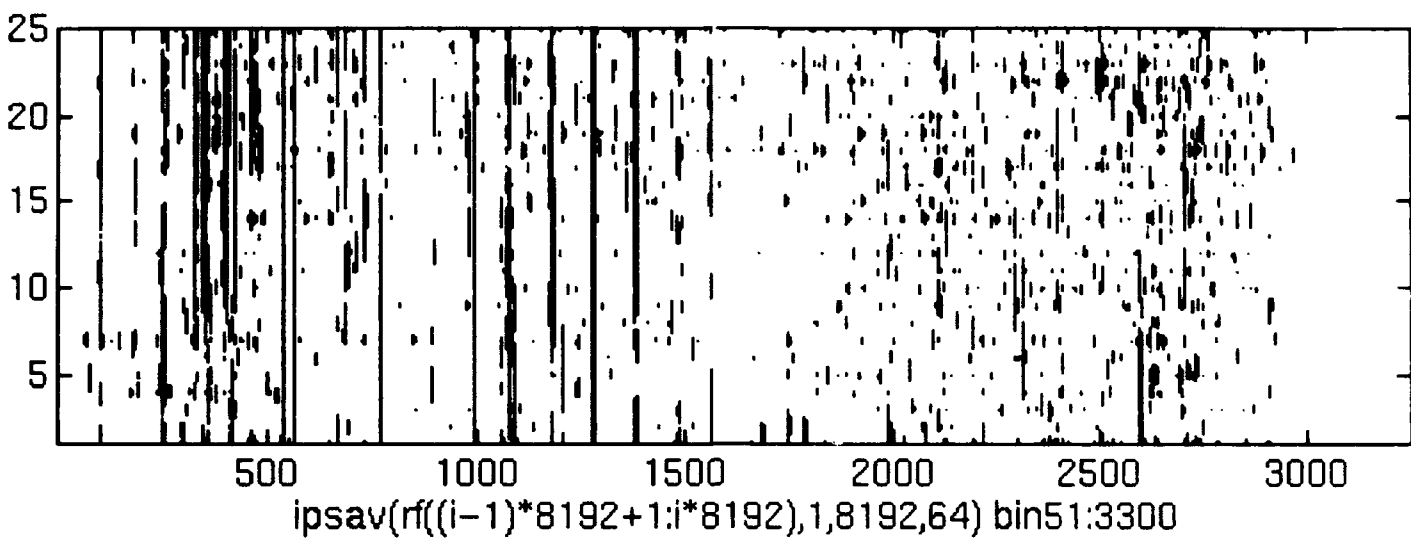


Fig. 21

7. Program Listings:

All algorithms are implemented (including their hard copy functions) using MATLAB software (The Mathworks Inc.). The programs can be executed on MS-DOS personal computers (i.e. 386 + co-processor or 486 based IBM compatible PC's) or on SUN work stations. Due to the long data sequence and large T-F surfaces most of the work is done on SUN work stations. The hard copies provided are obtained by using the contour plotting function of MATLAB. One note of caution is appropriate when interpreting the T-F plots. Due to the way contour lines are drawn, equal height spectral peaks can appear different if they differ in T-F spread, that is a narrow peak will be darker than a wide peak even though these peaks are of the same height. This is due to the density of contour lines which is higher for narrow peaks than it is for wide peaks. Better results are obtained when displaying the data on gray scale or color scale output devices. The new 4.0 MATLAB version supports the function 'image' which on a gray scale or color monitor will improve the readability of LOFARGRAMs.

The color output (using MATLAB 3.5i) on a SUN SPARC-2 work station shows superior detail when compared to the hard copies supplied in this report. The hard copies are obtained using a screen dump routine which preserves less detail than a postscript derived output. The postscript output is not used due to the length of time involved generating it on the processing system.

```

>> %typical setup for obtaining IPS and CUM like surfaces
>> %for i=start:finish
>> %p(i,:)=ipsav(rf((i-1)*shft+1:(i-1)*shft+N),1,N,step);
>> %q(i,:)=cumav(rf((i-1)*shft+1:(i-1)*shft+N),1,N,step);
>> % N= proc length, step=stepsize, N/step=number of terms averaged to
>> %create one spectral line, shft = amount of data shifted to create
>> %the next surface which will be averaged to create one spectral
>> %line at location i
>> %end
>>
>> %typical setup for obtaining LOFAR like surfaces
>> %for i=start:finish
>> %po(i,:)=lofarm(rf((i-1)*shft+1:(i-1)*shft+N),id,st,t1);
>> %id=number of data points in transform, st=stepsize,
>> %t1=transform length
>> % Note: rf = input sequence,
>> % Note: in all run executed id=st=t1
>> % So the overlap was controlled with shft
>>
>>
```

```

```

%function [P,freqindex]=ipsav(data,wintype,winlen,step);
%This function will calculate a single averaged Instantan. Power Spectral (IPS)
% line.
%The IPS surface characteristics are determined by the selection of window
%type (wintype), window length (winlen) and the distance that the window
%is moved through the data sequence (step).
%
%The P matrix plots only positive frequencies (in magnitude). The
%outputs timeindex and freqindex can be used in plots to interpret the
%results.
%The inputs are:
%data - The input data string row vector
%wintype: '0' Rectangular Window
% '1' Hamming Window
%winlen - The desired width of the window, normally half of the siglen
%step - Time step desired, normally '1' or a multiple of '2'
%See also IPSSURF, IPSLOFAR

function [P,freqindex]=ipsav(data,wintype,winlen,step)
[datarows,datacolumns]=size(data);
if datarows ~=1
 data=data.';
end

siglen=length(data);
if wintype==0
 win=ones(winlen-1,1);
elseif wintype==1
 win=hamming(winlen-1);
end
W=[win(winlen/2:-1:1)];
x=[zeros(1,winlen) data zeros(1,winlen)];
P=zeros(1,winlen/2);

for n=winlen+1:step:siglen+winlen-step+1
 Xm=[conj(x(n:-1:n-(winlen/2-1))).' x(n:n+(winlen/2-1)).'];
 Xn=[x(n);conj(x(n))];
 product=((Xm*Xn).*W).'';
 product=[product 0 conj(product(winlen/2:-1:2))];
 ptemp=fftshift(real(.5*fft(product)));
 P=P+abs(ptemp(winlen/2+1:winlen));
end

[prow,pcolumn]=size(P);
freqindex=[0:pcolumn-1];

```

```

%function [P,freqindex,timeindex]=cumav(data,wintype,winlen,step);
%This function will calculate the 1.5 D Spectral surface.
%this surface consists of averaged (shorter) cumulant based surfaces
%in a power or magnitude averaged sense
%The 1.5 D surface characteristics are determined by the selection of window
%type (wintype), window length (winlen) and the distance that the window
%is moved through the data sequence (step).
%The surface is placed sequentially in the P matrix for display.
%The P matrix plots only the positive half of the spectral plane. The
%outputs timeindex and freqindex can be used in plots to interpret the
%results.
%The inputs are:
%data - The input data string must be in row vector form
%wintype: '0' Rectangular Window
% '1' Hamming Window
%winlen - The desired width of the window, normally half of the siglen
%step - Time step desired, normally '1' or a multiple of '2'
%See also ONESURF, ONELOFAR

```

```

function [P,freqindex]=cumav(data,wintype,winlen,step)
[datarows,datacolumns]=size(data);
if datarows~=1
data=data.';
end

siglen=length(data);
if wintype==0
 win=ones(winlen-1,1);
elseif wintype==1
 win=hamming(winlen-1);
end
W=[win(winlen/2:-1:1)];
x=[zeros(1,winlen) data zeros(1,winlen)];
P=zeros(1,winlen/2);
for n=winlen+1:step:siglen+winlen-step+1
 Xn=[abs(x(n))^2;abs(x(n))^2];
 Xm=[conj(x(n-1:n-(winlen/2-1))).' x(n:n+(winlen/2-1)).'];
 product=((Xm*Xn).*W).';
 product=[product 0 conj(product(winlen/2:-1:2))];
 ptemp=fftshift(real(.5*fft(product)));
 P=P+abs(ptemp(winlen/2+1:winlen));
P=abs(P);
end
[prow,pcolumn]=size(P);

freqindex=[0:pcolumn-1];

```

```

% This program computes the LOFARGRAM based on windowed periodograms and displays the result
% id=no of points in xform, step = shift, tlen=transform length
% [P]=lofarm(name,id,step,tlen)
function [P]=lofarm(name,id,step,tlen)
clear pow
%name=input(' name of input file is ');
[drow,dcolumn]=size(name);
if drow~=1
 name=name.';
end
len=length(name);
%id=input(' No. of non-zero data points in transform ');
%step=input(' shift (step size) in data points ');
%tlen=input('transform length ');
i=fix((len-id)/step)+1;
win=hamming(id).';
for ic=1:i
 ppow=abs(fft(name(1+(ic-1)*step:id+(ic-1)*step).*win,tlen));
 pow(ic,:)=ppow(1:tlen/2);
end
P=pow;
clear name drow dcolumn len id step tlen i ic win ppow

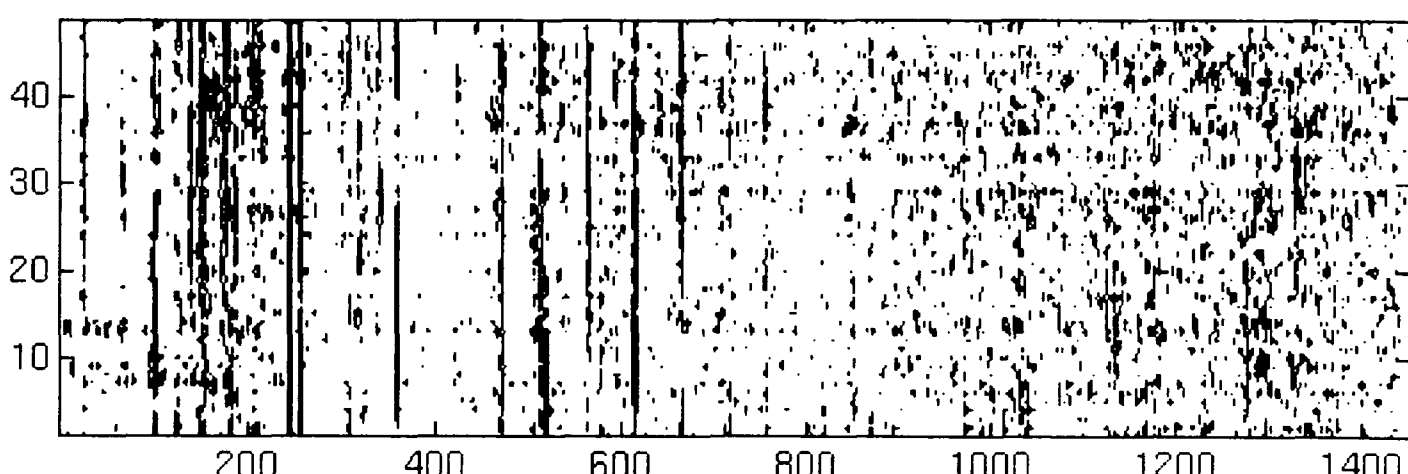
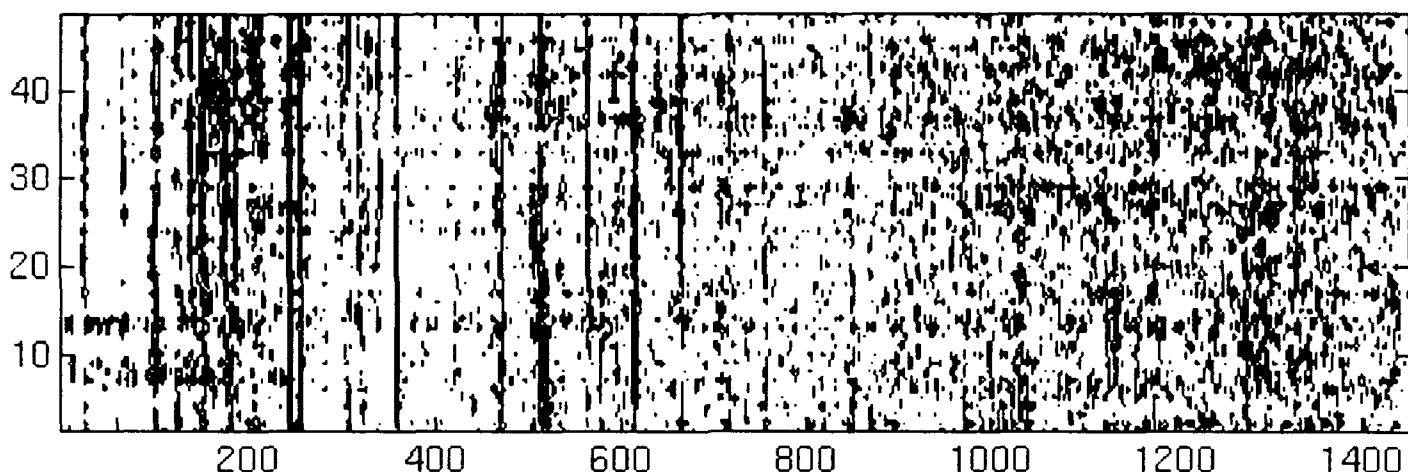
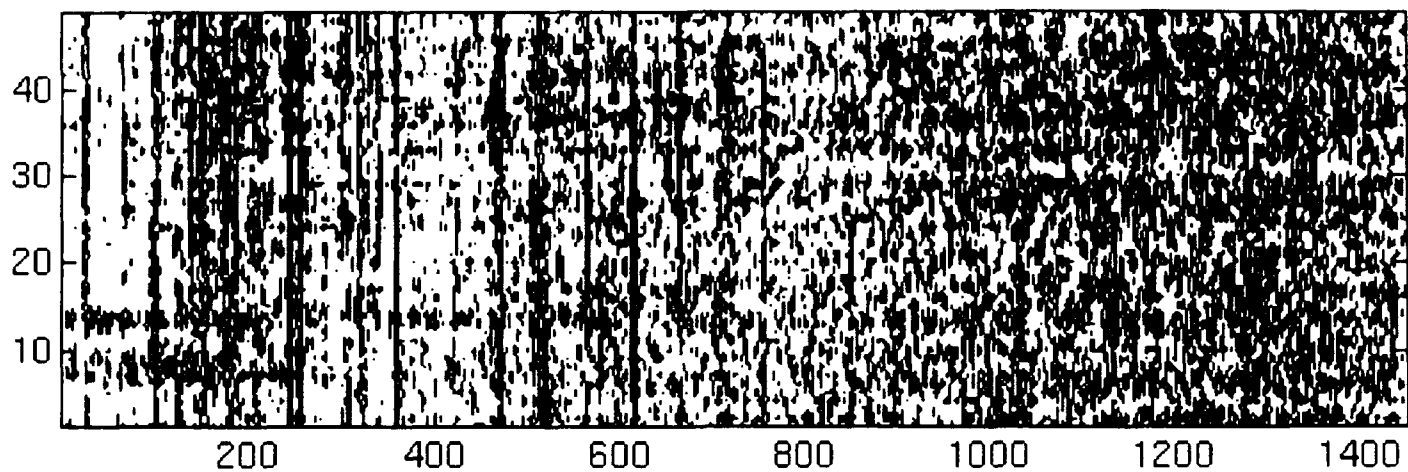
```

## **8. References**

- [1]: L. Cohen, "Time-Frequency Distributions - A Review," IEEE Proceedings, Vol. 77, No. 7, July 1989.
- [2]: R. Hippenstiel and P. Oliveira, "Time Varying Spectral Estimation using the Instantaneous Power Spectrum (IPS)," IEEE Transaction on Acoustics, Speech, and Signal Processing, Vol. 38, No. 10, October 1990.
- [3]: P. M. D. Monica de Oliveira, "Instantaneous Power Spectrum," Engineer's Thesis, Naval Postgraduate School, Monterey, California, 1989.
- [4]: K. A. Hagerman, "Instantaneous Power Spectrum and 1½D Instantaneous Power Spectrum Techniques," Master's Thesis, Naval Postgraduate School, Monterey, California, 1992.
- [5]: J. M. Mendel, "Tutorial on Higher Order Statistics (Spectra) in Signal Processing and System Theory: Theoretical results and some Applications," Proceedings of the IEEE, Vol. 79, pp. 278-305, 1991.
- [6]: J. F. McAloon, "Comparison of Higher Order Moment Spectrum Estimation Techniques," Master's Thesis, Naval Postgraduate School, Monterey, California, 1993.
- [7]: A. P. Petropulu, "Detection of Multiple Chirp Signals based on a Slice of the Instantaneous Higher Order Moments," Proceedings of the IEEE-SP International Symposium on Time Frequency and Time-Scale Analysis, pp. 261-264, IEEE Press, Victoria, B. C. Canada, Catalog No. 92TH0478-8, October 1992.

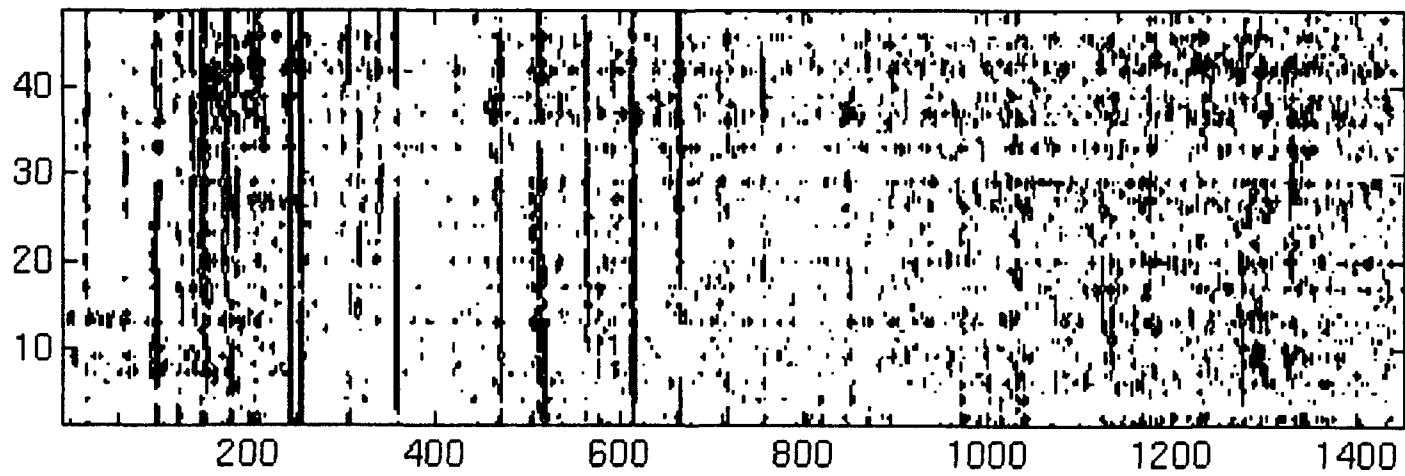
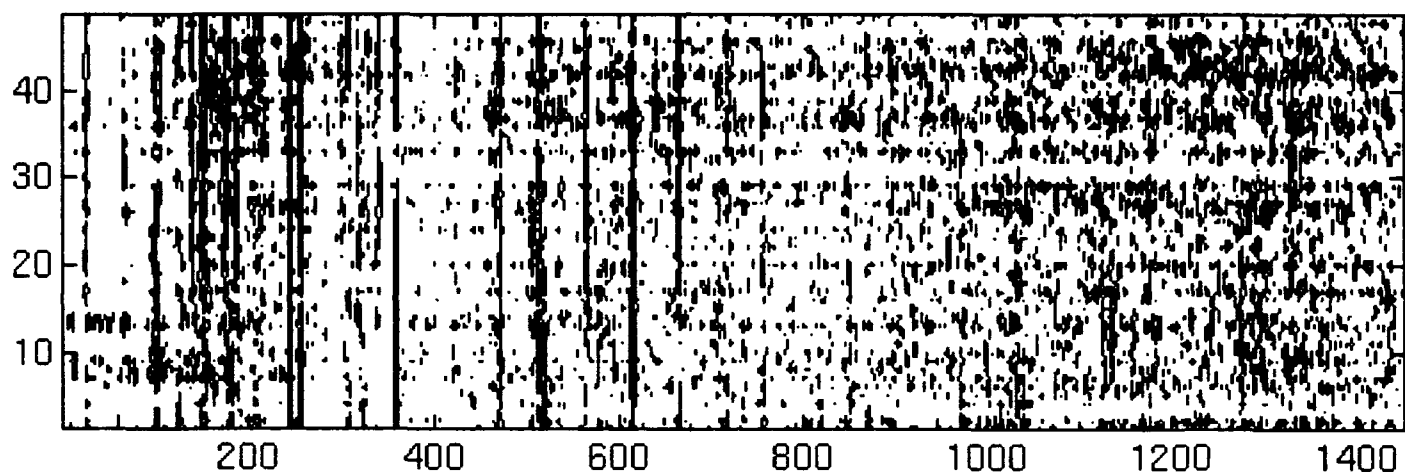
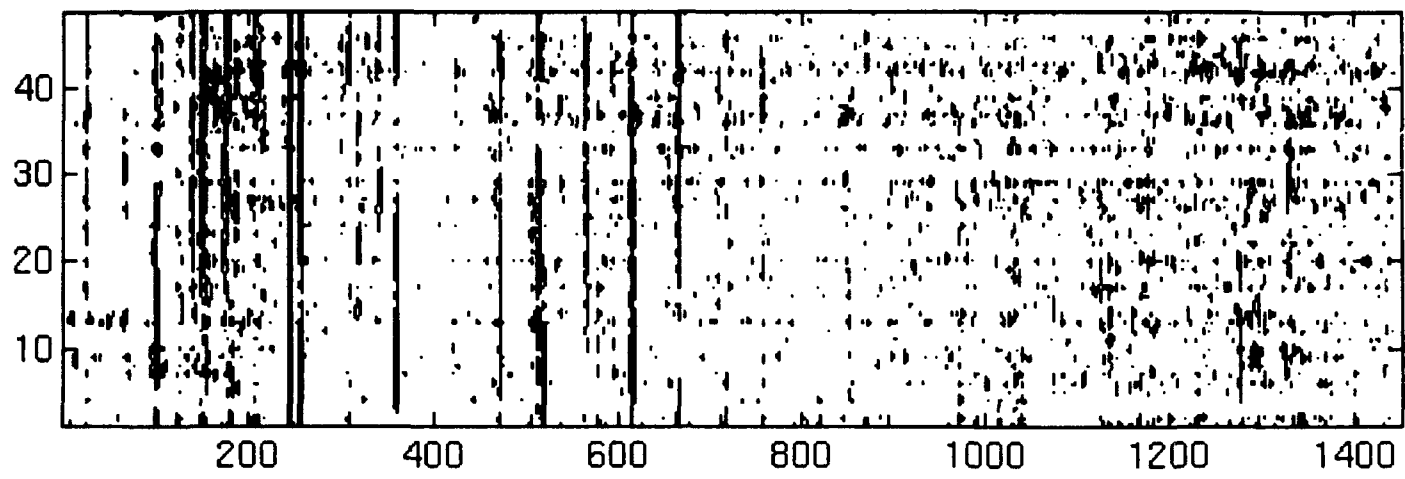
## **9. Appendix A**

This appendix provides 3 figures which illustrate the effects of level selection when using a simple (no-gray scale , no color ) printer. All three figures use a shift of 4096 (i.e. no overlap of data between successive spectral lines). Fig A.1, A.2 and A.3 show IPS, CUM, and LOFAR respectively. The number of quantization levels is different on each figure. The label on each figure is self explanatory.



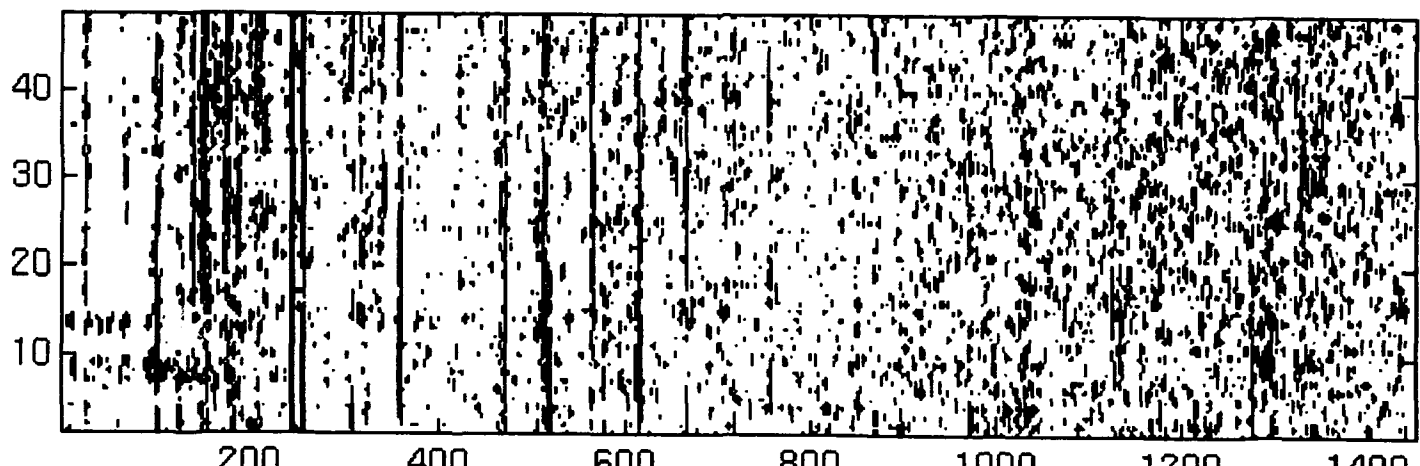
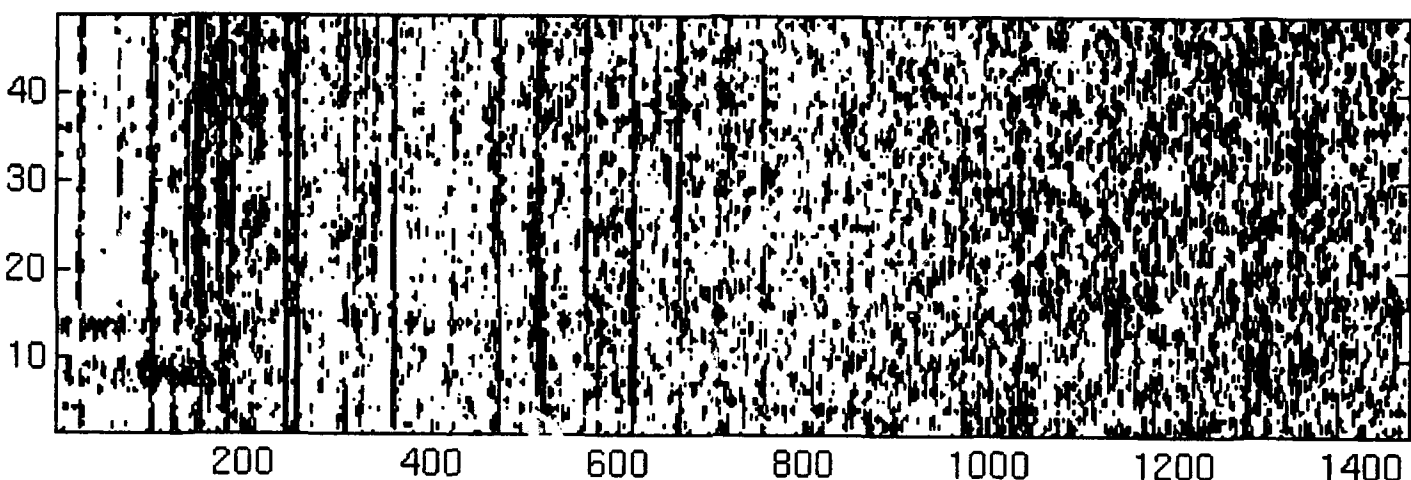
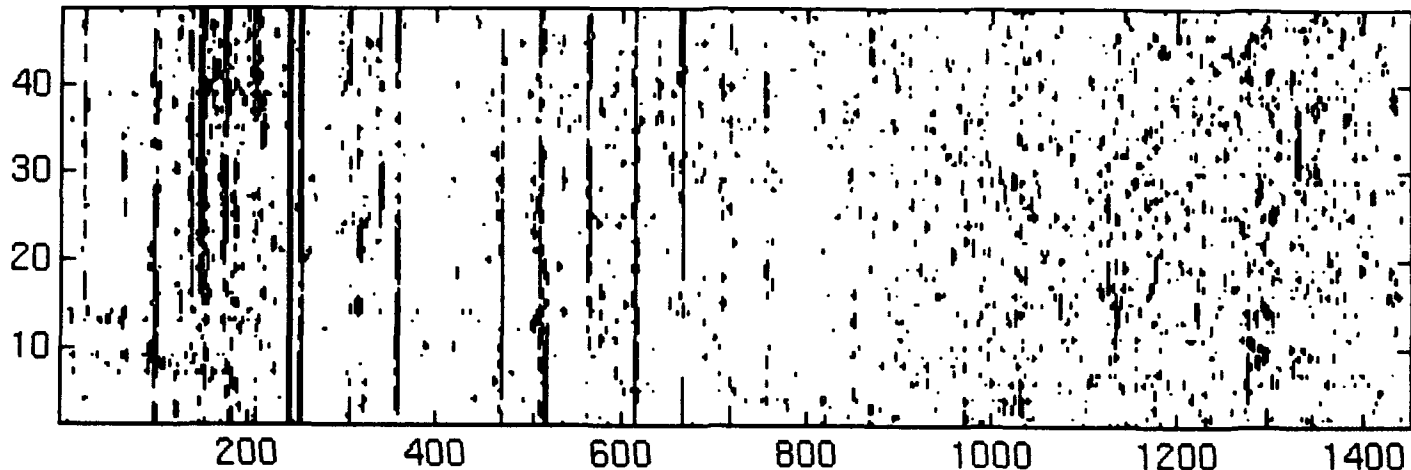
ipsav(rf,1,4096,32) bin51:1500 level:def,7,6 top:bottom

Fig. A.1



cumav(rf,1,4096,32) bin51:1500 level: def,8,7 top:bottom

Fig. A.2



lofarm(rf,4096,4096,4096) bin51:1500 level:def,7,6 top:bottom

Fig. A.3

## INITIAL DISTRIBUTION LIST

|                                                                                                                                                              | No. Copies |
|--------------------------------------------------------------------------------------------------------------------------------------------------------------|------------|
| 1. Defense Technical Information Center<br>Cameron Station<br>Alexandria, VA 22304-6145                                                                      | 2          |
| 2. Dudley Knox Library, Code 52<br>Naval Postgraduate School<br>Monterey, CA 93943-5002                                                                      | 2          |
| 3. Chairman, Code EC<br>Department of Electrical and Computer Engineering<br>Naval Postgraduate School<br>833 Dyer Road, Room 437<br>Monterey, CA 93943-5121 | 1          |
| 4. Professor Ralph Hippenstiel, Code EC/HI<br>Department of Electrical and Computer Engineering<br>Naval Postgraduate School<br>Monterey, CA 93943-5121      | 3          |
| 5. Dr. Charles Persons<br>Code 732<br>Naval Command Control & Ocean Surveillance Center<br>271 Catalina Blvd.<br>San Diego, CA 92152-5000                    | 2          |